Capacity Improvement Using Adaptive Sectorisation in WCDMA Cellular Systems with Non-Uniform and Packet Mode Traffic

Trung Van Nguyen

B.Eng., M.Sc.

SUBMITTED IN FULFILLMENT FOR THE REQUIREMENTS OF THE DEGREE OF DOCTOR OF PHILOSOPHY

School of Electrical Engineering

Faculty of Science, Engineering and Technology

Victoria University

Melbourne, Australia

March 2005

Declaration

I declare that, to the best of my knowledge, the research described herein is the result of my own work, except where otherwise stated. I also declare that this work has not been submitted for this degree before and is not being submitted concurrently for any other degree.

Signature of Author Date: **March 2005**

*To my dear wife **Thuy Thanh Phuong** and*
*my lovely daughter **Evonne Nguyen***

Table of Contents

Abstract

CDMA cellular mobile systems find widespread acceptance particularly in regional centres where there are large geographical areas to cover. However, temporal changes of user density due to formation of congregated population centres (called hot spots) can seriously undermine the system design goals in terms of quality of service (QoS) and system capacity. This investigation deals with the problem of hot spots in a bid to improve system capacity at acceptable quality of service levels. Among the techniques considered is the adaptive sectorisation and its implementation with finite antenna beam switching.

The future wireless communications systems are expected to offer a wide variety of services, which have vastly differing QoS requirements. To handle this, the third generation cellular mobile communication systems are designed to carry packet mode traffic. This investigation also deals with the impact of third generation cellular system traffic on system capacity. It examines the system activity in the presence of mixed mode traffic and the capacity and QoS trade-offs possible in Wideband CDMA (WCDMA) cellular systems. Application of adaptive sectorisation to improve capacity in such systems when confronted with hot spots is also investigated.

It is found that in all situations the adaptive sectorisation brings an overall improvement to system capacity and this is particularly significant when the user concentration in hot spots is substantially bigger than that of the rest of the cell.

Acknowledgements

I am most grateful to my supervisor, Dr. Prem Dassanayake who has guided me through this work. I am indebted to him for his unceasing encouragement, support and advice. His knowledge, experience and commitment have benefited me tremendously during this research. It is my great pleasure to have had such an opportunity to work with him.

My deep gratitude goes to Professor Mike Faulkner, my co-supervisor, for his support and help in my research. His enthusiasm for research and devotion to work have been constant sources of inspiration and encouragement for my advancement.

I am truly indebted to head of school Professor Aladin Zayegh, Professor Jack Singh, Associate Professor Fu-Chun Zheng, Dr. Greg Martin, Ms Shirley Herrewyn, Dr. Ying Tan and Mr Foster Hayward for their genuine help.

My thanks should also go to my colleagues at Centre for Telecommunications and Micro-Electronics. The memories I shared with Gavin, Andrew, Hanh, Nghia, Melvyn, Alamgir, Shane, Guillaume, Jason, Michael, Phuoc, Hai, Lei, Wei, Kai, Don, Alex, Ronny, and Leon will always remain with me.

Special thanks should go to Australian Telecommunications Cooperative Research Centre (ATcrc) for its financial support.

Words cannot express my deepest gratitude and appreciation to my wife, my parents, my brother, and my sisters, for their encouragement and support throughout the period of this work. Without them this work would never have come into existence.

Abbreviations

3G	3^{rd} Generation
3GPP	3^{rd} Generation Project Partnership
AMPS	Advanced Mobile Phone System
ARIB	Association of Radio Industries and Bussiness
AWGN	Additive White Gaussian Noise
BCH	Broadcast Channel
BER	Bit-Error-Rate
BS	Base Station
CDMA	Code Division Multiple Access
cdma2000	Code Division Multiple Access 2000
CIR	Carrier-to-Interference Ratio
DL	Down Link
DPCCH	Dedicated Physical Control Channel
DPDCH	Dedicated Physical Data Channel
DQPSK	Differentially Encoded Quadrature Phase Shift Keying
DS	Direct Sequence
ETSI	Europe Telecommunications Standards Institute
FBI	Feedback Information
FDD	Frequency Division Duplexing
FDMA	Frequency Division Multiple Access
FIFO	First-In-First-Out
GPRS	General Packet Radio Service
GSM	Global System For Mobile Commnications

HR	High Rate
HS	Hot Spot
HSA	Hot Spot Area
HSCSD	High Speed Circuit Switched Data
HSS	Hot Spot Sector
IMT-2000	International Mobile Telecommunications - 2000
ISI	Inter-Symbol Interference
ISR	Interference-to-Signal Ratio
LR	Low Rate
MAI	Multiple Access Anterferenc
MC	Multicode
MR	Mixed Rate
MS	Mobile Station
MSC	Mobile Switching Center
OVSF	Orthogonal Variable Spreading Factor
PCS	Personal Communication Systems
PDC	Personal Digital Cellular
PG	Processing Gain
Pr	Blocking Probability
PRACH	Physical Random Access Channel
PSTN	Public Switching Telephone Network
QoS	Quality of Service
RV	Random Variable
SIR	Signal-to-Interference Ratio
SINR	Signal-to-Interference-Plus-Noise Ratio
SNR	Signal-to-Noise Ratio
TCC	Telecommunication Technology Committee
TDD	Time Division Duplexing
TDMA	Time Division Multiple Access
TFCI	Transport Format Combination Indicator
TIA	Telecommunications Industry Association

TPC	Transmit Power Control
VCR	Variable Chip Rate
VSF	Variable Spreading Factor
UE	User Equipment
UL	Up Link
UMTS	Universal Mobile Telecommunications Sevice
UTRA	UMTS Terrestrial Radio Access
WCDMA	Wideband Code Division Multiple Access
WLAN	Wireless Local Area Network

Notations

Variables

t_{ai}	Time of arrival of the i^{th} user
A_i	Inter-arrival time between $(i-1)^{th}$ and i^{th} arrivals, $(t_{ai} - t_{a(i-1)})$
S_i	Service time of i^{th} user (exclusive of customer's delay in queue)
D_i	Delay time of the i^{th} user in the queue
t_{di}	Time of departure of i^{th} user after receiving service, $(T_{ai} + D_i + S_i)$
N	Average number of users in the system
$N(t)$	Number of users in the system at any given time
$\gamma(t)$	Number of arrivals (total)
$\beta(t)$	Number of departures (total)

Chapter 1

Introduction

This chapter provides an overview of the investigation that forms the subject of this thesis. It introduces the basic concepts on which the investigation has been launched and provides a historical development of the subject. It identifies the author's contribution to the knowledge in this field and outline the thesis layout.

1.1 Capacity of CDMA cellular systems

Personal mobile communication has become a way of life in the present day society. Its widespread acceptance among people in all walks of life has created an ever increasing demand on the services of cellular mobile phone systems. Adding to that is the range of services that continually expand covering a vast variety of applications that involve traffic arising from voice, data, multimedia, and the like. The aim of mobile communications has always been the extension of all wireline service facilities to wireless environment. With the emergence of the third generation cellular systems this aim has become close to reality and the issue of system capacity has moved to the fore front.

In CDMA cellular systems the capacity is a function of interference and reducing interference leads to capacity improvement. The interference that a user confronts consists of back ground noise and the signals generated by other users in the system. Therefore, the user distribution in a cell is a crucial factor in estimating the capacity of a cell. With the power control mechanisms employed in CDMA systems the base station (BS) of a cell is able to control the power generated by the mobile station (MS) within the cell but it has no control over the power generated by the mobile stations in the neighbour cells. Since the interference consists of the signals generated by other users including those in neighbour cells, the location of these other users in neighbour cells plays an important part in estimation of the systems capacity.

1.2 Hot Spots and Adaptive Sectorisation

Most of the studies that deal with the capacity estimation assume that the users are evenly distributed in cells throughout the coverage area of the system. In practice however this is an unlikely situation and users are more likely to be distributed unevenly. What is of particular importance is the occurrence of small areas within a cell where there are collections of users densely packed. These areas (called hot spots) generate disproportionate amount of interference and can seriously effect the system capacity.

Adaptive sectorisation is one way the system can adapt to changing traffic environment. By judiciously selecting sector size and positioning them in such a way so as to distribute the interference arising from hot spots as evenly as possible among the sectors the system capacity can be improved. the sector size and boundaries can be varied so as to include either fully or partially a given hot spot in a cell, and hence, limit the interference appearing at a given BS. There are many techniques that can be used to implement adaptive sectorisation. Among these, a simple and robust techniques is the employment of finite beam switching using linear antenna arrays. By adjusting the length and the spacing of the antenna array elements, and the phase of their feed currents, its is possible to stear the main beam of the array to cover a sector of desired size, in a cell.

1.3 System Capacity with 3G Traffic

Third generation cellular systems are poised to cater for mixed mode traffic consisting of voice, data, interactive multimedia, and the like, much of it associated with the Internet. The third generation partnership project (3GPP) has identified this need and has developed a traffic model that can closely resemble the practical situations that are most likely to be confronted by the 3G cellular systems. This model consists of 3 tiers in which packets, packet calls, and sessions are included in a single packet connection. The arrival and duration statistics of each category (i.e., packet, packet calls, and sessions) determine the particular traffic environment and hence can represent most types of traffic commonly found in Internet.

Third generation systems which deal with packet mode traffic can extend system capacity by employing inactivity periods inherently present among packets, packet calls, and sessions. Depending on the quality of service, if bandwidth is not reserved for nominated connections, this system inactivity periods could be utilised to increase the system capacity quite substantially.

This investigation looks at each of the above aspects in order to examine the ways in which the system capacity can be improved in the third generation cellular mobile communication systems.

1.4 Results and Conclusions

It is shown in this report that in almost all situations irrespective of the traffic environment, in CDMA cellular systems dealing with hot spots, the system capacity can be increased by the employing adaptive sectorisation. This capacity increase is particularly significant when the user density in hot spots is considerably higher (by several orders of magnitude) when compared to the user density in rest of the cell.

1.5 Contribution to Knowledge

This thesis, except where otherwise stated, is author's own. In particular the section 4.3 and chapter 5 describe the analysis of influence of hot spots on the capacity of multicell CDMA cellular systems, and the examination of possible improvement to capacity using adaptive setorisation. Similarly, the chapter 5 describes the modeling of traffic in third generation cellular systems and the examination of the capacity performance of WCDMA cellular mobile systems with adaptive sectorisation.

1.6 Layout of the Thesis

The rest of the thesis is organized as follows: Chapter 2 reviews the cellular mobile communication systems and their capacity estimation. Chapter 3 reviews some of the techniques used to improve the capacity of CDMA cellular systems. In Chapter 4, the methods of evaluating interference in CDMA cellular systems in multicell structures are developed. Chapter 5 discuses the capacity improvement of CDMA cellular systems in non-uniform traffic environments using adaptive sectorisation. Chapter 6 describes the WCDMA air interface to lay the foundation for the study of 3G systems and their capacities. Chapter 7 describes the modelling of 3G traffic in WCDMA cellular systems and its application in estimating the system capacity. Finally, the Chapter 8 presents the conclusions and some thoughts for future work on this subject.

Chapter 2

Cellular Mobile Communication Systems and Their Capacity

This Chapter provides the background material necessary for the study of the capacity of cellular mobile communication systems. The concepts of FDMA, TDMA, and CDMA are explained, and a basic introduction to the first, second, and third generation cellular systems is given. The issues involved in the estimation of capacity of these systems are highlighted.

2.1 Mobile Communication and Cellular Concept

The cellular concept arose out of the necessity to share the spectrum which is a premium and a limited resource in mobile communication. It is centered around the ability to control the radio frequency energy within a confined area of space (called a cell) so that the same spectrum can be reused as many times as desired, within each cell. Thus the capacity of the system can be increased by making cells smaller in area and also by sub dividing a cell area into smaller parts (called sectors). The users in a cell are allowed to

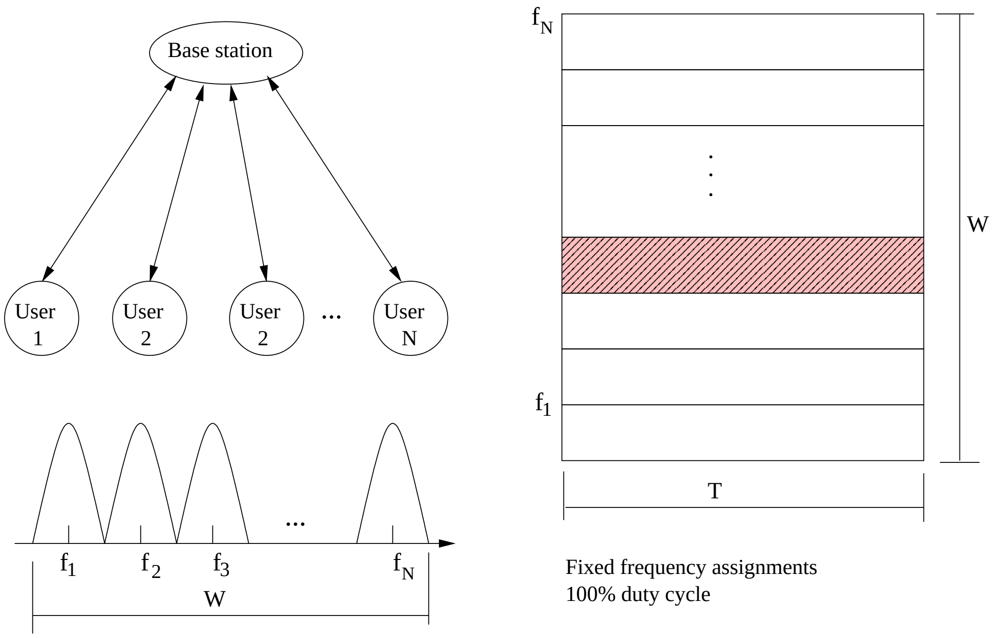

Figure 2.1: Frequency division multiple access [1].

get access to the available spectrum by employing a multiple access technique. In cellular mobile communication systems, the widely adopted multiple access techniques are the Frequency Division Multiple Access (FDMA), Time Division Multiple Access (TDMA), and Code Division Multiple Access (CDMA), as described below.

2.1.1 FDMA

In FDMA system, the time frequency plane is divided into N discrete frequency channels, continuous along the frequency axis as shown in Fig. 2.1. Each user is assigned a channel for the entire duration of the user's conversation. Other users can access the channel after the first user's conversation has ended.

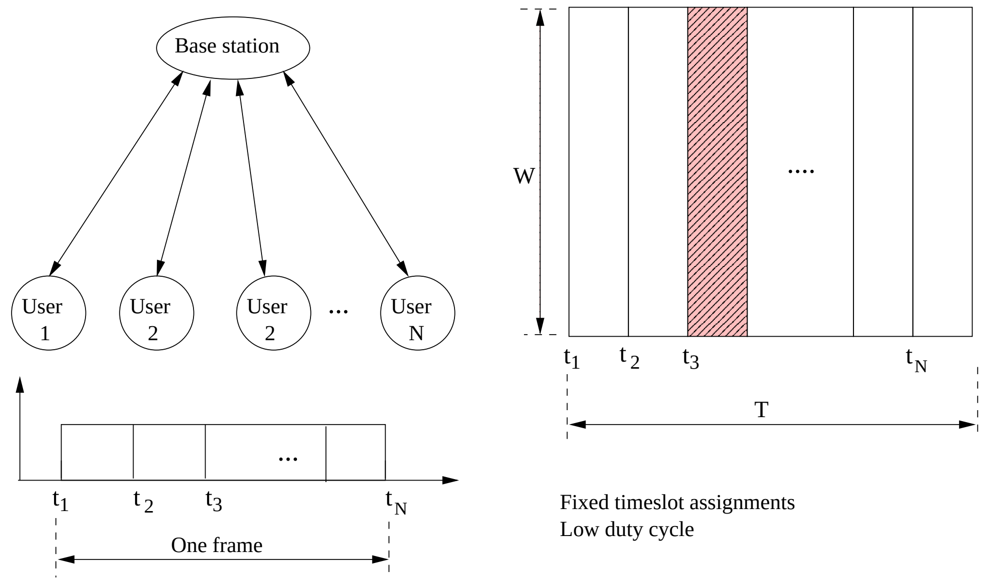

Figure 2.2: Time division multiple access [1].

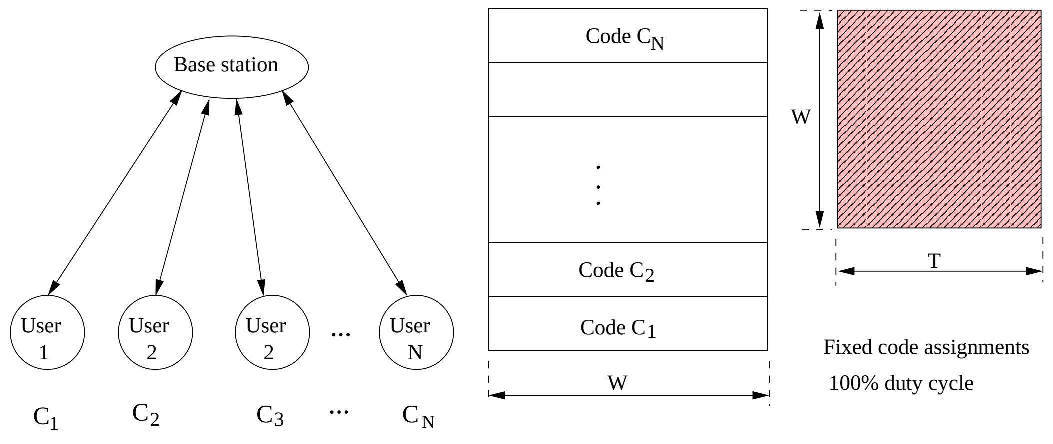

Figure 2.3: Code division multiple access [1].

2.1.2 TDMA

In TDMA the time frequency plane is divided into N discrete timeslots, continuous along the time axis as shown in Fig. 2.2. With this technique, multiple users can make use of the band assigned to the communication at different moments of time.

Mixed TDMA-FDMA techniques are used, where the bandwidth assigned to an operator is divided among different FDMA carriers, each of which is shared by the users with the TDMA technique. This technique is used by the second generation digital cellular systems such as Global System for Mobile (GSM) and Personal Digital Cellular (PDC).

2.1.3 CDMA

In CDMA system, the signal energy is continuously distributed throughout the entire time frequency plane. Each user employs a wideband coded signalling waveform, as shown in Fig. 2.3. The user data to be transmitted is uniquely coded such that it can be distinguished from those of the other users. Each data bit is subdivided to accommodate the code word in it and as a result this technique leads to spectrum spreading. CDMA is a direct sequence spread spectrum system and is the subject of the present investigation.

2.2 Early Cellular Systems

Early cellular systems were all analog systems and need FDMA with Frequency Division Duplexing (FDD). The systems were designed to handle voice and the voice signal was frequency modulated. Part of UHF spectrum were utilised to cover sizable areas where in today's terms could be categorised as macro cells. The capacity was not a main issue in these systems as demand was not great.

2.2.1 First Generation Systems

The first successful cellular mobile communication system was the Advanced Mobile Phone Service (AMPS) developed in USA in 1970s. It used FDMA technology with FDD and employed 20 MHz bandwidth in the 800 MHz region. AMPS at present operates with a 25 MHz bandwidth in each direction over the frequency allocations of 824-849 MHz for the Uplink (UL) (from mobile to base station), and 869-894 MHz for the Downlink (DL) (from base station to mobile) [1]. This spectrum is divided into 832 frequency channels leaving 416 channels in the uplink and another 416 channels in the downlink. Some of these channels are used to carry system information and control signal while the rest carries voice and data in analog form. In AMPS, each channel occupies 30 kHz of bandwidth using analog Frequency Modulation (FM) [1]. TACS, NMT and AMPS are among the first generation cellular systems.

Although cell division techniques are frequently employed by the first generation system, reduction of cell sizes below a few hundred meters eventually renders cell division infeasible. Moreover, analog modulation is sensitive to interference from other users in the system, and the voice quality is quite vulnerable to various kinds of noise. As a consequence of these, other means of capacity improvement such as efficient modulation schemes were sought for the second generation.

2.2.2 Second Generation Systems

In the second generation cellular systems, digital technology enabled the use of signal processing techniques to increase the robustness against interference. It also reduced the spectral bandwidth required for each user and hence provided a higher capacity. The second generation systems provide about 3 to 4 times the capacity of the first generation system for the same spectral resource without adding new base stations. Since digital systems are more immune to noise, an Interference-to-Signal (ISR) ratio of about 15 dB is acceptable in digital systems (whereas 18 dB is required for the analog systems under same circumstances [3]). This allowed the use of smaller reuse clusters, thereby increasing the capacity of the system.

The second generation cellular mobile systems were based on Time Division Multiple Access (TDMA) technology, or a combination of TDMA and FDMA. The IS-54 TDMA digital cellular system employs digital voice produced at 10 kbps (8 kbps speech plus over head), and transmitted with $\pi/4$ Differentially encoded Quadrature Phase Shift Keying ($\pi/4$ DQPSK) modulation. The IS-54 system permits 3 callers per 30 kHz channel spacing (30 kHz/10 kbps), therefore, increasing capacity three times that of AMPS.

In 1990, Qualcomm, Inc., proposed a digital cellular telephone system based on Code Division Multiple access (CDMA) technology. In July 1993, the second U.S digital cellular standard (IS-95) was adopted. Using spread spectrum techniques, the IS-95 system provides a very high capacity [1].

2.2.3 Third Generation Systems

WCDMA Air Interfaces

In principle, all third generation cellular systems have adopted WCDMA as the air interface. However, there are minor differences between the WCDMA air interface adopted by cdma2000 and IMT-2000.

The cdma2000 (USA)

Within the standardization committee of Telecommunications Industry Association (TIA), the subcommittee TR45.5.4 was responsible for the specifications of the basic cdma2000 scheme [4]. Like for all other wideband CDMA schemes, the goal for cdma2000 has been to provide data rates that meet the IMT-2000 performance requirements. That is at least 144 Kbps in a vehicular environment, 384 Kbps in a pedestrian environment, and 2048 Kbps for indoor office environment. The main focus of standardization has been to provide 144 Kbps and 384 Kbps bit rates with approximately 5 MHz bandwidth.

There are two main alternatives currently existing for the down link channel structure of cdma2000. They are the multicarrier and direct spread options [4]. The multicarrier approach maintains orthogonality between the cdma2000 and IS-95 carriers. In the downlink this is important because the power control can not balance the interfering power between different layers, as it can in the uplink. Transmission on the multicarrier downlink is achieved by using three consecutive IS-95B carriers where each carrier has a chip rate of 1.2288 Mcps as shown in Fig. 2.4. For the direct spread option, transmission on the downlink is achieved by using normal chip rate of 3.6864 Mcps [4].

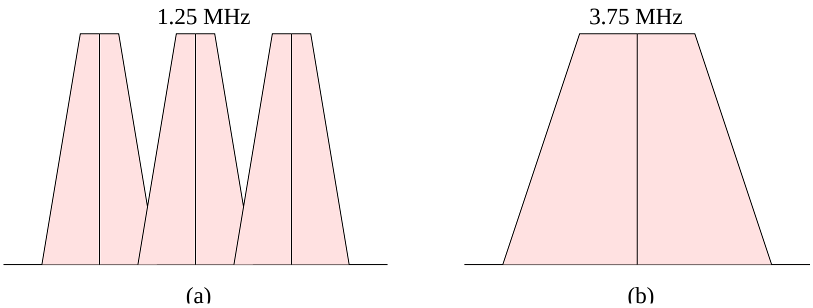

Figure 2.4: Illustration of (a) multicarrier and (b) direct spread downlink for cdma2000.

The starting point for bandwidth design for cdma2000 has been the PCS spectrum allocation in the United State. The PCS spectrum is allocated in 5 MHz blocks and 15 MHz blocks. One 3.6864 Mcps carrier can be deployed within 5 MHz spectrum allocation including guardbands. For a 15 MHz block, three 3.6864 Mcps carriers and one 1.2288 Mcps carrier can be deployed [4] [5].

The cdma2000 system chip rate is in fact three times the chip rate used in the IS-95 standards, which is 1.2288 Mcps. Higher chip rates on the order of $M \times 1.2288$ Mcps, $M = 6$, 9, 12 are also supported. In the Direct-Spread Modulation Mode (DSMM), the symbols are spread according to the chip-rate and transmitted using a single carrier, giving a bandwidth of M×1.25 MHz. In Multicarrier modulation, the symbols to be transmitted are de-multiplexed into separate signals, each of which is then spread at a chip rate of 1.2288 Mcps. M different carrier frequencies are used to transmitted these spread signals, each of which has a bandwidth of 1.25 MHz [6] [7].

By using multiple carriers, cdma2000 is capable of overlaying its signals on the existing IS-95 1.25 MHz channels and its own channels, while maintaining orthogonality. Similar, to UTRA and IMT-2000, cdma2000 also supports TDD operation in unpaired frequency bands [8].

In contrast to UTRA and IMT-2000, where the pilot symbols are time multiplexed with the dedicated data channel on the downlink, cdma2000 employs a common code multiplexed continuous pilot channel on the downlink. The advantage of a common downlink pilot channel is that no additional overhead is incurred for each user. Another difference with respect to UTRA and IMT-2000 is that the BSs are operated in synchronous mode in cdma2000 [9].

IMT-2000 (Europe)

The Europe Telecommunications Standards Institute (ETSI) has been working on the Universal Mobile Telecommunication Services (UMTS), which is to be the European standard for the third generation mobile systems. UMTS will appear as one of the family members within the IMT-2000 family. (Any system/network based on specification that supports the IMT-2000 capabilities and interfaces defined by the ITU will be considered as an IMT-2000 system/network.) ETSI has agreed on UTRA (UMTS Terrestrial Radio Access) as the radio transmission technology for UMTS. This Radio Transmission Technology (RTT), which utilizes WCDMA with FDD for paired frequency bands and a hybrid WCDMA/TDMA with TDD for unpaired frequency bands, has been submitted to the ITU-R as a candidate for IMT-2000 [5]. UMTS will utilize the GSM network interfaces as the basis for its network interfaces and proposals. The current GSM network capabilities, which include General Packet Radio Service (GPRS), High Speed Circuit

Switched Data (HSCSD), and Customized Application for Mobile Enhanced service Logic (CAMEL), will be enhanced to support UMTS capabilities in terms of services like virtual home environment and multimedia, as well as higher bit rates [5].

The WCDMA technology in Japan is very similar to that of Europe. The Association of Radio Industries and Businesses (ARIB) in Japan has their technology in line with ETSI's WCDMA. The outcome of the ARIB selection process in 1997 was WCDMA, with both FDD and TDD modes of operation [5]. Since the creation of 3GPP for the third generation standardisation framework, ARIB has contributed to 3GPP, in the same way as ETSI has contributed UTRA. In Japan, the IMT-2000 standardization is divided between two standardization organization: the Association of Radio Industries and Businesses (ARIB) and the Telecommunication Technology Committee (TTC). ARIB is responsible for the standardization of radio interface while TTC is responsible for the standardization of network interface.

In Korea, two wideband CDMA air interfaces are being considered: Telecommunications Technologies Association's standard I (TTA I) and Telecommunications Technologies Association's standard II (TTA II) [5]. The Electronics and Telecommunications Research Institute (ETRI) in Korea has established an R&D consortium to define the Korean proposal for IMT-2000 during 1997 and 1999. The main features of these air interfaces are listed in Table 2.1. TTA II concept is closer to cdma2000 while TTA I resembles WCDMA [5].

The IMT-2000 system is aiming to be flexible in order to operate in any propagation environment, such as indoor to outdoor, outdoor to indoor, and vehicular environments.

Table 2.1: Parameters of Korean WCDMA Schemes

	TTA I	TTA II
Channel spacing	1.25 MHz / 5 MHz / 20 MHz	1.25 MHz / 5 MHz / 10 MHz / 20 MHz
Chip rate	0.92 Mcps / 3.68 Mcps / 14.77456 Mcps	1.024 Mcps / 4.096 Mcps / 8.192 Mcps / 1.384 Mcps
Frame length	20 ms	10 ms
Spreading	Walsh and long codes	Walsh and long codes
Pilot for coherent detection	UL: pilot symbol based DL: common pilot	UL: pilot symbol based DL: common pilot
Base station synchronization	Synchronous	Asynchronous

It is also aiming to be sufficiently flexible to be able to handle circuit as well as packet mode services, and services involing variable data rates [10].

The spectrum allocation for WCDMA in Europe, Japan, Korea, and USA is shown in Fig. 2.5 [6]. In Europe and in most of Asia, the International Mobile Telecommunication (IMT) - 2000 band consists of 2×60 MHz (1920 -1980 MHz plus 2110-2170 MHz). In Japan and Korea, the IMT-2000 FDD band is the same as that of the rest of Asia and Europe. In USA no new spectrum has yet been made available for the third generation systems. Third generation services can be implemented by reforming second generation systems within the existing Personal Communication Systems (PCS) spectrum [10]. Table 2.2 summarises the main features related to the WCDMA air interface [6].

2.3 Capacity of Early Cellular Systems

The capacity of first and second generation cellular mobile systems was governed by the available number of r.f. channels within the allocated spectrum. Once the acceptable

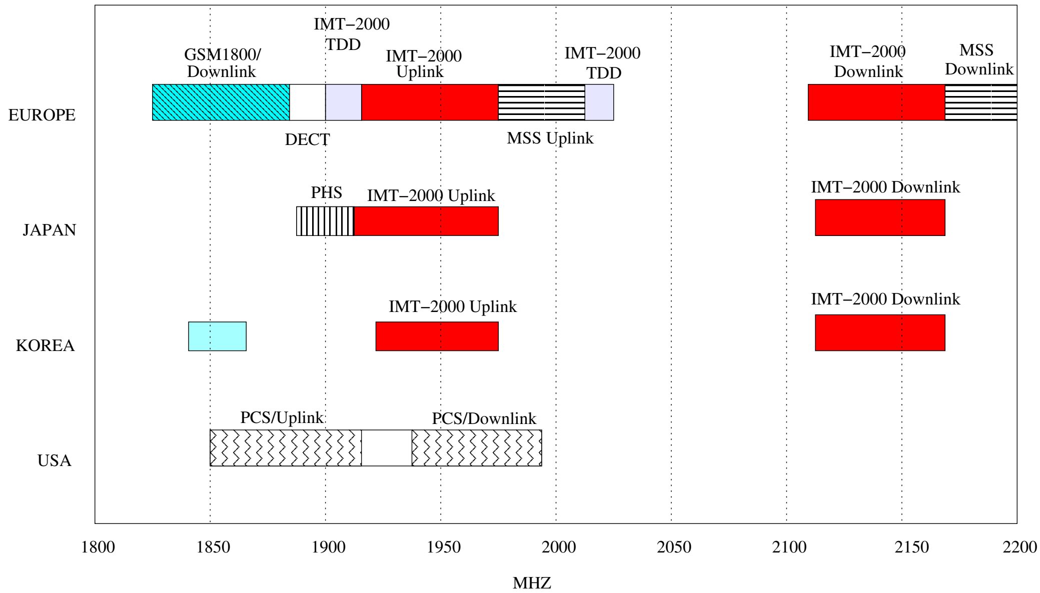

Figure 2.5: Spectrum allocation for WCDMA in Europe, Japan, Korea, and USA [6].

Table 2.2: Main WCDMA features [6]

Multiple access method	Direct Sequence Code Division multiple Access
Duplexing method	Frequency Division Duplex / Time Division Duplex
BS synchronisation	Asynchronous
Chip rate	3.84 Mcps
Frame length	10 ms
Service multiplexing	Multiple service with different QoS requirements multiplexed on one connection
Multirate concept	Variable spreading factor and multicode
Detection	Coherent using pilot symbols or common pilot
Multiuser detection, smart antenna	Supported by the standard. Optional in the implementation

Table 2.3: 7-cell OMNI channel grouping scheme

Cell number, K	1	2	3	4	5	6	7
Channel Number:							
K	1	2	3	4	5	6	7
K + 7	8	9	10	11	12	13	14
K + 14	15	16	17	18	19	20	21
.	.	.					
.	.	.					

grade of service (GoS) is specified, the amount of traffic that could be offered in the system with the given number of channels is determined, and this has set a hard limit on the system capacity. The GoS in turn is determined by the signal to interference (or carrier-to-interference) ratio of the system.

2.3.1 Capacity in AMPS System

The AMPS cellular system at 850 MHz, is a high capacity system. There are two separate frequency bands, adjacent to each other, each band providing 416 channel pairs, having 30 KHz channel separation [11]. Out of 416 channels, 21 channels are designated as control channels. Control channels are used for call setup and management. The remaining channels (395) are used as voice channels. Channel assignment is based on the following sequence: $(K, K+7, K+14, ...)$ where K is the cell number (K = 1, 2, ..., 7 for 7-cell cluster). The channel grouping scheme is shown in Table 2.3 and the corresponding cell cluster is shown in Fig. 2.6,

As seen in Fig. 2.6 that the minimal separation (D_S) required between two nearby

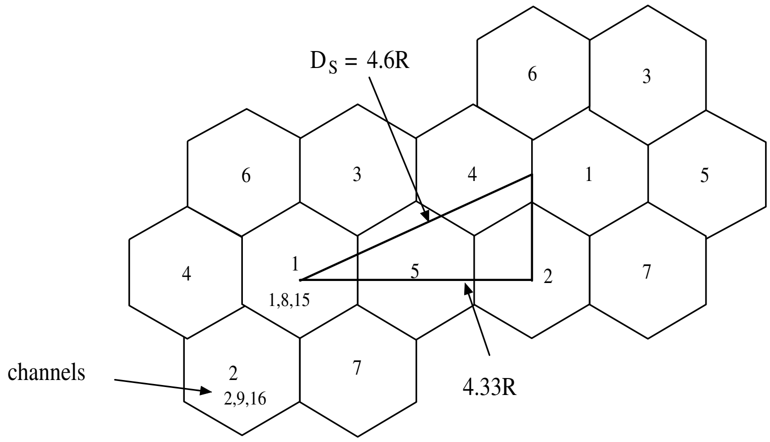

Figure 2.6: Channel allocation in 7-cell cluster system.

co-channel cells is based on specifying a tolerable co-channel interference, which is measured by the carrier-to-interference ratio (CIR). The CIR is also a function of minimum acceptable voice quality of the system. The CIR of AMPS is defined [12] as,

$$\left(\frac{C}{I}\right)_{AMPS} = 10log\left[\frac{1}{j}\left(\frac{D_S}{R}\right)^{\gamma}\right] \tag{2.3.1}$$

where j is the number of co-channel cells (j = 1, 2,.., 6), γ is the propagation exponent, D_S is the frequency reuse distance, and R is the cell radius. The co-channel interference reduction factor, q_s, is defined as,

$$q_s = \frac{D_S}{R} \tag{2.3.2}$$

With $\gamma = 4$, $D_s = 4.6$, and $j = 6$, the CIR becomes

$$\left(\frac{C}{I}\right)_{AMPS} = 18dB \tag{2.3.3}$$

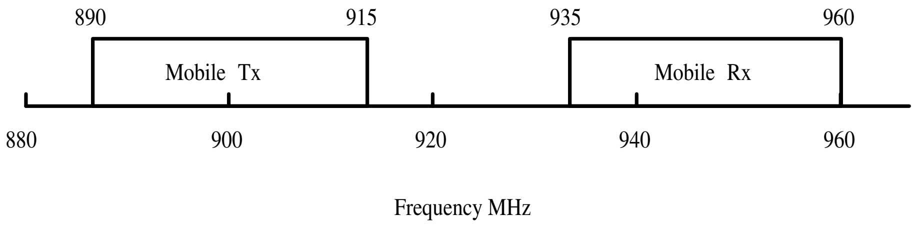

Figure 2.7: GSM spectrum allocation.

2.3.2 Capacity in GSM System

GSM uses a Time Division Multiple Access (TDMA) with Frequency Division Duplex (FDD) technique on a total of 125 carrier pairs in the 900 MHz band as shown in Fig. 2.7. Each carrier conveys 8 time divided channels making a total of 125×8=1000 channels. The GSM used Gaussian minimum shift keying (GMSK) modulation with a bandwidth-to-bit-period product (B.T) of 0.3. The spectrum of this signal is tailored to enable it on a radio frequency carrier of 200 KHz bandwidth. The TDMA frame is produced by multiplexing eight channel encoded speech sources in time division. Eight timeslots each of duration 0.577 ms make up one TDMA frame of 4.62 ms and is transmitted on the radio path at a bit rate of 270.833 kbps [13]. The salient features of the air interface of GSM system are shown in Table 2.4. Because of the inherently greater robustness to interference, the GSM system is designed to operate at a lower carrier-to-interference ratio of 12 dB (compared with 18 dB for AMPS).

Table 2.4: Basic air interface parameters of GSM

Feature	*Parameter*
Channel spacing	200 kHz
Modulation	GMSK
Modulation depth	B.T = 0.3
Data transmission rate	1270.833 Kbps
Number of channels/band	8 (16) Kbps
User data rate (nominal)	16 (8) Kbps
TDMA frame period	4.62 ms
Time slot duration	0.58 ms

2.4 Conclusions

This chapter reviewed early cellular networks with particular emphasis to their capacity aspect. The fundamentals of FDMA, TDMA and CDMA access strategies and the evolution of first, second and third generation cellular systems were examined. It was shown that the second generation systems provide three to four times capacity of the first generation systems with the same infrastructure (i.e., Base Station) layout. It was also shown that the capacity of the third generation systems are determined by the amount of the co-channel interference that can be tolerated, and is to be discussed in detail in the next chapter.

Chapter 3

Capacity of CDMA Cellular Systems

Due to increasing demand in cellular mobile communications, the efficient use of spectrum resource to maximize system capacity remains an important issue in system design. The capacity of a CDMA cellular network is determined by the amount of co-channel interference it can tolerate. This chapter introduces the concept of Signal-to-Interference ratio (SIR) in CDMA cellular systems (section 3.1), and then derive expressions for intra-cell and inter-cell interference (section 3.2). System capacity estimation with blocking probability as a performance measure is given in section 3.3, the factors effecting the capacity of CDMA cellular systems are discussed in section 3.4, and section 3.5 we present our conclusions.

3.1 Signal-to-Interference Ratio (SNR)

In digital systems, we are primarily interested in the link metric called E_b/N_0 or energy per bit to noise power spectral density ratio. This quantity can be related to the conventional

Signal-to-Noise-Ratio (SNR) by recognizing that energy per bit equates to the average signal power allocated to each bit duration, such that

$$E_b = ST \tag{3.1.1}$$

where S is the average signal power and T is the time duration of bit. We can further analyse (3.1.1) by substituting the bit rate R_b, which is the inverse of bit duration T:

$$E_b = \frac{S}{R_b} \tag{3.1.2}$$

The noise-power-spectral-density N_0, is the total interference power I divided by the transmission bandwidth W, i.e.,

$$N_0 = \frac{I}{W} \tag{3.1.3}$$

The total interference power I at the Base Station (BS) receiver could be defined as,

$$\begin{aligned} I &= I_{intra} + I_{inter} + \eta \\ &\equiv \ same\ cell\ interference\ power \\ &+ \ other\ cell\ interference\ power\ +\ background\ thermal\ noise\ power \end{aligned} \tag{3.1.4}$$

Therefore,

$$\left(\frac{E_b}{N_0}\right) = \left(\frac{S}{I}\right) \cdot \left(\frac{W}{R_b}\right) \tag{3.1.5}$$

The ratio W/R_b is known as the processing gain of the system. Therefore, in general, we can write,

$$\left(\frac{S}{I}\right) = \frac{S}{I_{intra} + I_{inter} + \eta} = \frac{E_b/N_0}{W/R_b} \tag{3.1.6}$$

where S is the received signal power. The power control in the uplink is used to ensure that the power received at the BS from every mobile user is the same. I_{intra} and I_{inter} will be discussed in the next section.

3.2 Interference

As mentioned previously the interference consists of intra-cell interference, inter-cell interference, and background noise due to thermal activity. Quantitative analyses have shown that the amount of back ground thermal noise is often insignificant in comparison to interference occurring due to the presence of other users in the system.

3.2.1 Intra-cell Interference

The same-cell (I_{intra}) interference on the reverse link consists of the superposition of signals from other mobile stations (MSs) at the base station (BS) receiver. Almost all of the noise received at the BS receiver is due to interference signals. The system capacity is maximized by making each signal'a power the same at the BS and as low as possible while achieving satisfactory link performance [1]. Let N denote the number of mobile users per cell (or sector). Assume that S is the signal power received by a cell BS when perfect power control is in place, so that this value is the same for every mobile in the same cell

(Fig. 3.1). The interference from the intracell mobiles is equal to,

$$I_{intra} = S \cdot (N - 1) \tag{3.2.1}$$

Thus given N mobile users per cell, the total intracell interference is never greater than $S(N-1)$. But this interference is reduced further with the employment of the voice activity factor, υ, which will be discussed in more detail in section 3.4.3.

3.2.2 Inter-cell Interference

Let the interfering MS is in the neighbour cell (Fig. 3.2), at a distance r from its respective controlling base station, BS_1, and r_0 from the home cell base station, BS_0. Fig. 3.3 depicts the geometry of this situation. The inter-cell interference on the reverse link (with perfect power control in place), can then be observed as,

$$\begin{aligned} I(r, r_0)_{inter} &= S \cdot \left(\frac{10^{\zeta_0/10}}{r_0^n}\right)\left(\frac{r^n}{10^{\zeta/10}}\right) \\ &= S \cdot \left(\frac{r}{r_0}\right)^n 10^{(\zeta_0 - \zeta)/10} \leq 1 \end{aligned} \tag{3.2.2}$$

where n is propagation loss exponent, r is the distance of the MS from its own base station, BS_1, r_0 is the distance of the MS from the home cell base station, BS_0, and ζ_0 and ζ are random variables representing the log-normal shadowing process in neighbour cell and home cell respectively. Since ζ_0 and ζ are independent random variables of zero mean and standard deviation, δ, the difference (ζ_0 - ζ) is also a random variable of zero

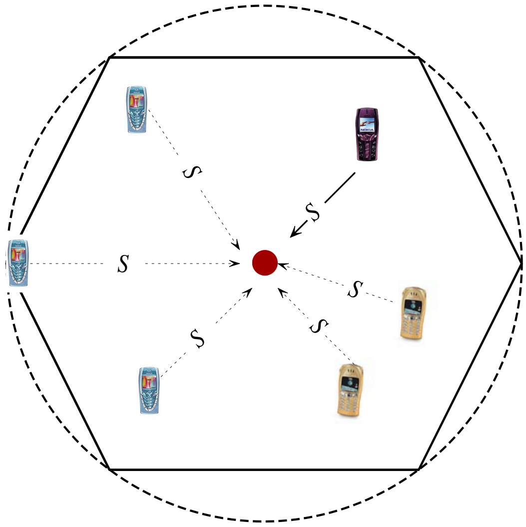

(a)

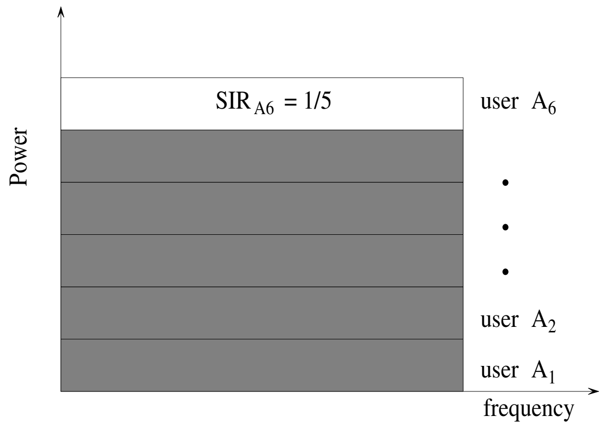

(b)

Figure 3.1: 3.1(a) Reverse link home cell interference with perfect power control. 3.1 (b) In CDMA the total interference power in the band is equal to the sum of powers from individual users. Therefore, if there are six users in the cell, with perfect power control, the SIR experience by any one user is 1/5

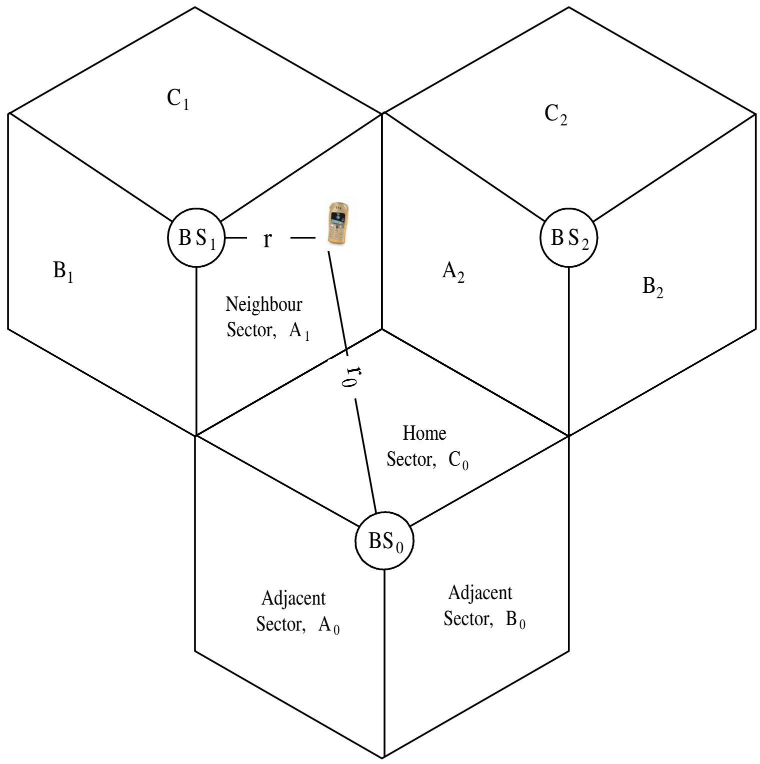

Figure 3.2: Configuration of sectorised multi-cell system and inter-sector interference.

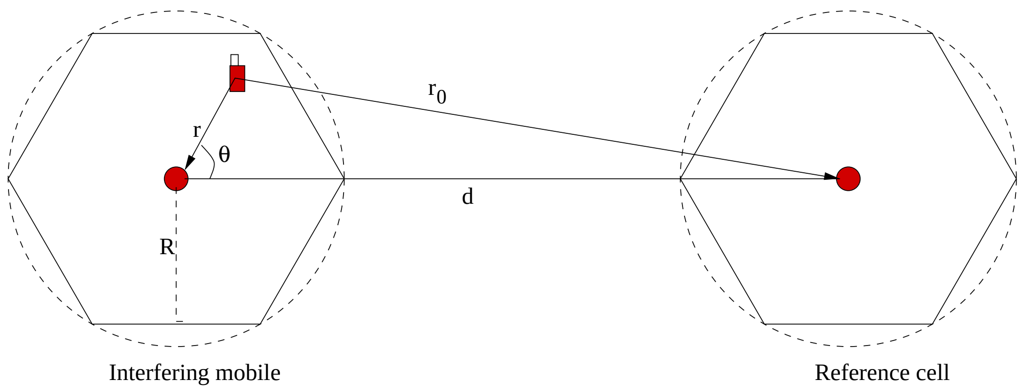

Figure 3.3: Geometry related to MS location in assessment of reverse link inter cell interference.

mean and variance $2\sigma^2$. The equation (3.2.2) takes into account of the fact that perfect power control is in place in the uplink in all cells. Let d be the distance between the base stations BS_0 and BS_1, and θ be the direction in which the MS is located with respect to the line joining the two base stations. Then,

$$r_0 = \sqrt{r^2 + d^2 - 2rd\cos\theta} \tag{3.2.3}$$

Assume that there are N users in the interfering cell, and they are uniformly distributed in the cell. Then the user density in the cell, ρ is $2N/(3\sqrt{3}R^2)$. (Please refer to appendix B)

The total interference power received at the home cell base station, BS_0, due to users in the interfering cell can be found as,

$$I_{inter} = 2\int_0^{\pi} d\theta \int_0^{R} \left(\frac{2N}{3\sqrt{3}R^2}\right) \cdot S\left(\frac{r}{r_0}\right)^n 10^{(\zeta_0 - \zeta/10)} \cdot \Theta(\zeta_0 - \zeta, r_0/r) \cdot r \cdot \theta dr \tag{3.2.4}$$

and

$$\Theta(\zeta_0 - \zeta,\ r_0/r) = \begin{cases} 1, & if \ \left(\frac{r}{r_0}\right)^n 10^{(\zeta_0 - \zeta)/10} \leq 1 \\ 0, & \text{otherwise} \end{cases} \tag{3.2.5}$$

Therefore the SIR of reverse link can be found by substituting (3.2.1) and (3.2.4) in (3.1.6),

$$
\begin{aligned}
\left(\frac{S}{I}\right) &= \frac{S}{\left(S(N-1) + 2S\int\limits_{0}^{\pi} d\theta \int\limits_{0}^{R} \left(\frac{r}{r_0}\right)^{n} 10^{(\zeta_0 - \zeta/10)} \left(\frac{2N}{3\sqrt{3}R^2}\right) \cdot rdr + \eta\right)} \\
&= \frac{1}{\left((N-1) + 2\int\limits_{0}^{\pi} d\theta \int\limits_{0}^{R} \left(\frac{r}{r_0}\right)^{n} 10^{(\zeta_0 - \zeta/10)} \left(\frac{2N}{3\sqrt{3}R^2}\right) \cdot rdr + \eta/S\right)}
\end{aligned}
\tag{3.2.6}
$$

3.3 Estimation of Capacity in a CDMA Cellular System

When an MS chooses to access a certain sector's BS, the sector's BS will check whether the SIR prevailing there is greater than the minimum (threshold) value required. If the SIR is less than the threshold, the MS is blocked. This threshold value, SIR_{th}, is

$$
\left(\frac{S}{I}\right)_{th} = \left(\frac{E_b/N_0}{W/R_b}\right) \tag{3.3.1}
$$

The quantity E_b/N_0 is the bit energy-to-noise power spectral density ratio and W/R_b is the processing gain of the system. The E_b/N_0 required in a CDMA system is about 7 dB if it were to have a bit-error rate (BER) not exceeding 10^{-3} [14]. If outage probability is also taken into account this value is about 7.4 dB [15].

The SIR_{th} based algorithm for call administration is a distributed mechanism [15]. It can be used by each sector's BS to determine whether or not a sector admits a call. If $SIR > SIR_{th}$, the call request is accepted. Otherwise, the call request is rejected. Therefore, the call blocking probability can be defined as,

$$
P_b = Pr(SIR \leq SIR_{th}) \tag{3.3.2}
$$

Estimation of capacity involves the placement of users in the system (in home sector as well as adjacent and neighbour sector) in a random fashion, successively increasing the number of users in the system. Every time a new user is to be added, the prevailing S/I ratio in the uplink at all base stations are evaluated. New users are added as long as the prevailing S/I is greater than the SIR_{th}. At the point when a new user causes the SIR to fall below the SIR_{th} the new user is blocked and the system capacity is evaluated as the total number of users already in the system.

3.4 Factors Influencing the Capacity of CDMA Systems

The actual capacity of a CDMA cell depends on the actual interference power introduced by other users in the same cell and in neighbouring cells. This in turn depends on many different factors, such as sectorisation, power control accuracy, voice activity, antenna gain, etc.

3.4.1 Sectorisation

The capacity of a CDMA system can be increased by cell sectorisation as it reduces the intra-cell interference (I_{intra}). Since the capacity is directly affected by the interference, less interference yield a higher system capacity. With uniform traffic distribution, the capacity of cellular system with sectorisation is increased by a factor equal to the number of sectors because the interference is effectively reduced by the same factor. That is, if N_s is the number of users per sector, the cell capacity (i.e. number of users per cell), N, is given by

$$N = \Delta \cdot N_s \tag{3.4.1}$$

where Δ is the number of sectors per cell. In the case of a three sector cell ($\Delta = 3$), (120^0 sectors) the interference sources seen by an antenna are approximately one-third of those seen by an omnidirectional antenna. Therefore, the number of users per sectorised cell is given by,

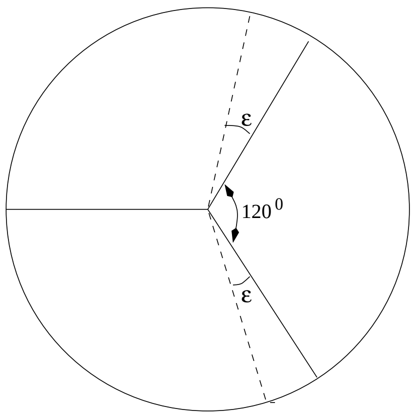

Figure 3.4: Sector coverage with an imperfect directional antenna with overlap angle ϵ and 120^0 sectors

$$N = 3N_s \tag{3.4.2}$$

Sectorisation is proposed as a method of increasing the system capacity in CDMA/WCDMA cellular systems. However, the obtainable capacity increase is often less than the theoretically predicted value. For instance, a 3-sector configuration tends to perform better than the 6-sector system at small cell radii [16] [17]. Also, higher sectorisation increases the inter-cell interference level of the system. Capacity gain at higher sectorisation will experience diminishing returns. The biggest problem in higher sectorisation is the control of the sector overlapping due to too wide antenna beam width [18]. With increasing overlap there will be an increase in soft/softer handovers creating unacceptable load on the switch gear of the system [18]. Since practical antennas have side lobes, perfect sectorisation does not exist in practice.

To model imperfect sectorisation, the overlap angle ϵ is introduced as shown in Fig. 3.4. The the capacity with imperfect sectorisation $N_{(imp)}$ is given by,

$$N_{(imp)} = \frac{360}{(360/\Delta) + 2\epsilon} \cdot N_s \tag{3.4.3}$$

If overlap angle is too big, interference is leaking through to the other sectors directly reducing it's capacity. The overlap in the antenna radiation patterns as well as the influence of the propagation environment on the pattern itself make it difficult to control the interference leakage into neighbouring sectors [18].

3.4.2 Tilted Antenna

Tilted antenna is another technique that can be used to improve the system capacity. The tilted antenna generally reduces the interference (Fig. 3.5) by controlling the range of coverage over a sector. This is because the main beam when tilted does not deliver as much power towards other BS as it normally does, and therefore most of the radiated power is directed to an area where it is intended [15] [19]. However, the tilted antenna will shrink the coverage area [15]. It causes the signal strength to be less at the mobile station (MS) when the MS is close to the sector boundary.

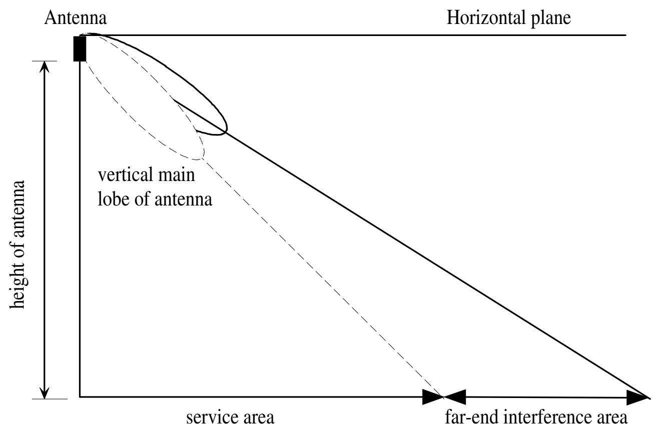

Figure 3.5: Tilted antenna cell coverage.

3.4.3 Channel Activity

Equation (3.2.6) assumes that users are active in transmitting 100% of the time. In practice, the vocoder (such as the one used in IS-95 system) is a variable rate vocoder, which means that the output bit rate of the vocoder is adjusted according to a user's speech pattern [20].

Therefore, CDMA system can take advantage in voice transmission in that the interference can be further reduced with the use of voice activation. The studies have shown that a speaker is active only for about 35% to 40% of the time [14] [21]. We assume that the voice activity factor, $\upsilon = 37.5\%$ *or* 3/8, throughout, this investigation. Thus with voice activity factor employed, the equation (3.2.6) becomes,

$$\left(\frac{S}{I}\right) = \frac{1}{\upsilon\left((N-1) + 2\int\limits_{0}^{\pi} d\theta \int\limits_{0}^{R} \left(\frac{r}{r_0}\right)^n \cdot 10^{(\zeta_0 - \zeta/10)} \cdot \left(\frac{2N}{3\sqrt{3}R^2}\right) \cdot r \cdot \theta dr + \eta/S\right)} \tag{3.4.4}$$

3.4.4 Power Control

Power control is critical in CDMA systems to keep interference under control. Each base station (BS) controls the transmit power of its own users. However, a given BS is unable to control the power of users in neighbouring cells; and these users introduce intercell interference, thereby reducing the capacity of the reverse link [22] [23]. Thus, to minimize the total received power in a cell while all users get their minimum required power, the cell should be sectored such that each sector has the same number of active users [24].

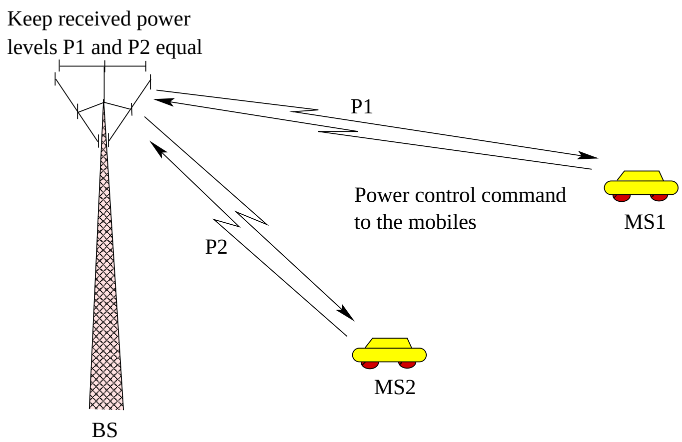

Figure 3.6: Closed-loop power control CDMA/WCDMA

Tight and fast power control is perhaps the most important aspect in WCDMA, in

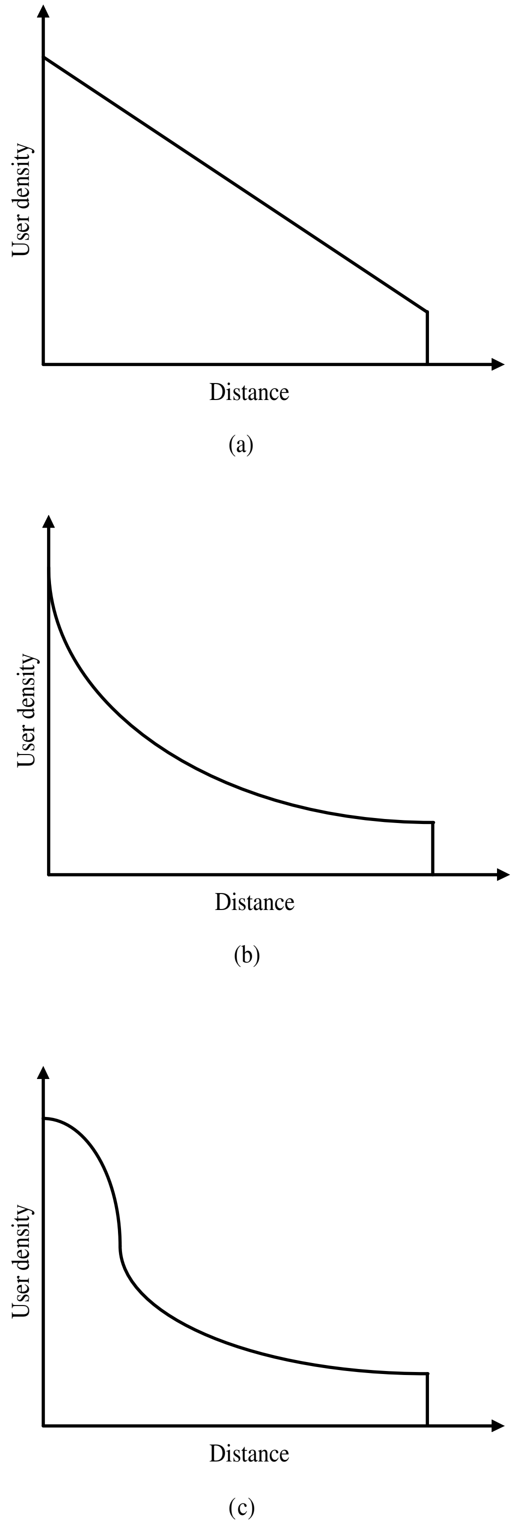

Figure 3.7: The non-uniform user density distributions [26]: (a) linear, (b) exponential, (c) gaussian

particular on the uplink. Without it, a single overpower mobile could block a whole cell. The solution to power control in WCDMA is fast closed-loop power control [6], (Fig. 3.6). In closed-loop power control in uplink, the BS performs frequent estimates of the received SIR and compares it to a target SIR. If the measured SIR is higher than the target SIR, the BS will command the MS to lower its power, and if measured SIR is too low, it will command the MS to increase its power [6]. Closed-loop power control will prevent any power imbalance among all the uplink signals received at the BS. The same closed-loop power control techniques also used on downlink, though here the motivation is different [6]. These power control mechanisms are based on constant bit rate traffic and is not directly applicable to the case of WCDMA when non-uniform and mixed traffic are involved.

3.4.5 Non-uniform Traffic

The analysis so far assumed that the user distribution in a cell or a sector is uniform. However, this is not the case always. In case of non-uniform traffic loads in cells, the inter-cell interference factor can be in the range from zero (no external interference) to highest (all the interference is external) [25].

Further it is necessary to make the SIR as small as possible, to satisfy the needs of the dynamic range characteristics of transmitters/receivers, as well as to adhere to power consumption requirements [25]. When compared with the more general case of non-uniform user distributions, the uniform user distribution leads to lower multi-user interference and consequently higher system capacity [26]. The results in [26] indicate that intra-cell multi-user interference dominates the total interference levels in most cases.

However, the works of [27] [26] have been limited only to non-uniform user density models described by a) linear, b) exponential, and c) Gaussian distributions (Fig. 3.7). In reality the non-uniform traffic occurs in a more sporadic and discrete fashion (as hot spots) in a cell space.

3.5 Conclusions

This chapter discussed fundamentals of capacity assessment in CDMA cellular systems taking into account of both intra-cell and inter-cell interference. The cases of sectorisation, tilted antenna, as well as channel activity factor have been considered. The system capacity estimation with blocking probability as a performance parameter and the factors that effecting the capacity estimation have been studied. The effects of non-uniform user distribution within cell and sector areas have also been discussed. The affects of non-uniform user distribution in multi-cell environment are to be discussed next.

Chapter 4

Interference in CDMA Cellular Systems: Multicell Structures

The capacity of a CDMA cellular mobile system is determined by the interference associated with it. In a multi-cell (or sector) system this interference consists of intra-cell interference generated within the cell and inter-cell interference arriving from neighbour cells. In estimating system capacity of these systems it is customary to consider the activity in uplink as it is the weaker link in terms of signal-to-interference ratio. Further, it is not unrealistic to assume that perfect power control is in place in the up link.

Under these conditions, the interference power received at a the Base Station (BS) of a given cell can be estimated by knowing the number of users in the cell, and the number of users and their locations in the neighbouring cells. In a macro cell environment, it is more likely that there exist small areas of higher user concentration (called hot spots). It would be of interest to the cellular mobile system designers to know the effects of this Hot Spot (HS) formation and its influence on the system capacity.

This chapter investigates the effect of HSs in a CDMA macro cellular system. The chapter layout is as follows: In Section 4.1 we present the system model considered for the present investigation. The mobile radio channel is described in Section 4.2. Section 4.3 deals with the estimation of interference due to uneven distribution of user populations (hot spots) in the cell. The section concludes with the results obtained from a simulation study.

4.1 Multicell System Model

In this investigation, the system model considers only the first tier of interfering cells, which means that there are six interfering (neighbouring) cells. Therefore, the geometry of the interference model can be represented as shown in Fig. 4.1(a). The interference from second and third tiers to the home cell is extremely small [15] [1], and thus is ignored.

The Fig. 4.1(b) shows the rotational symmetry of the hexagonal grid system that has hexagonal rings of cells round a center [1]. The diagram consists of the center cell and one of six 60^0 sectors around the origin. The coordinates of a cell in the sector are $(a,\ b)$, where a is the ring number and $b = 1, 2, ...a$, indexes the cells in the sector that are in ring a. The distance of the bth cell in the ath ring is

$$d(a,b) = 2R\sqrt{a^2 + b^2 - ab} \tag{4.1.1}$$

With this notation, the normalized distance of an interfering cell is,

$$r_{a,b} = \frac{d(a,b)}{R} = 2\sqrt{a^2 + b^2 - ab} \tag{4.1.2}$$

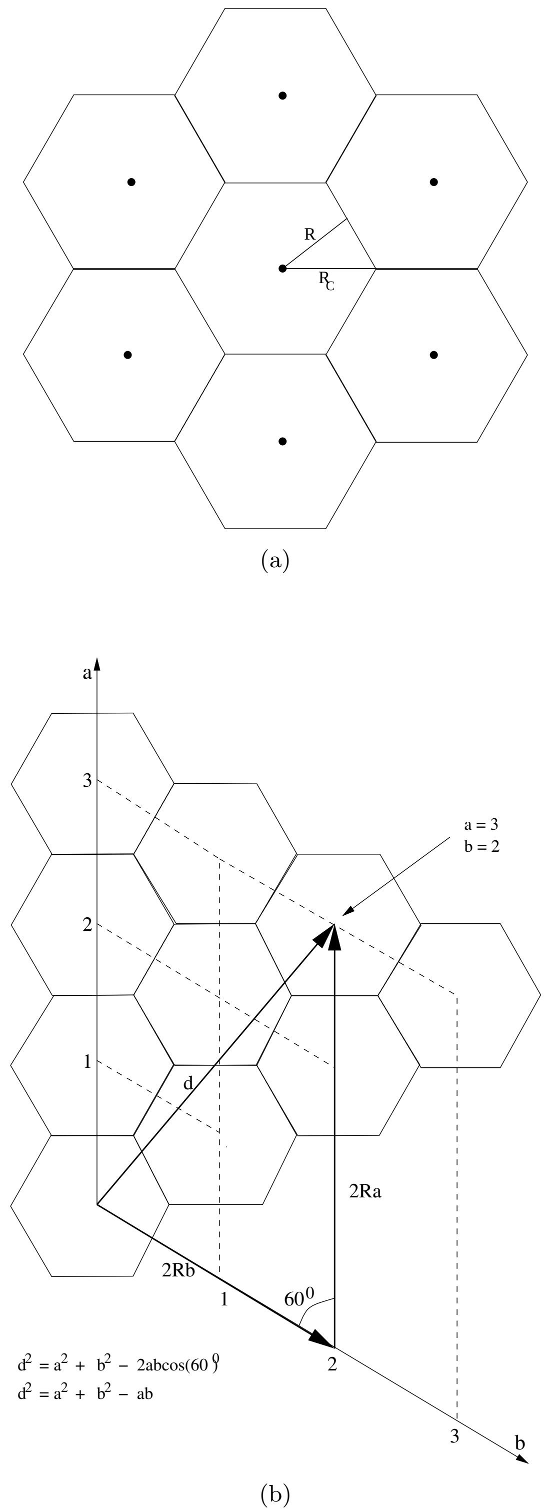

Figure 4.1: 4.1(a) Geometry of the system model for interference evaluation, 4.1(b) Ring cellular coordinate system [1].

Table 4.1: Reverse link intercell interference calculation

a = Ring	b	$d(a,b)/R$	I
1	0	2	$0.2844 \cdot (\upsilon NS)$
2	0	4	$0.2940 \cdot (\upsilon NS)$
	1	$2\sqrt{3}$	$0.3120 \cdot (\upsilon NS)$
3	0	6	$0.3138 \cdot (\upsilon NS)$
	1	$2\sqrt{7}$	$0.3168 \cdot (\upsilon NS)$
	2	$2\sqrt{7}$	$0.3198 \cdot (\upsilon NS)$
$\vdots$	$\vdots$		$\vdots$
100	0	20	.
	$\vdots$	$\vdots$	$\vdots$
	99	$2\sqrt{9901}$	$0.33 \cdot (\upsilon NS)$

$$I = (N\upsilon S) \cdot 6 \sum_{a=1}^{n} \sum_{b=1}^{a} 2 \left[2r^2 \ln \left(\frac{r^2}{r^2 - 1} \right) - \frac{4r^2 - 6r^2 + 1}{2(r^2 - 1)^2} \right]_{r = r_{a,b}} \tag{4.1.3}$$

Using (4.1.2) and (4.1.3), it is possible to evaluate n tiers of interfering cells. According to [1], a 100 tier evaluation shows that only the interference from first tier has a significant effect (Table 4.1).

It shows that the first tier interference is approximately 28.4% of intracell interference and the total interference from 100 tiers is approximately 33% of the intracell interference. Thus the contribution to interference from the second and higher tiers is extremely small compared to that of the first tier.

4.2 Mobile Radio Channel

A mobile radio channel is usually characterised by the superposition of three different, mutually independent, multiplicative and approximately separable components with small, medium and large scale propagation effects. The small scale quasi-stationary variations, mostly referred to as *multipath fading*, are fairly rapid in space. Medium scale effect, mostly referred to shadowing, is influenced by the spatial movements of the order of tens of wavelengths and creates random variation in the average power of the received signal which typically follows a lognormal distribution. In the large scale, spatial movement of the order of hundreds of meters make the median average power level vary in power-law fashion with path length. Large scale variation is mostly referred to as *path loss*. Shadowing creates local variation (narrow area median), while path loss creates long range variation (wide area median).

Local scatterers around the mobile produce several time delayed and attenuated versions of the original transmitted signal. consequently, the received signal comprises a summation of several signals which can add together either constructively or destructively. The resultant field strength in such an environment follows a spatially fluctuating standing wave pattern with minimum and maximum values a quarter wavelength apart. Movement of a mobile station through such a space selective fading field makes the receiver sense a time selective fading signal. The rate of fluctuation depends on the velocity of the mobile and the result is a received signal level which experiences vary large and fast variations. The assumption that different scattered wave components are mutually uncorrelated with random phase leads to the conclusion that the local statistics of the received signal envelope follows a Rayleigh distribution.

As the mobile station moves, changes in the obstacles along the propagation path lead to the gradual changes in local mean signal level. Analysis of mobile radio propagation measurement results from different surveys has shown that the local mean of the signal envelope r is adequately described by a lognormal distribution. That is, the mean $s = 20log_{10}\gamma$ in dB is a Gaussian random variable, with a probability density function given by

$$f(s) = \frac{1}{\sqrt{2\pi}\sigma_s} e^{\frac{-(s-\mu)^2}{2\sigma_s^2}} \tag{4.2.1}$$

where σ_s is the standard deviation of the local mean in dB due to the shadowing of the signal (location variability) and $\mu = \langle s \rangle$ is the average of the received signal local mean level (area average) in dB. Area average reflects the median logarithmic attenuation and can be determined by the path loss.

In the mobile radio environment, due to the fact that the mobile antenna height is close to the ground, the signal received from the base station is affected by three main sources of loss, namely, free space loss, ground wave loss and diffraction loss. The path attenuation depends on many variable, some of which can be controlled (e.g., frequency, antenna height); some can be measured (e.g., distance) and some can neither be controlled nor be measured deterministically (e.g., terrain, topograph of the environment). Considering all these factors, it is apparent that the path loss prediction of mobile radio signal is a formidable task. Although, there is no easy analytical solution to the problem, it is possible to create a propagation prediction model to estimate the median path loss. These ,models vary in complexity, accuracy and capability. Among different methods, Hata's empirical formula based on Okumura's measurements is the most widely used relation that predicts the median propagation path loss in macro-cells [28]. The median path loss, L_p, in decibels between two isotropic base and mobile antennas, with a separation distance denoted by d in kilometer is formulated as:

$$L_p = A + 10\gamma log(d) \tag{4.2.2}$$

where γ is the slope factor and depends on the base station effective antenna height h_b and is weakly affected by the carrier frequency. A good approximation yields $\gamma = 4.49 - 0.655log(h_b)$. The value of A for different frequency and environment settings such as urban area, suburban area, open area can be obtained through Hata and Okumura recommendations [28]. Therefore, in the case a transmitter emits a signal with the power of $P_{tx}[dB]$, the received signal level $P_{rx}[dB]$ due to the path loss will be

$$P_{rx} = P_{tx} - L_P = K_1 - K_2 log(d) \tag{4.2.3}$$

where $K_1 = P_{tx} - A$ and $K_2 = 10\gamma$. Hata's formula does not consider propagation from low base station antenna heights (less than 30 m) or over the short distance (less than 1 Km). Therefore, in a micro-cellular environment, where cell radius is usually below 1 Km and base station antenna height is lowered down the surrounding building at the street lamp elevation, Hata's formula is not valid.

One of the main distinctions between the propagation characteristics of the microcell and macrocell is the existence of a line-of-sight (LOS) wave. The presence of a LOS path in the microcell environment implies that near the base station, the environment features are unlikely to have a prominent influence on the propagation conditions, and the path loss exponent will be very close to that of free space propagation. When the link distance grows beyond a limit, namely a breakpoint distance, environmental factors dominate and the path loss exponent increases, leading to extra attenuation.

A relatively simple semi-empirical propagation model used to calculate path loss is Lonley-Rice model [1]. According to Lonley-Rice model, the path lose is given by,

$$L(dB) = \underbrace{A_{ref}(dB) + L_{fs}(dB)}_{L_{med}} + \sigma(dB) \times G(0,1) \tag{4.2.4}$$

where $G(0,1)$ denotes a zero mean Gaussian random variable (RV) with unit variance, σ is the standard deviation of shadow fading (Fig. 4.2), L_{fs} is the free space propagation loss and A_{ref} is the reference (median) excess attenuation or propagation loss due to terrain. A typical value of σ is between 8 to 10 dB. Equation (4.2.4) can be written as

$$L(dB) = L_{med}(dB) + \sigma(dB)\chi \tag{4.2.5}$$

where χ is a Gaussian random variable of zero mean and unity variance. Then, in absolute number, the propagation loss is the RV L_a, where

$$L_a = 10^{[L_{med}(dB)+\sigma(dB)\chi]/10} \tag{4.2.6}$$

The variation in L_{med} is due to many factors, including the presence or absence of

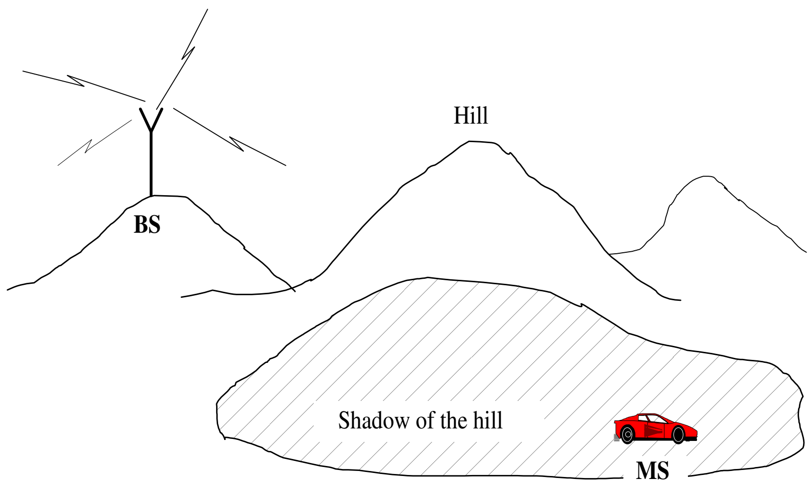

Figure 4.2: Lognormal shadow zone

obstacles in line of sight (LOS) that can cast shadows on the receiver. The term shadowing refers to the fact that a hill or other obstruction can block the radio signal, much like it does for the light from the sun, as depicted in Fig. 4.2

The zero mean, unit variance Gaussian RV X can be between $-\infty$ and ∞; however, over 99% of its variation is within the range $-3 < X < 3$. Thus that over 99% of the variation in the propagation loss is within $\pm 3\sigma$ (dB) or

$$-3\sigma + L_{med} < L < L_{med} + 3\sigma \quad \textit{with probability} \; > 0.99 \tag{4.2.7}$$

In this investigation, the signal propagation in the mobile channel is modeled as a product of two components, one inversely proportional to a power of the distance representing the path loss and the other a random variable with lognormal distribution representing the shadowing losses. The shadowing represents slow variations in signal strength even for

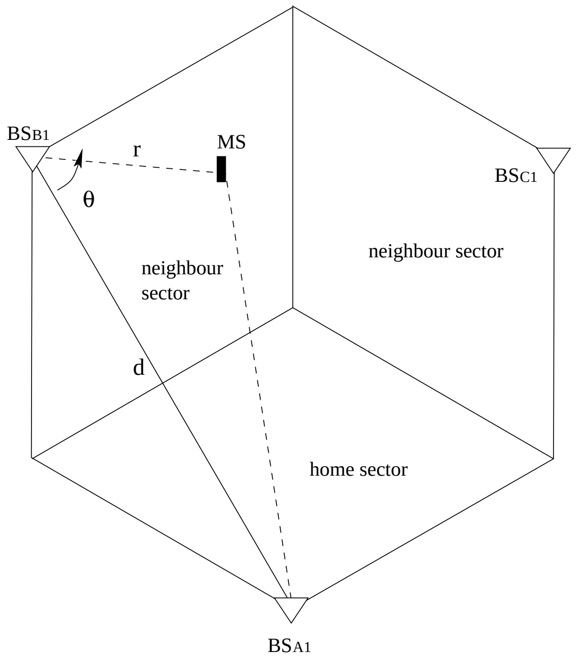

Figure 4.3: Geometry of the home and neighbour sectors.

mobile users. On the other hand, fast fading, which is largely due to multipath propagation, can be assumed to have no effect in the average signal power level [29] and therefore can be ignored. Hence, for a user at a distance r from a Base station (BS) at an angle θ as per Fig. 4.3, the total propagation path loss is a function of r, ζ, and $A(\theta)$, given by

$$PL(r, \zeta, \theta) = r^{-n} \cdot 10^{\zeta/10} \cdot A(\theta) \tag{4.2.8}$$

where ζ is the standard deviation of a gaussian random variable representing the log-normal shadowing process, $A(\theta)$ is the antenna gain in the direction of MS, and n is the propagation path loss exponent which has a typical value of 4.

4.3 Interference due to uneven distribution of user population - Hot Spots

Most interference studies found in the literature are based on uniformly distributed mobile populations over cell and sector coverage area. However, in practice, situations arise where users are congregated in a small area within a cell or a sector. Such areas are called Hot spots (HS) and systems confronted with hot spots require special consideration when dealing with capacity estimation.

In this investigation, the system model considers only the first tier of interfering cells, which means that there are six interfering (neighbouring) cells. Therefore, the geometry of the interference model can be represented as shown in Fig. 4.4. The interference from second and third tiers to the home cell is extremely small [as shown in the previous section] and thus is ignored. In Fig. 4.4 home cell A consists of sector A_1, A_2, and A_3 of which A_1 is the home sector. The hot spot is located in the neighbour sector B_1. A_2 and A_3 are adjacent sectors, and B_1, B_2, B_3, C_1, C_2, and C_3 are neighbour sectors from which the home sector may receive interference. In this investigation the mobility characteristics of users are ignored. Also, the effects of soft handover are ignored. Cells are assumed to be hexagonal in shape and identical in size.

4.3.1 Case of Hot Spots in Macro Cells

The occurrence of HSs in macro cells corresponds to the situation where a large number of users gather in a relatively small area in a cell (or sector). An example of this is a

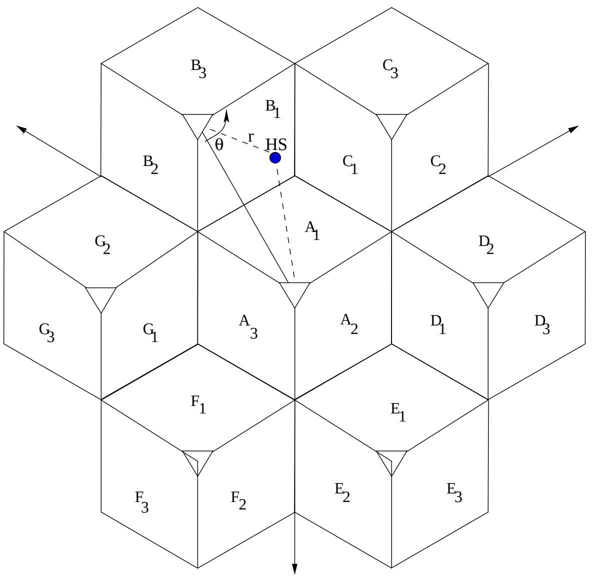

Figure 4.4: Geometry of the system model for interference evaluation. The HS is located in neighbour sector B_1 at (r, θ) where r is the distance to HS from BS of B_1 and θ is the angle measured from the line joining the BSs of B_1 and A_1.

crowd gathering in a sports stadium. Evaluation of the cell (or sector) areas and HS areas (in a macro cell environment) reveals that for most purposes a HS in a macrocell can be considered (geometrically) as a single point in a cell (or sector), (Fig. 4.5(a)). Fig. 4.5(b) shows the dimensional significance of hot spot in a macro and micro cell. It can be seen (Fig. 4.5(b)) that when the HS dimension is of the order of a tenth or less of the dimension of the sector, the area occupied by the HS is negligibly small in comparison to the sector area. Thus the interference arising from a HS in a macrocell consisting of M users could be considered as M times the interference due to one user, in the same location.

Let $I(r, \theta)$ be the interference power received at home cell (sector) BS due to a user at location (r, θ) in the neighbour cell (sector), where r is the distance of interfering MS from

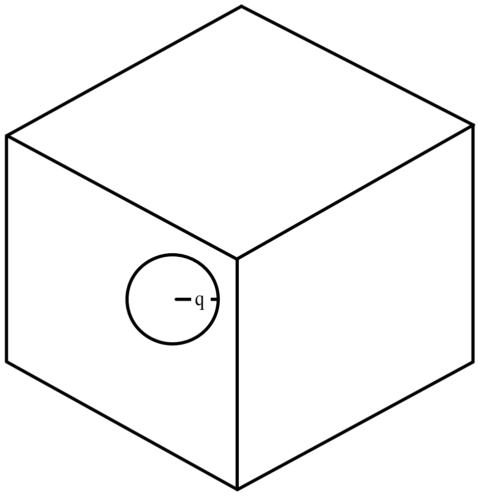

(a)

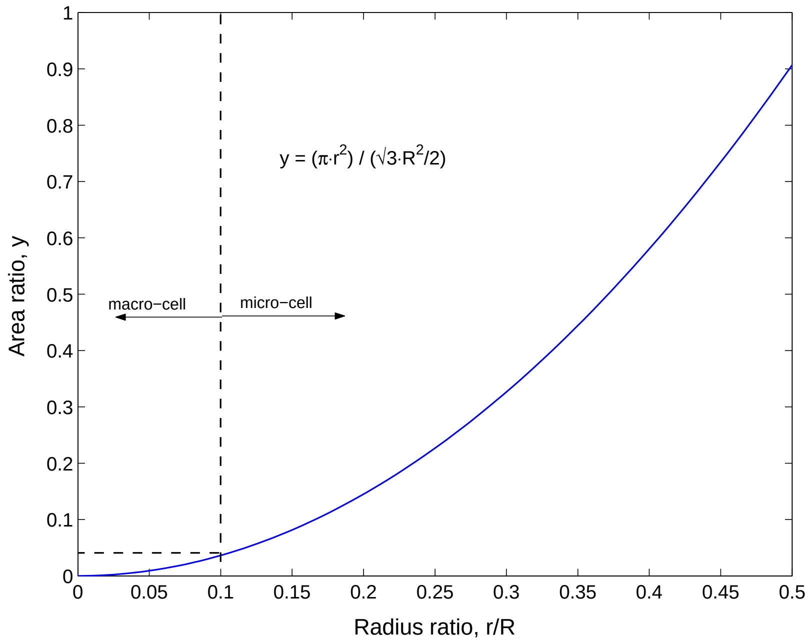

(b)

Figure 4.5: 4.5(a) Hot spot formation in macrocells. q = HS radius, R = cell radius, 4.5(b) Dimensional significance of HS in micro and macro cells. $y = \frac{\pi r^2}{\frac{\sqrt{3}}{2} R^2}$.

its BS and θ is its direction from the line joining the BSs at home and neighbour sectors (Fig. 4.4). Then the total interference due to the presence of a HS of M users at location (r, θ) in the neighbour cell is $M \cdot [I(r, \theta)]$. If N is the number of users in the home cell (sector), and S is the signal power received at every BS, the S/I at the home cell (sector) BS is given by,

$$\begin{aligned} \left(\frac{S}{I}\right) &= \left(\frac{S}{(N-1) \cdot S + I(r,\theta) \cdot M}\right) \\ &= \left(\frac{1}{(N-1) + \frac{M}{S} \cdot I(r,\theta)}\right) \end{aligned} \tag{4.3.1}$$

Using (4.3.1), system capacity could be estimated in terms of number of users that can be accommodated in the home sector, N, in relation to a HS with a given user concentration, M, in a neighbour sector at a given location, (r, θ), for an acceptable (S/I) at the home sector BS. In the present study, the acceptable (S/I) is taken as -13.6 dB [15].

Profile of $I(r, \theta)$

For the purpose of determining the profile of $I(r, \theta)$ we can ignore the effects of shadowing and consider the interference power received by the home sector A_1 base station, due to the presence of a mobile station in the neighbour sector, B_1 (Fig. 4.4). The three dimensional view of the profile of $I(r, \theta)$ shown in Fig. 4.6 exhibits the strong non-linearity of $I(r, \theta)$ associated with its parameters r and θ. It is to be emphasized that r is the distance of the interfering MS from its own BS and not from the home sector BS. Similarly, θ is the direction of the interfering MS measured from the BS of the interfering MS, and not from

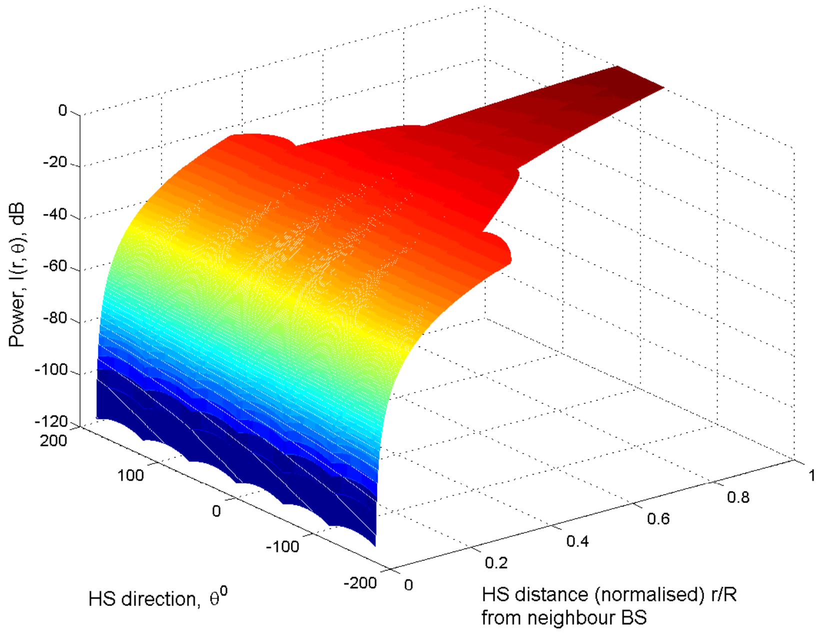

Figure 4.6: Interfering signal strength at home sector A_1 due to a user in neighbour cell B (in terms of the signal power received at home sector BS due to a MS in home sector) (Please refer to Fig. 4.4).

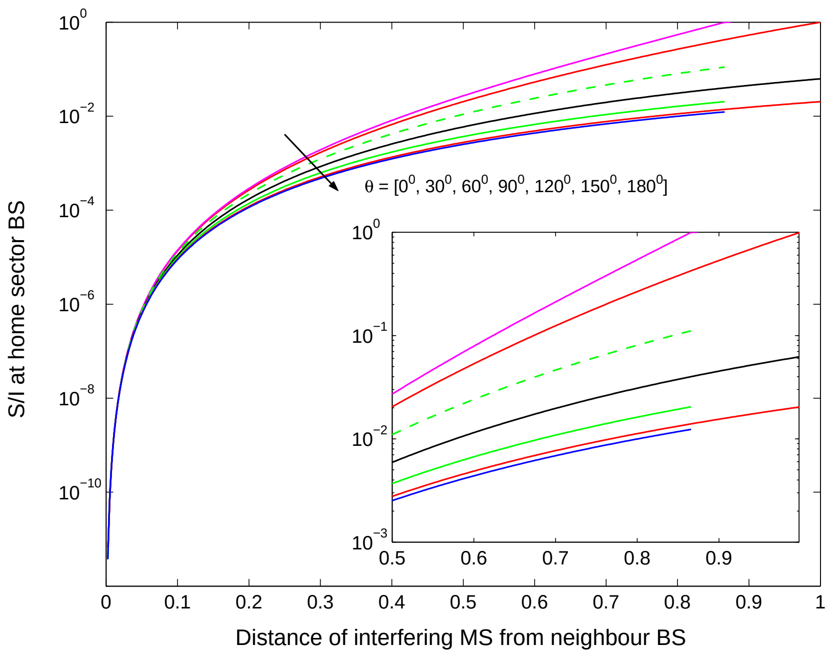

Figure 4.7: S/I ratio at home sector BS (A_1) due to a MS in neighbour cell (B). (Only one MS in home sector)

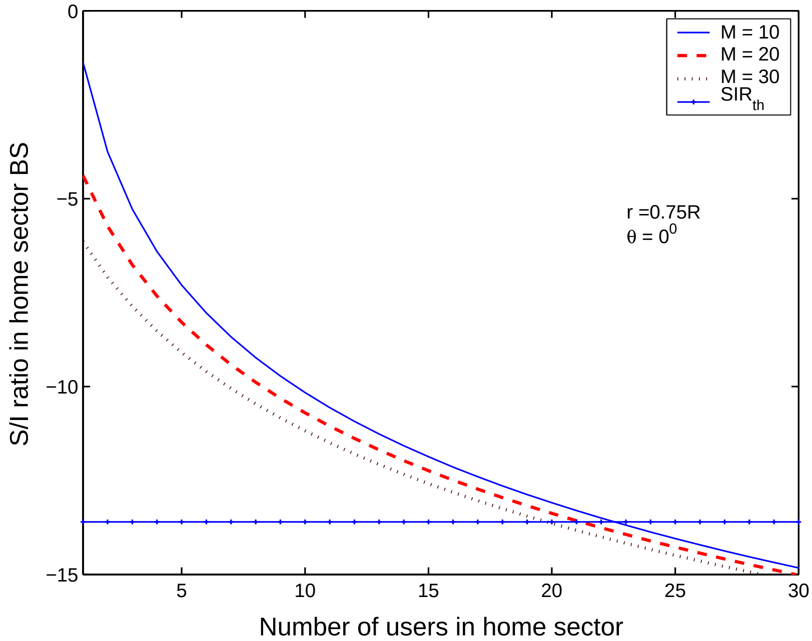

Figure 4.8: S/I ratio at home sector BS against the number of users in home sector, with different hot spot concentrations. (Hot spot location r = 0.75R, $\theta = 0^0$)

the BS of the home sector. Fig. 4.7 highlights these results and shows that the location of the MS is significant in estimating its interference power. When the MS distance from the neighbour BS is approximately 0.2 of cell radius or less, the interfering power at the home sector BS is about 40 dB or more below the received signal power at the BS irrespective of which direction the MS is located. On the other hand, when the distance of the MS (from the neighbour BS) is greater than 0.4 (of the cell radius) the interfering power is dependent on the direction of the MS location, and its variation could be as much as 20 dB. (Note that when the distance of the MS from the neighbour BS gets larger, it gets closer to the home sector BS and hence interference gets bigger.)

Fig. 4.8 to Fig. 4.10 show the S/I at the home sector BS as evaluated per (4.3.1) against the number of users in the home sector. Shown also (in Fig. 4.8 to Fig. 4.10) is the

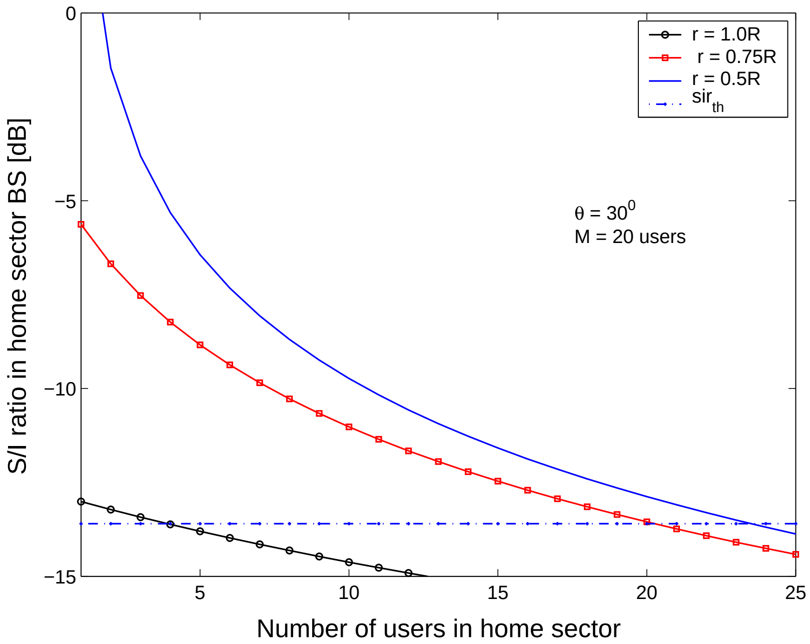

Figure 4.9: S/I ratio at home sector BS against the number of users in home sector, with different hot spot locations ($\theta = 30^0$ and $M = 20$ users)

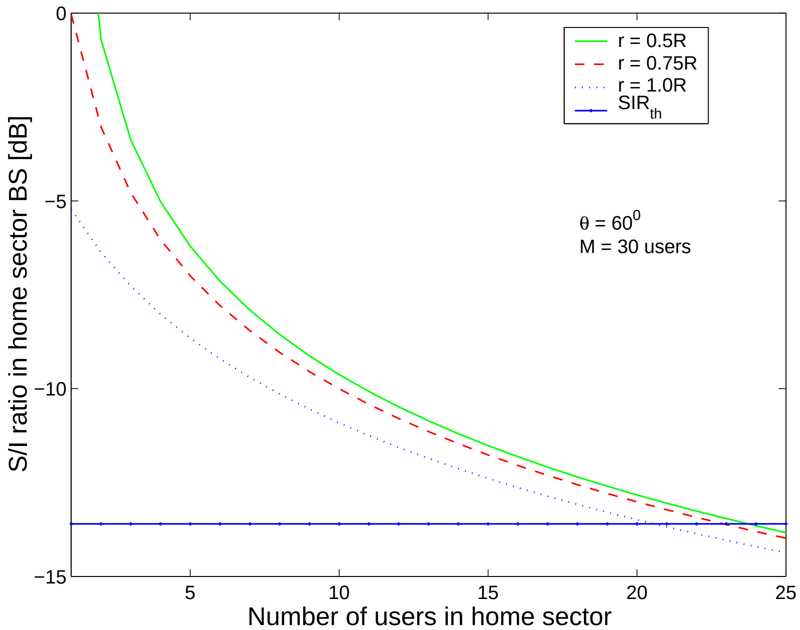

Figure 4.10: S/I ratio at home sector BS against the number of users in home sector, with different hot spot locations ($\theta = 60^0$ and $M = 30$ users)

threshold S/I required for satisfactory operation [15]. It can be observed (Fig. 4.8) that as the neighbour sector hot spot intensity rises from 10 to 30 the home sector capacity falls from 23 to 19. Fig. 4.10 shows the effect of movement of hot spot in the neighbour sector. As the hot spot (in this case consisting of 30 users) move from the sector boundary to halfway towards the neighbour sector BS, the home sector capacity increases from 20 users to 24 users. In this case the direction of the hot spot movement is kept at an angle of 60^0 from the line joining the sector BSs.

Influence of Shadowing

To obtain a more realistic picture of the HS phenomenon we can incorporate lognormal shadowing into (4.3.1). Then the S/I at the home cell (sector) BS is given by,

$$\left(\frac{S}{I}\right)_{shad} = \left(\frac{1}{(N-1) + \frac{M}{S} \cdot I(r,\theta) \cdot 10^{\zeta/10}}\right) \tag{4.3.2}$$

where ζ is the standard deviation of a gaussian random variable representing the log-normal shadowing process. Fig. 4.11 shows the results corresponding to the case of Fig. 4.6 but obtained with a simulation which incorporates shadowing process. The amount of shadowing is taken as 8 dB. It shows that at moderate shadowing the predictable interference profile is not significantly affected.

Fig. 4.12 to Fig. 4.15 show the S/I at the home sector BS as evaluated against the number of users in the home sector with different locations and concentrations of hot spot, obtained by simulation (4.3.2). The amount of shadowing was kept at 8 dB. Fig. 4.12 shows that the movement of HS in the direction $\theta = 0^0$ causes a significant variation in the home

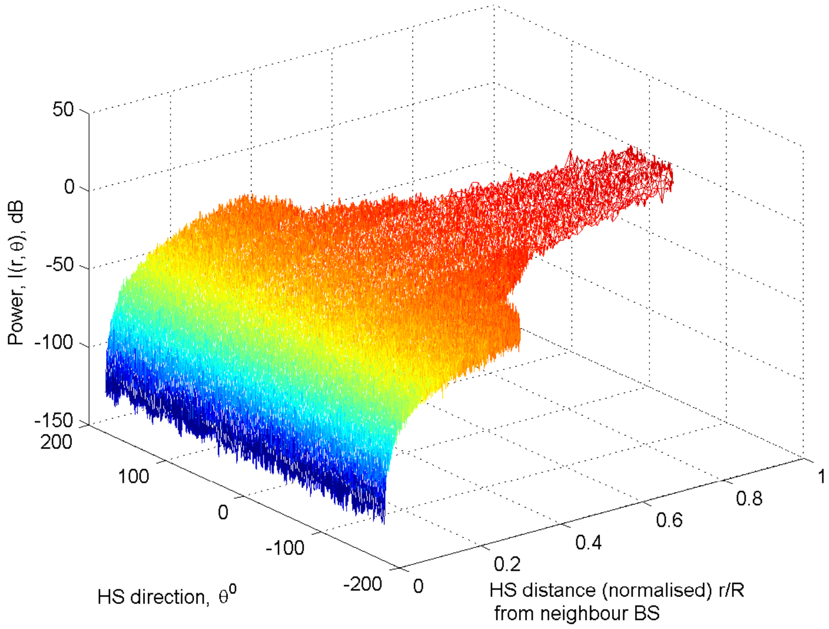

Figure 4.11: Interfering signal strength at home sector A_1 due to a user in neighbour cell B_1 (in terms of the signal power received at home sector BS due to a MS in home sector), standard deviation of shadowing fading = 8 dB (1000 averaging) (Please refer to Fig. 4.4).

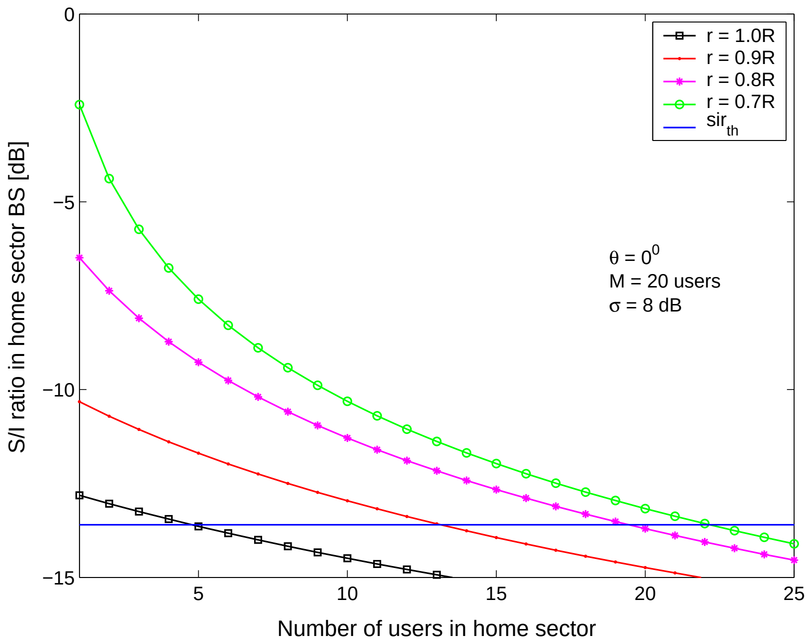

Figure 4.12: S/I ratio at home sector BS against the number of users in home sector, at different hot spot locations. Shadowing = 8 dB.

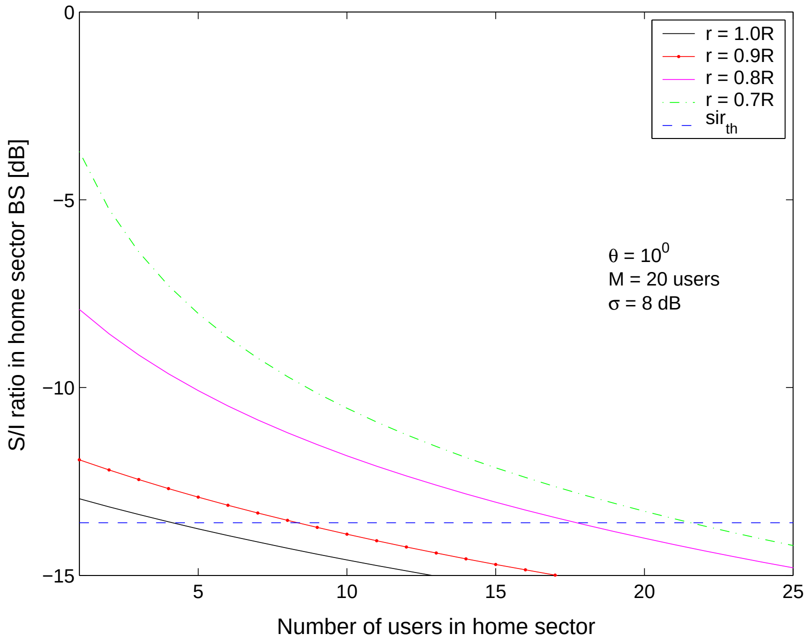

Figure 4.13: S/I ratio at home sector BS against the number of users in home sector, at different hot spot locations. Shadowing = 8 dB.

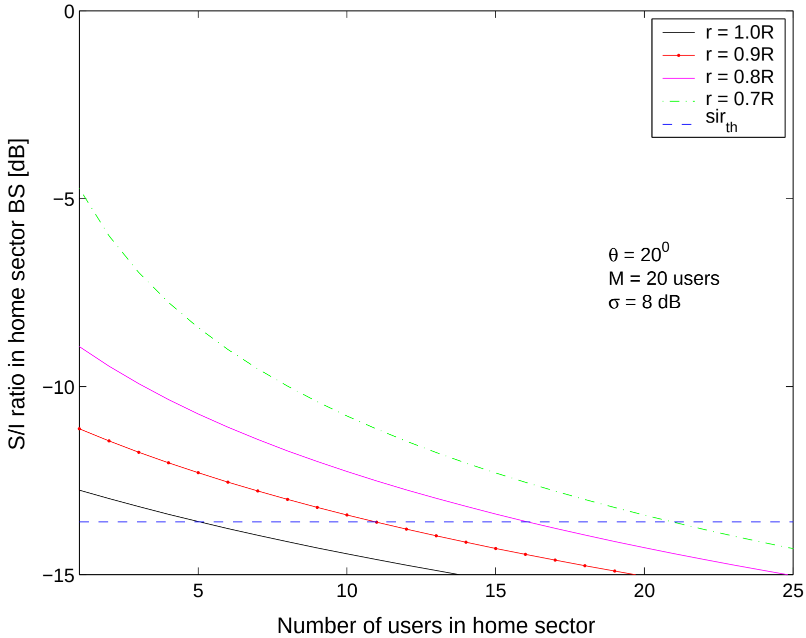

Figure 4.14: S/I ratio at home sector BS against the number of users in home sector, at different hot spot locations. Shadowing = 8 dB.

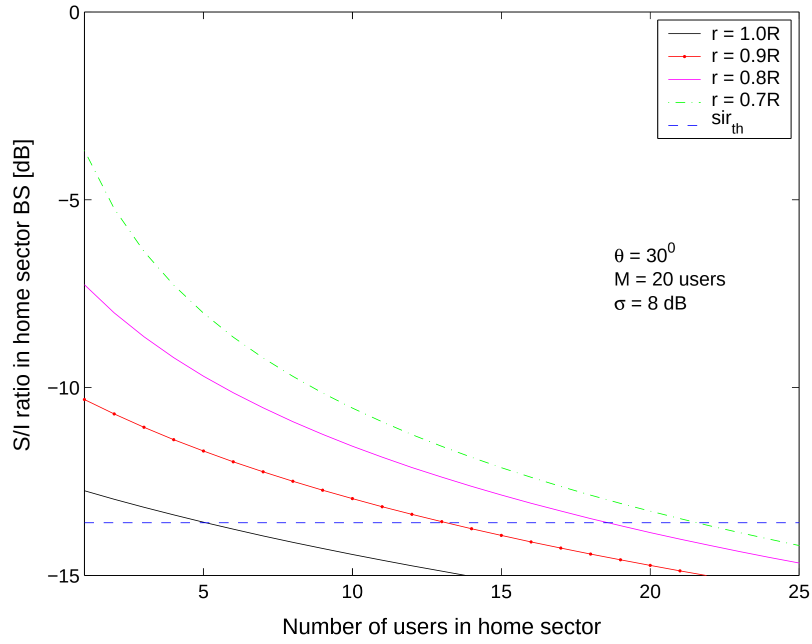

Figure 4.15: S/I ratio at home sector BS against the number of users in home sector, at different hot spot locations. Shadowing = 8 dB.

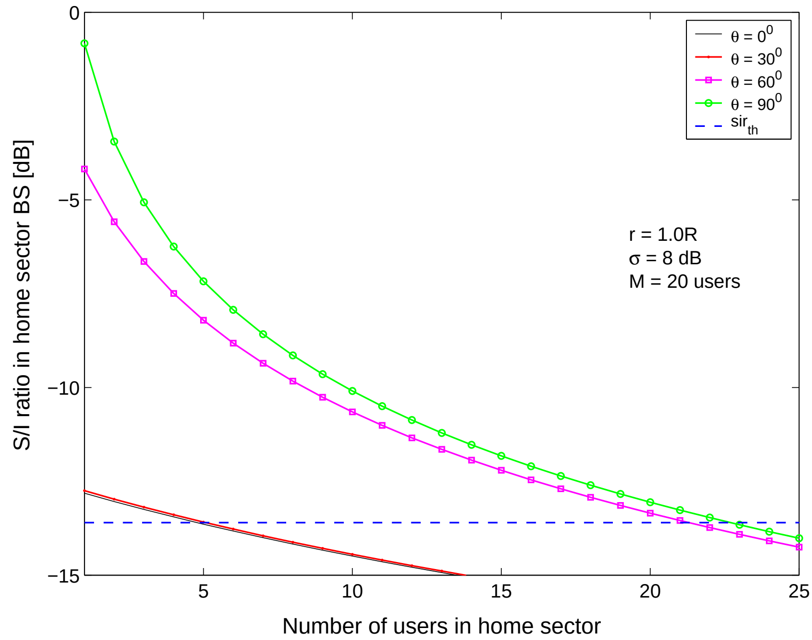

Figure 4.16: S/I ratio at home sector BS against the number of users in home sector, at different hot spot locations along the sector boundary. Shadowing = 8 dB.

sector capacity, when the (normalized) distance of HS is in the range 0.9 to 1.0 (i.e., close to the home sector boundary). At $\theta = 10^0$ (Fig. 4.13), and $\theta = 30^0$ (Fig. 4.15), this influential region shifts to be in the range 0.8 to 0.9 and 0.7 to 1.0 respectively of the (normalized) distance to HS.

Fig. 4.16 shows the S/I at the home sector BS as evaluated against the number of users in the home sector when the hot spot concentration is 20 users and the hot spot is on the neighbour sector boundary. The extent of shadowing is kept at 8 dB. The results show that the hot spot has a significant effect on the home sector capacity only when the direction of HS is at $\pm 30^0$ and its (normalized) distance is greater than 0.9.

4.4 Conclusions

The influence of non-uniform traffic distribution (hot spots) on the capacity of a CDMA cellular system was studied in this chapter. A macro cell environment was considered using a one-tier multi-cell model. Both slow frequency shadowing and free space path loss were incorporated in the propagation model. The simulation results indicate that the location of the hot spot is a significant factor in determining the system capacity. The use of adaptive sectorisation to improve the system capacity under hot spot conditions is to be examined in chapter 5.

Chapter 5

Capacity Improvement in Non-uniform Traffic Environment Using Adaptive Sectorisation

This Chapter discusses the application of adaptive sectorisation in the capacity enhancement of a CDMA cellular system dealing with non-uniform traffic. It considers the particular case where the traffic distribution consists of isolated areas of congested traffic called Hot Spots (HS). It is envisaged that the traffic density inside a HS is many times more than that outside the HS. A more even traffic distribution among sectors is attempted by re-adjustment of sector boundaries using finite antenna beam switching. System capacity is estimated on the basis of tolerable interference in a sector taking both intrasector and intersector interference into account in a multicell environment. Interference is evaluated under the assumption of perfect power control in the uplink. Normal propagation environment is assumed in the cell that allows path losses and shadowing losses in the mobile radio signal. Variation in the antenna gain is also accommodated by taking appropriate radiation pattern into account. It is shown that successive sector size adjustment with increasing HS traffic intensity can deter call blocking in the HS sector. It is also shown that a significant improvement in system capacity could be obtained with adaptive sectorisation particularly when the HS user density is several orders of magnitude higher than that outside the HS.

5.1 Adaptive Sectorisation

5.1.1 Sector Size Variation

Consider a hot spot in the home sector (BS_{A1}), Fig 5.1(a). It is assumed that the hot spot is confined to a strip of dimension $L \times W$ (Fig. 5.1(b)) where W is the width of HS and L is its length. Table 5.1 gives the relative magnitude of the hot spot area in relation to 120^0 sector area. The table shows that for the hot spot dimensions indicated, the area covered by the hot spot is 10% or more of the normal 120^0 sector area. This is a microcell situation and therefore the actual location of the mobile station within the hot spot has to be considered in the estimation of intercell interference.

Table 5.1: Relative magnitude of Hot Spot area in a 120^0 sector.

L	W	$\%\ Area\ \ of\ HS\ = \frac{HS\ area}{120^0\ sector\ area}$
$0.3R$	$0.35R$	10%
$0.3R$	$0.52R$	15%
$0.3R$	$0.70R$	20%
$0.3R$	$0.87R$	25%
$0.3R$	$1.05R$	30%

We consider a BS antenna structure that produces twelve fixed 30^0 beams per cell

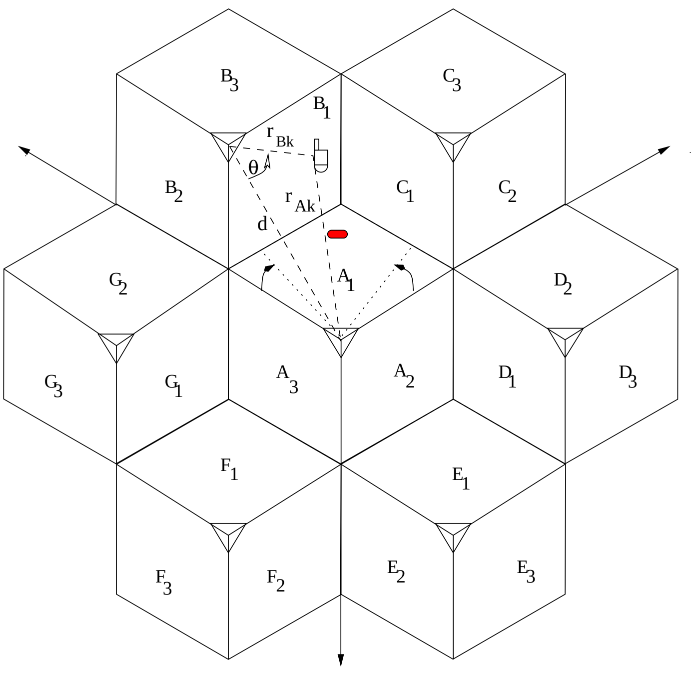

(a)

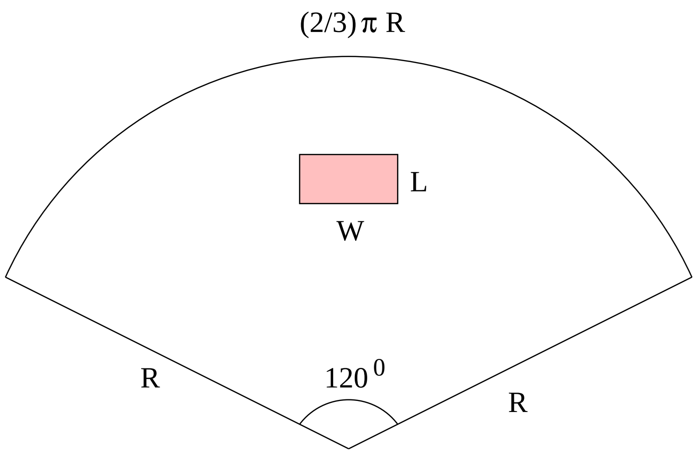

(b)

Figure 5.1: 5.1(a) Geometry of the system model for interference evaluation, 5.1(b) Dimensioning of Hot Spot. For example $W = 0.35R$ and $L = 0.3R$ where R is cell radius in both cases.

(Fig. 5.2(a)). These beams can be combined to obtain 3 fixed beams which would substitute for the beams provided by the normal 120^0 directional antennas. Next, keeping the number of sectors fixed at 3 per cell, we may adaptively change the sector size by combining appropriate number of narrow (30^0) beams (Fig. 5.2). This adaptive sectorisation allows sector beamwidths to be approximately 30, 60, 90, 120, 150, 180, or 210 degrees. Switched beams can adjust the sector size to include a hot spot either fully or partially. Using adaptive beam switching, operators can shift the traffic from a heavily loaded HS sector to sectors that are underutilized.

5.1.2 Capacity Estimation with Adaptive Sectors

In this investigation of CDMA system capacity, the number of users the system can support is evaluated using a computer simulation according to (3.3.1) and (3.3.2). The simulation software was written in MATLAB employing random number generators to represent call arrivals and MS locations. The simulation is based on the system parameters shown in Table 5.2.

Table 5.2: Simulation parameters

Data rate, R_b	9.6 kbps
Chip rate, W	1.2288 Mcps
Required E_b/N_0	7.4 dB
Standard deviation of shadow fading, δ	8 dB
Cell radius R	unity
Reverse link SIR_{th}	-13.6dB
Number of sectors Z	3

Consider a HS in the home sector (BS_{A1}), Fig. 5.1(b). As mentioned above, the HSS

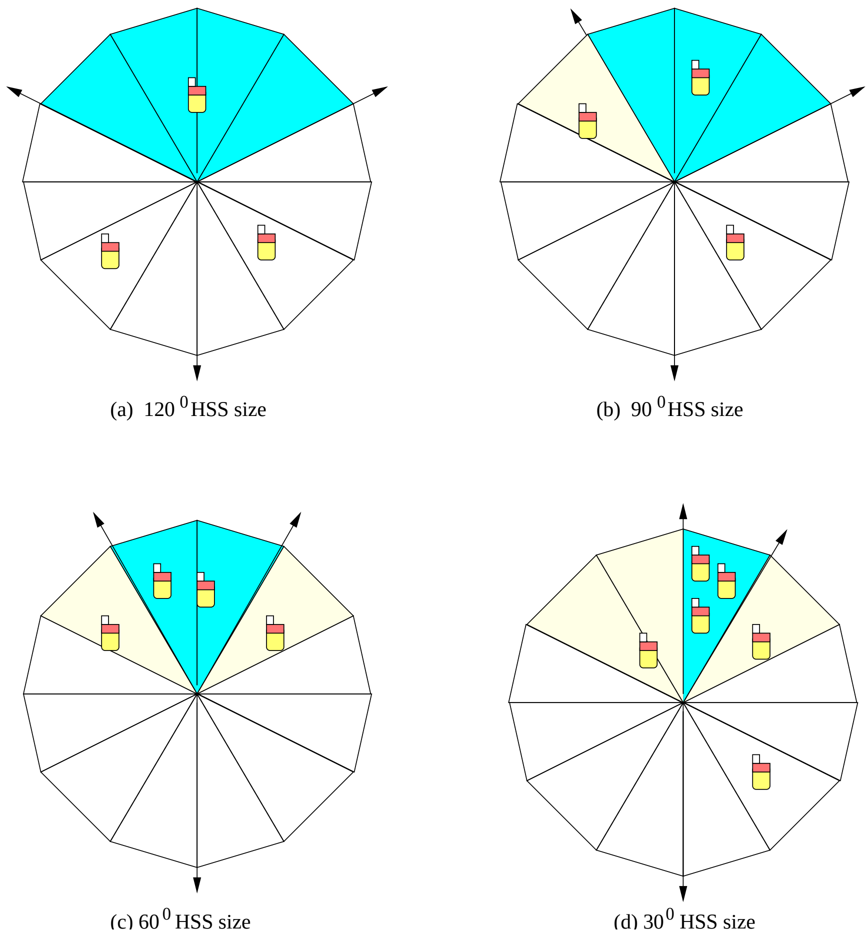

Figure 5.2: Adaptive sectorisation using switched beams, (a) before adaptation and (b, c and d) after adaptation. (HSS = Hot Spot Sector)

can vary from 120^0 to 30^0. In this investigation, we consider two cases, (i) hot spot area (HSA) completely inside the HSS and (ii) HSA extends beyond the HSS. The cell radii in all scenarios are normalized to unity. The conventional hexagonal cell pattern is assumed. Perfect power control in the uplink is also assumed so that the received power at the sector's BS from all mobiles within the sector is the same.

A uniformly distributed mobile population is generated with random locations within the home and the six neighbour sectors. This is done by generating two sets of random numbers that assign an angular position and a radial distance to each mobile. The radial position is the distance of the MS from the home BS. The individual path losses (coupled with the shadowing effect) are calculated for each MS in order to evaluate the SIR at the sector BS.

The system capacity is evaluated in terms of possible number of users in each sector when at most 1% new call blocking is experienced in any of the sectors. The cell capacity is the sum of three sector capacities.

The simulation starts with empty system (no users any where) and proceeds by adding users progressively, one user at a time, positioning each user at a randomly selected location in each sector and in HS region. Every time a user is added (anywhere in the system) the SIR at the BSs of all sectors are evaluated to see that with the added user the system blocking probability does not exceed the stipulated value. When the blocking probability does exceed the stipulated value the simulation terminates and the number of users in each sector is noted. The sector causing the simulation to terminate is also noted.

5.1.3 Case of Perfect Antenna

The case of a perfect antenna serves as a reference to examine the system under ideal conditions and to compare it with the practical case. The sector coverage in this case (with perfect antenna) is assumed to be uniform over the entire sector and there is no spillover of main lobe or occurrence of sidelobes in the radiation pattern.

Case of HS with $W = 0.35R$

Fig. 5.3(a) shows the number of users that can be accommodated in respective sectors when the overall system blocking probability is 1%. As mentioned earlier, in Fig. 5.1(a), A_1 is the HSS, A_2 and A_3 are the adjacent sectors, and B_1, B_2, B_3, C_1, C_2, C_3 are the neighbour sectors. In the absence of HSs there is uniform traffic in all sectors (HS to non-HS user density ratio is 1) and the system offers a traffic capacity of 34 users/sector. This serves as the reference. The results (Fig. 5.3(a)) indicate that when all sectors are of the same size (i.e. $A_1 = 120^0$), the possible number of users in hot spot sector A_1 increases with increasing user density in HS while the possible number of users in adjacent (A_2 or A_3) and neighbour ($B_1, C_1, ..$) sectors decreases with increasing user density in HS. Simulation shows that in this situation blocking always occurs first in A_1. This is in contrast to the situation when A_1 is 60^0 or 30^0. In these cases blocking first occurs in the adjacent sectors (A_2 or A_3) and then moves to A_1 as the HS to non-HS user density ratio reaches 5 and 10, respectively. Fig. 5.3(b) shows the change over of blocking sector as the HS to non-HS user density ratio increases from 1, in the three cases of sector sizes 120^0, 60^0, and 30^0. The system capacity (per cell) can be obtained as a function of HS

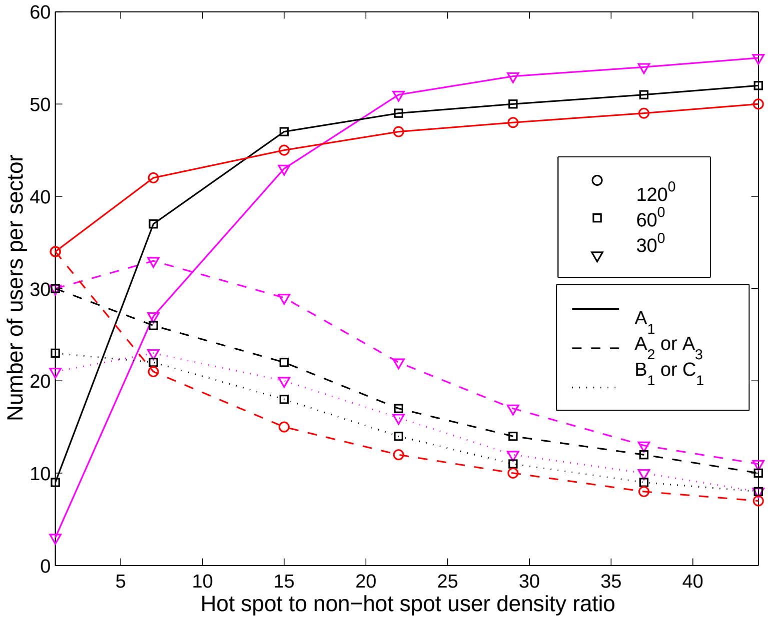

(a)

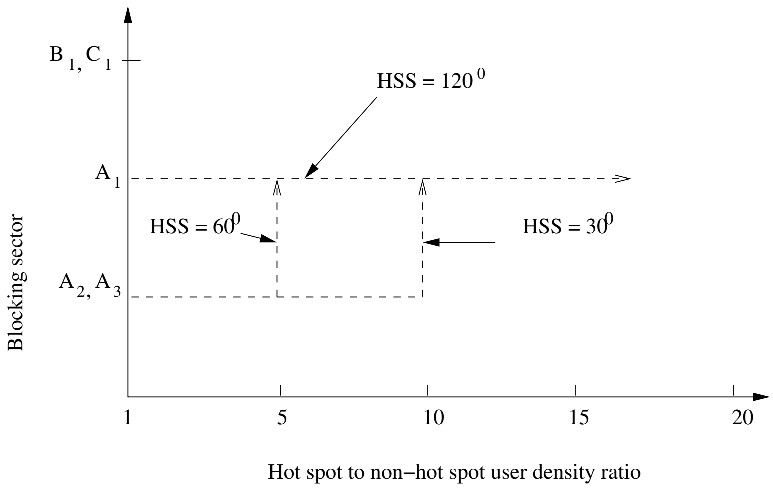

(b)

Figure 5.3: 5.3(a) Sector capacity versus hot-spot to non-hot spot user density ratio (Case I, $W = 0.35R$) (Case of perfect antenna), 5.3(b) The change over of blocking sector between HSS (A_1) and adjacent sectors (A_2 and A_3) (case I, $W = 0.35R$) (Case of perfect antenna).

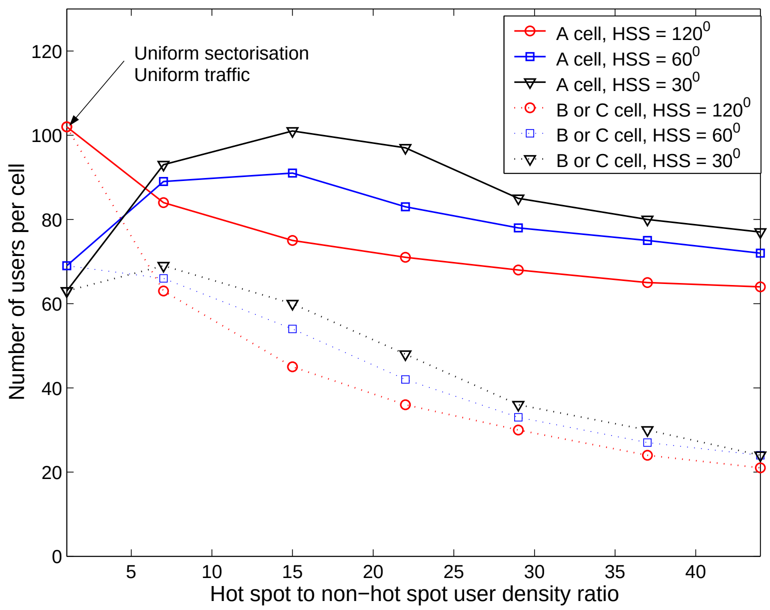

Figure 5.4: Cell capacity (of home cell A and neighbour cells B and C) versus hot spot to non-hot spot user density ratio at different HSS sizes. (120^0, 60^0, and 30^0). $W = 0.35R$ (Case of perfect antenna).

to non-HS user density ratio by summing up the number of users in each sector. Fig. 5.4 illustrates this situation and shows the cell capacity (both in home cell A and neighbour cells B and C)as a function of HS to non-HS user density ratio. As could be expected the cell capacity (in home cell as well as in neighbour cells) fall with increasing user density, in the case of nominal 120^0 sector cells. However, when the HSS size is changed to 60^0 (or 30^0) there is a relative increase in capacity in the home cell as well as in neighbour cells. It can be seen that there is an overall capacity improvement in the case of 60^0 and 30^0 HSS sizes over the nominal 120^0 sector size and that this improvement starts at a user density ratio of about 5.

Case of HS with $W = 1.05R$

Fig. 5.5 shows the system capacity in terms of number of users per sector paying attention to home, adjacent, and neighbour sectors. It can be seen that the home sector capacity increases with increasing user density ratio in all cases (i.e., HSS sizes of 120^0, 60^0, and 30^0). However, it is clear that HSS size of 60^0 outperforms the other two indicating that the control of HSS size has to be judiciously done. It is also clear that when the HSS size is 30^0, the capacity in adjacent sectors is virtually uneffected by the changes in user density ratio. At other HSS sizes however, both the adjacent and the neighbour sector capacities gradually fall with the increasing hot spot to non-hot spot user density ratio. For the case of HS with $W = 1.05R$, the blocking first occurs in the adjacent sectors and then moves to HSS when the HS to non-HS user density ratio reaches about 2 and 4, when HSS size is 60^0 and 30^0, respectively. Fig. 5.6 presents the blocking sector for this case. The results of Fig. 5.7 shows the case corresponding to Fig. 5.4 when the HS width $W = 1.05R$. The overall capacity improvement in this case starts to occur at a user density ratio of about 2 and stays steady particularly when HSS size is 30^0.

5.2 Practical Realization of Adaptive Sectorisation

5.2.1 Sector Size Variation by Finite Beam Switching

Fig. 5.8 shows the radiation pattern of a typical 120^0 commercial available (RFS Ltd.) [30] antenna element. Fig. 5.9 shows the radiation pattern of an antenna array consisting of 4 elements, corresponding to main beam directions -45^0, -15^0, 15^0 and 45^0. Fig. 5.10

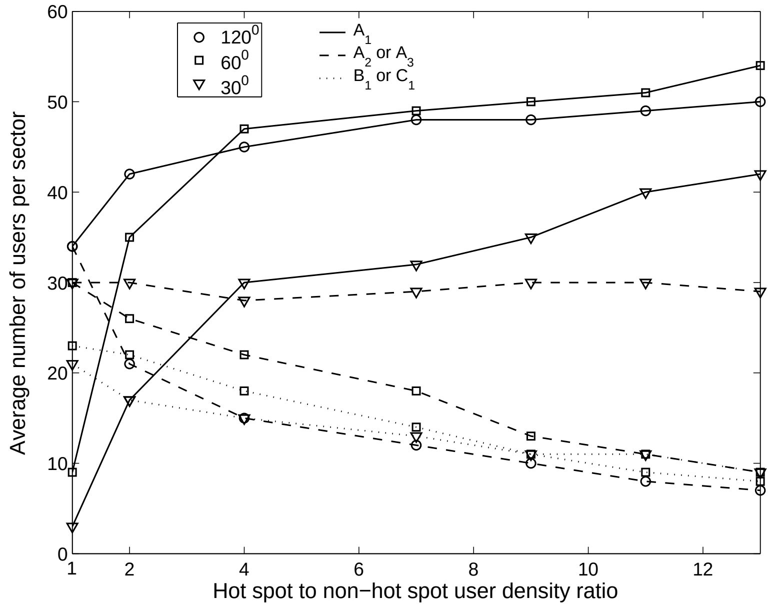

Figure 5.5: Sector capacity versus hot spot to non-HS user density ratio for different HSS sizes. (Case II, $W = 1.05R$). (Case of perfect antenna)

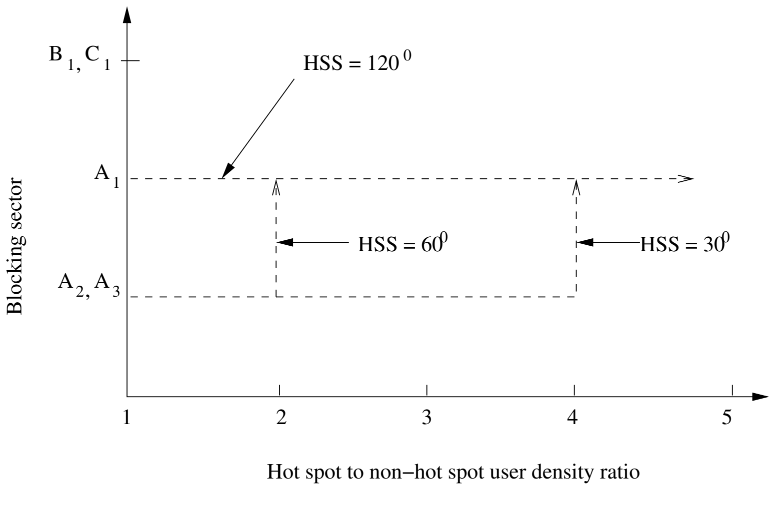

Figure 5.6: The change over of blocking sector between HSS (A_1), and adjacent sectors (A_2, A_3) (case II, $W = 1.05R$) (case of perfect antenna)

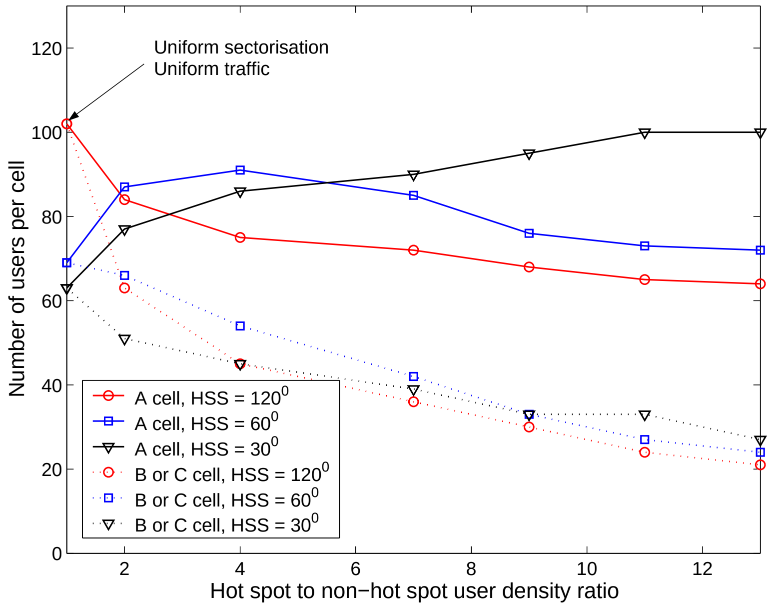

Figure 5.7: Cell capacity versus hot spot to non-HS user density ratio at different HSS sizes. $W = 1.05R$ (Case of perfect antenna)

shows the resultant antenna patterns obtained by pattern multiplication (Appendix C). Each element of the antenna array is an RFS dipole and the array spacing is $d = \lambda/2$. The phase of the feed current is controlled to obtain the desired radiation pattern. It can be seen that the main beam can be steered to cover a desired part of a sector.

5.2.2 Case of Practical Antenna Array

We assume that the radiation pattern of the practical antenna array can be represented by a theoretical model given by the parabolic function [31] (Fig. 5.11)

$$G_{th}(\theta) = \begin{cases} 1 - \dfrac{(1-b)}{(\pi/2)^2}\theta^2, & |\theta| \leq \sqrt{\dfrac{1-a}{1-b}}\dfrac{\pi}{3} \\ a; & \text{elsewhere} \end{cases} \tag{5.2.1}$$

where b represents the antenna gain level (normalized to the maximum gain) at $\pi/3$ sector

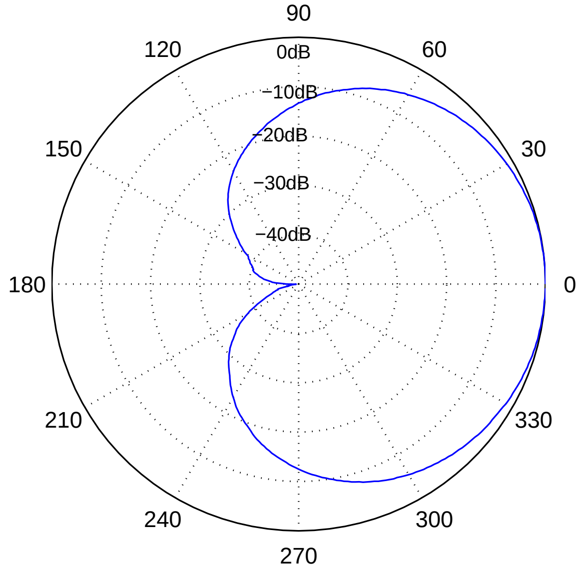

Figure 5.8: RFS (Radio Frequency Services) antenna element radiation pattern [30].

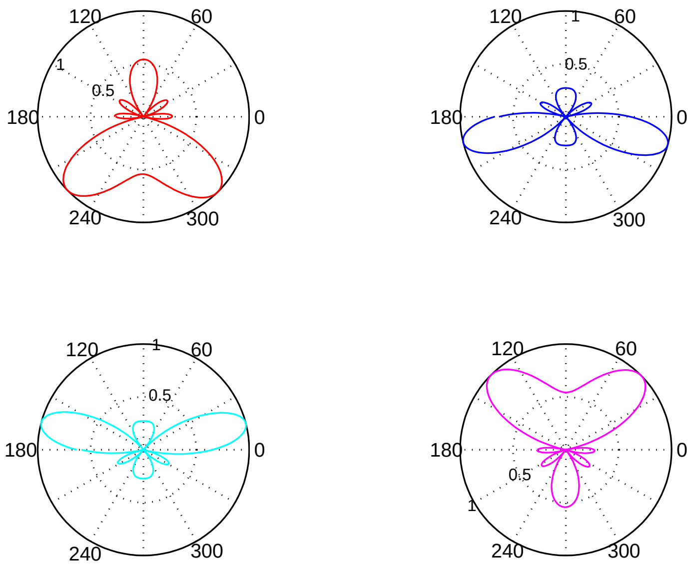

Figure 5.9: Array factor (clock wise from top left for $\theta_s = -45^0, -15^0, 15^0$ and 45^0)

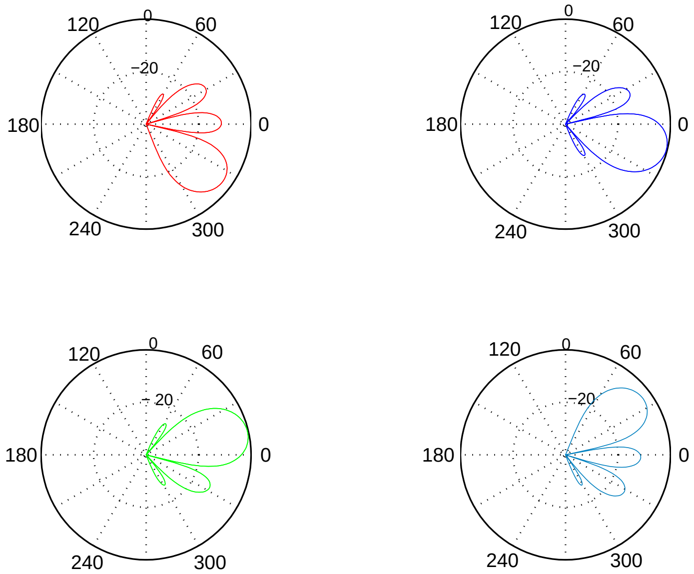

Figure 5.10: Resultant radiation pattern of practical array of 4 elements (clock wise from top left for $\theta_s = -45^0, -15^0, 15^0$, and 45^0)

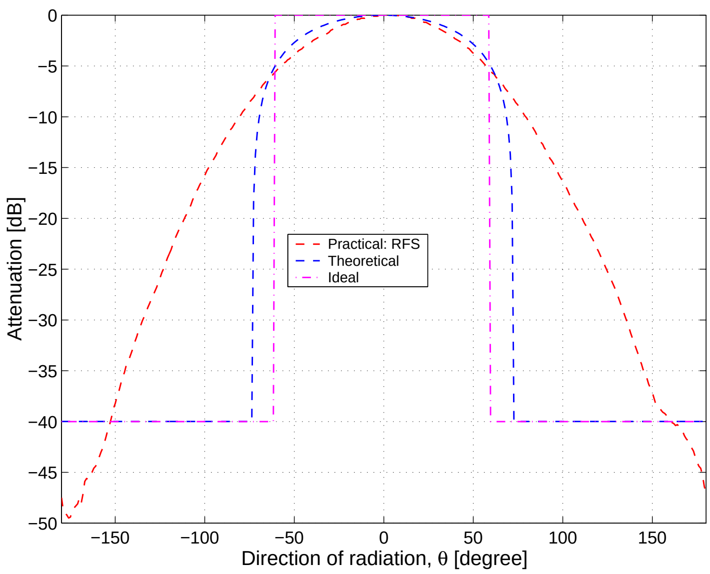

Figure 5.11: Radiation patterns for ideal, theoretical, and practical cases.

crossover from the maximum gain direction and a represents the average normalized gain level for the sidelobe. The values chosen (in the simulation) for a and b in (5.2.1) are -40 dB and -5 dB, respectively. Fig. 5.11 shows the comparison of antenna patterns for ideal, theoretical, and practical (RFS) cases.

5.2.3 Capacity Estimation with Practical Antenna

In this case the overall gain factor of the antenna array is taken into account (according to 5.2.1) in the direction of the MS location. Due account is also made of the fact that some sidelobes are present in the radiation pattern. Following a procedure similar to that of section 5.1.2, the system capacity is evaluated using a computer simulation. Once again the threshold measure of performance is taken as the system capacity at 1% blocking.

Case of HS with $W = 0.35R$

The blocking sector change over behaviour in this case is similar to the case of perfect antenna (Fig. 5.3(b)). The blocking always occur in A_1 when HSS size is 120^0. When HSS size is 60^0 and 30^0 the blocking first occurs in A_2, A_3 and then moves to A_1 when the user density ratio reaches about 5 and 7, respectively. Fig. 5.12 shows the cell capacity for the case of practical antenna. It can be seen that there is an overall improvement in system capacity with adaptive sectorisation although the improvement is not as much as in the case of perfect antenna.

When there is uniform traffic in every cell (user density ratio is 1) the system offers a traffic capacity of 32 users/sector, which is taken as the reference. The results indicate

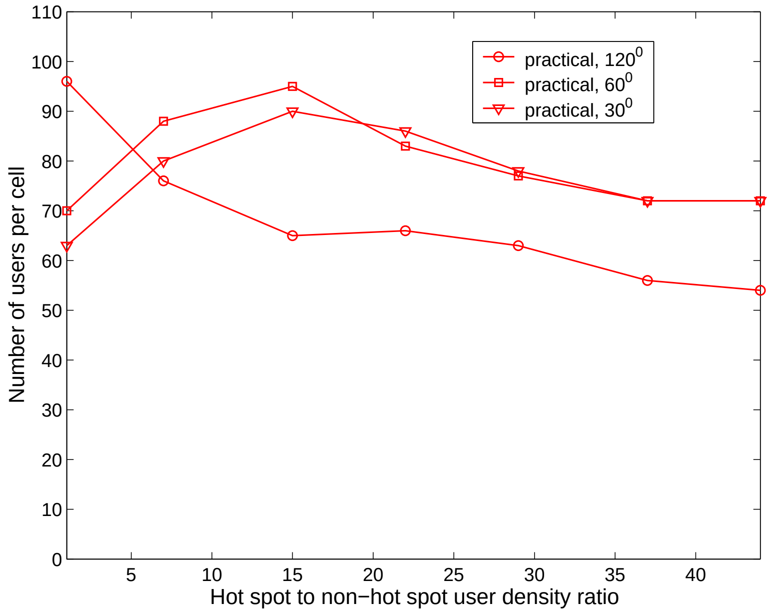

Figure 5.12: Cell capacity versus hot spot to non-HS user density ratio. Comparison between different HSS sizes with $W = 0.35R$. (Case of practical antenna)

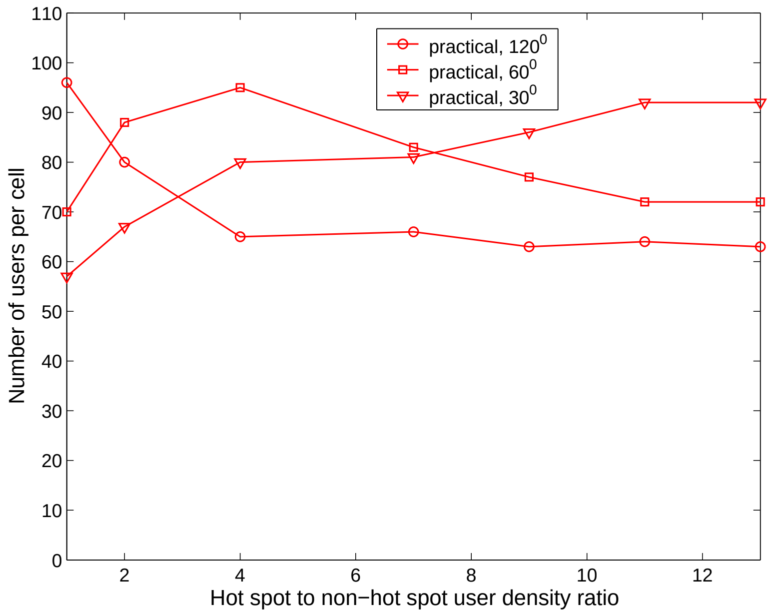

Figure 5.13: Cell capacity versus hot spot to non-HS user density ratio. Comparison between different HSS sizes with $W = 1.05R$. (Case of practical antenna)

that, similar to the case of perfect antenna, the possible number of users in HSS increases with increasing user density in HS while the possible number of users in adjacent and neighbour sectors decreases with increasing user density in HS. Fig. 5.12 also shows that the capacity improvement brought by reduction of HSS size (to 60^0 and 30^0) starts to occur at a user density ratio of about 5, and remains superior to nominal 120^0 sector situation at all higher concentration of HS.

Case of HS with $W = 1.05R$

The blocking sector behaviour in this case too is similar to the corresponding case of perfect antenna (Fig. 5.6). The blocking first occurs in A_2, A_3 and then moves to A_1 as the user density ratio reaches about 2 and 4, when HSS size is 60^0 and 30^0 respectively. Fig. 5.13 shows the cell capacity for this case and shows that the system capacity improvement with adaptive sectorisation starts to occur at a user density ratio of about 2 and 3 for HSS size 60^0 and 30^0 respectively. This improvement reaches a maximum at a user density ratio of 4 when HSS size is 60^0. When the HSS size is 30^0 there is a steady increase in capacity with increasing HS concentration.

5.3 Multi-rate CDMA and Adaptive Sectorisation

In DS/CDMA systems, there are three main options to implement multi-rate multiuser communications. They are, the variable spreading factor (VSF), multicode (MC), and variable chip rate (VCR) transmissions [32][33]. The VSF systems employ the same chip rate for all the users, and data streams at different rates are modulated by spreading codes of different length. In other words, for a VSF CDMA system with M different data rates, we have

$$T_c = \frac{T_0}{N_0} = \cdots = \frac{T_{M-1}}{N_{M-1}} \tag{5.3.1}$$

where T_c is the chip duration, and T_i and N_i (i=0,...,M-1) are symbol period and the spreading factor for rate i users, respectively.

In the MC systems, all data rates are assumed to be multiples of a basic rate. Each data stream is converted into several parallel basic rate substreams, followed by spreading with different codes. Orthogonal codes are used to prevent interference between the substreams [34]. However, the presence of a dispersive wireless channel results in a loss of this orthogonality. Note that all the users share the same bandwidth in both VSF and MC systems.

In the VCR systems, data streams at different rates are spread with different codes of the same length, i.e., different rate users use different chip rates. This means that the available bandwidths for the different rate users are different. Fig. 5.14 shows an example of how two different rate users would be supported by these three access methods, where the rate ratio is 2:3.

The best scheme for multi-rate transmission depends on many factors. Since the VCR scheme introduces extra difficulty in chip synchronization and frequency planning [35], MC and VSF solutions are preferred to the VCR scheme. Indeed, the 3G wireless networks employ the VSF and MC multi-rate access strategies [6], [7].

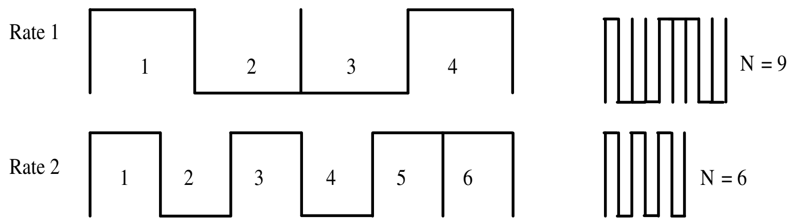

(a) Variable spreading factor scheme

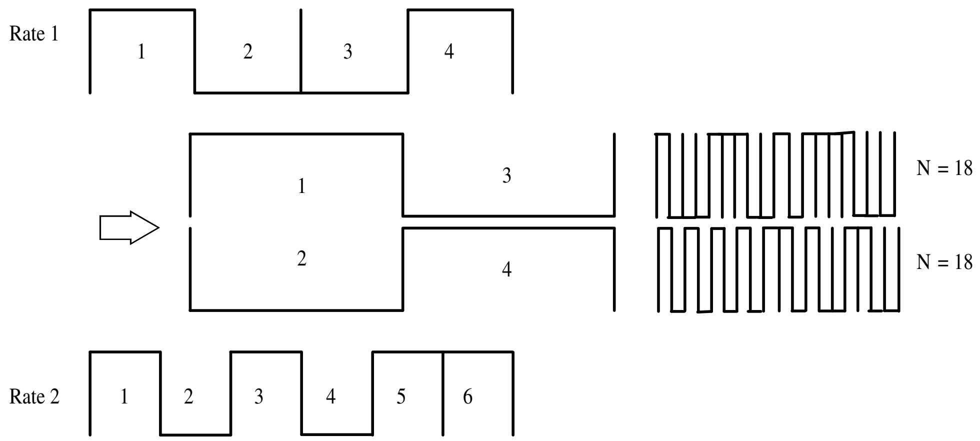

(b) Multicode scheme

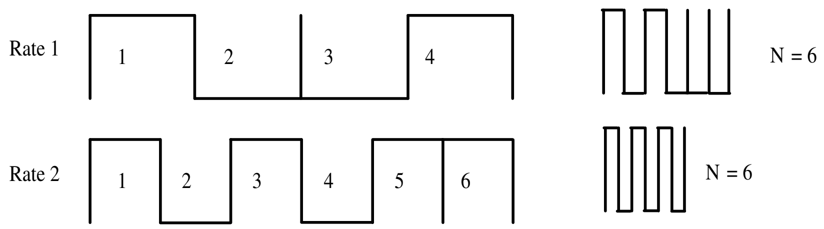

(c) Variable chip rate scheme

Figure 5.14: Three main multi-rate access strategies.

Compared to MC solution the provision of orthogonal channels in the forward link is more difficult in VSF scheme. This is because in the VSF scheme, orthogonal codes can be found only if the spreading factors are constrained to 2^n where n is a positive integer, e.g., orthogonal variable spreading factor (OVSF) codes used in the 3G wireless systems [6], [7]. Also, because of the larger spreading factor, MC multi-rate scheme experiences less ISI than the VSF multi-rate signals. This leads to less complexity of the receiver in the MC case compared to the VSF solution. However, the MC system requires linear power amplifier, especially in the reverse link direction, since multiple channels for a particular user can give rise to large amplitude variations. In this investigation we consider only the MC multi-rate access scheme for capacity improvement.

5.4 High Bit Rate using Multicode Transmission

In the Multi Code (MC) CDMA system, as shown in Fig. 5.15, the high bit rate data stream is split into M parallel data sreams, each of fixed basic data rate R_b. This basic data rate is spread with the same spreading gain, but different code sequences C_i $(i = 1, .., M)$ over the entire transmission bandwidth [36], where M denotes the maximum number of parallel channels per Mobile Station (MS). M is limited by the MS hardware. According to [36] MS is allowed to use up to $M = 8$ channels in parallel and each MS is capable of transmitting and receiving multiple channels. All active channels of one MS are superimposed and modulated afterward. The bit rate to be supported by a single MS is assumed to be exactly equal to the nominal bit rate achievable by a single code. In case of a data bit rate M times greater than the voice bit rate, this means that a data user causes an interference

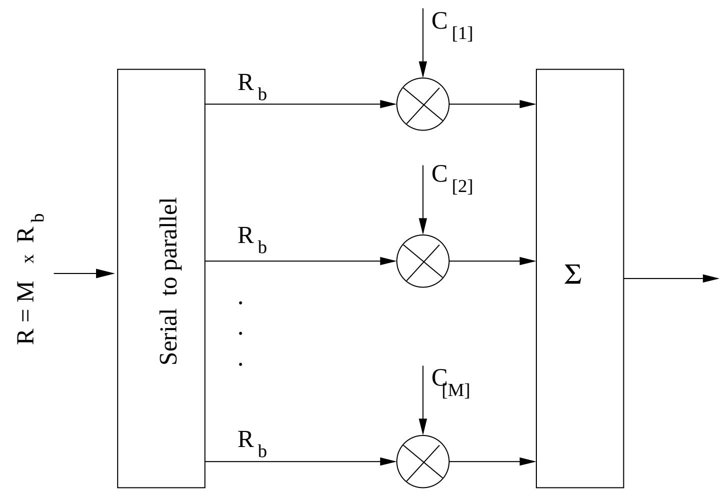

Figure 5.15: Multicode CDMA transmission.

to a voice user as if there were M voice users [37].

For MC transmission, pilot symbols may be inserted in one CDMA channel only (single-code pilot) or in all parallel channels (multicode pilot) [38]. In the first case, the relative pilot overhead is reduced as the number of parallel channels is increased, while, in the second case, the relative overhead remains constant.

In all cases, reverse link power control is necessary to get acceptable performance. With variable rate MC transmission, the transmit power of each channel does not vary with the bit rate as long as at least one of the parallel channels is always transmitted. For variable rate single code transmission, the transmit power on the CDMA data channel will vary with the bit rate. Power control can not be based on power measurements on the data channel, unless the rate is known in advance [15]. For MC transmission scheme, reverse link code allocation is not a problem at all. Given the bit rate, the BS receiver will then implicitly know what codes to receive. The system only needs to make sure that the total load in the cell does not exceed a certain level. Total self interference will be the same as for a single code transmission. However, with MC transmission, each CDMA channel will also receive interference from the $M-1$ parallel channels.

5.4.1 System Simulation

In this investigation of CDMA system capacity, the number of users the system can support is evaluated using a computer simulation. The cell radii in all scenarios are normalized to unity. The conventional hexagonal cell pattern is assumed. No mobility model is considered for this capacity simulation. A uniformly distributed mobile population is generated with random locations within home and the 18 neighbour sectors. This is done by generating random numbers that assign an angular position and a radial distance to each MS with respect to the home BS (see Fig. 4.4). The individual path losses (coupled with the shadowing effect) are calculated for each MS in order to evaluate the SIR at sector BSs. The simulation software was written in MATLAB employing random number generators to represent call arrivals. Simulations for three adaptive sector configurations were performed to estimate the uplink capacity taking both intra-sector and inter-sector interference into account. The sector coverage is obtained by using adaptive antennas in practical settings with associated antenna patterns including sidelobes. For each loading (in terms of users), we ran simulation more than 20,000 times and obtained an average value for the blocking probability.

Fig. 5.16 shows the blocking probability of the system as a function of the number

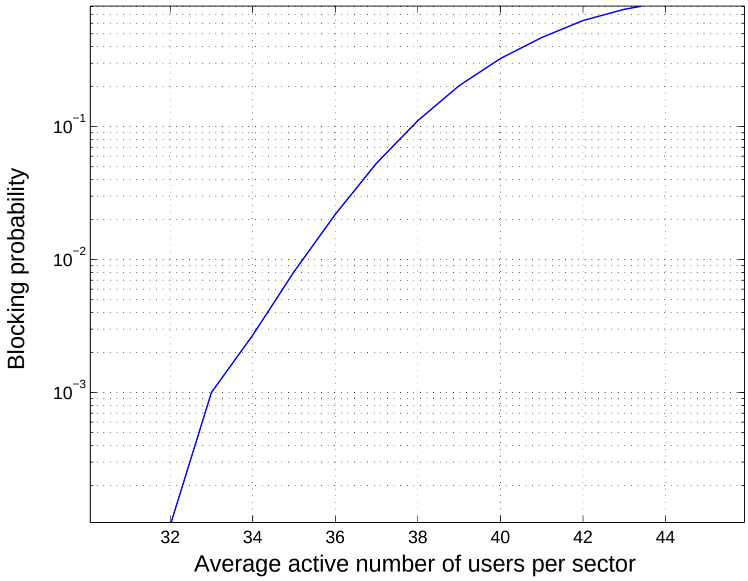

Figure 5.16: Blocking probability of the system with voice users only.

of voice users with constant bit rate (9.6 kbps). The voice activity factor is taken to be 37.5%. It can be seen from the plot that the capacity of system is 35 voice users per sector (or 105 user per cell) at 1% blocking and 37 users (or 111 users per cell) at 5% blocking.

In Fig. 5.17, we plot the blocking experienced when only one data user per sector (operating in circuit switched mode) at 38.4 kbps and 76.8 kbps respectively ($8 - codes$ and $2 \times 8 - codes$ aggregated, each at 9.6 kbps). Since the $M - codes$ corresponding to the data user are active all the time, the activity factor of the circuit switched mode data user is 1. We observe that when the data user is operating in circuit switched mode, the system can support 23 and 12 users with $M = 8$ and $M = 16$, respectively, at 1% blocking.

In order to integrate voice and data service, we will have only one data user, and use all the remaining capacity for voice users. Fig. 5.18 shows the number of voice users

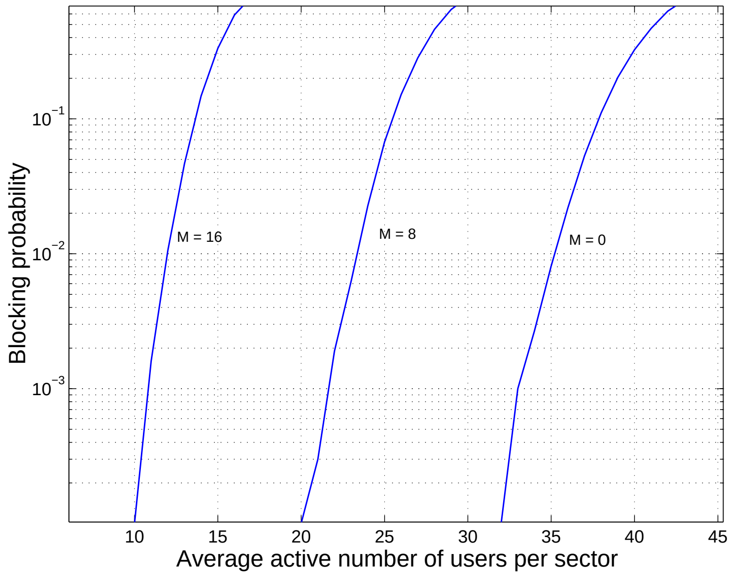

Figure 5.17: Blocking probability with one high speed data channel at 4 times and 8 times normal bit rate, and data activity factor = 1.

against the number of parallel codes in a multi cells system. We see that there is a linear relationship between the number of voice users and the number of multi codes used in parallel transmission. Our simulation agrees with the results shown in [37] although the results of [37] is focused on single cell systems only.

We study the system behaviour as the high data rate user is in a Hot Spot Sector (HSS) and uniform traffic persists with normal bit rate, R_b, in every neighbour cell. The results of Fig. 5.19 indicate how the possible number of users in HSS decreases with increasing bit rate of the high data rate user in the HS.

The simulation also shows that in this situation (at 1% blocking), there is a capacity improvement of about (37 - 23)/23 = 60% and (18 - 11)/11 = 63% at $M = 8$ and $M = 26$, respectively, with adaptive sectorisation. At data user data rate of about 24 times the

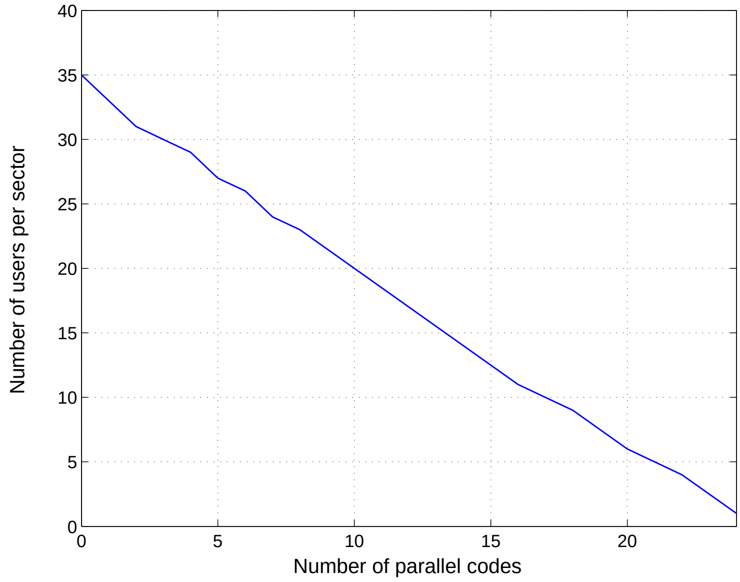

Figure 5.18: Number of users per sector Vs number of parallel codes at 1% blocking probability.

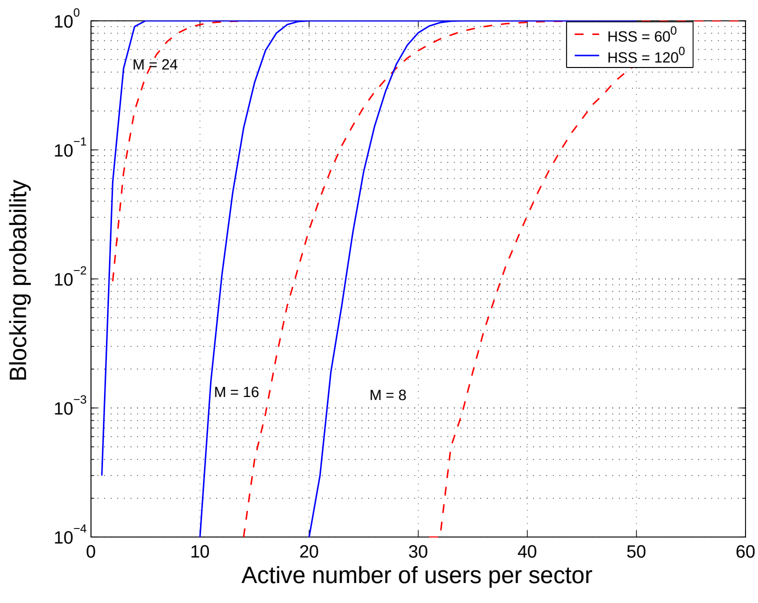

Figure 5.19: Adaptive sector with HSS $= 60^0$ Vs fixed sector (with HSS $= 120^0$). Blocking probability with only one high speed data channel at $M = 8$, 16, and 24 times the normal bit rate. (data activity factor $= 1$.)

normal ($R = 24 \times R_b$), there is only a very small improvement in system capacity. This is to be expected because the interference caused by the data user is excessively large.

5.5 Conclusions

Adaptive sectorisation can be used to improve the capacity of a CDMA cellular system when a cell or a sector contains an area of congested traffic (i.e., a hot spot). A simple and robust technique to achieve adaptive sectorisation is to employ finite beam switching with a suitable array antenna at the sector BS. The available capacity improvement is a function of the ratio of the user densities in the congested and non-congested areas of the sector and it appears that the improvement is particularly significant when the user density in the congested area is an order of magnitude higher than that of the rest. A simple beam forming dipole array antenna structure such as the one considered here, can be used for the implementation of adaptive sectorisation. Adaptive sectorisation can also be used for capacity improvement in multi-rate CDMA systems, that use multi-codes.

Chapter 6

Capacity of WCDMA Cellular Systems

To investigate the capacity of WCDMA cellular systems it is necessary to examine the air interface of third generation (3G) cellular systems. This chapter gives an overview of the emerging 3G cellular systems and draws attention to IMT-2000 standard which employs WCDMA as its air interface [39]. WCDMA is also known as UMTS Terrestrial Radio Access (UTRA) scheme.

6.1 WCDMA Air Interface

WCDMA has been widely accepted as the air interface for the third generation cellular systems. Its specifications have been drawn by the joint standardisation body called 3GPP (3^{rd} Generation Partnership Project).

6.1.1 Frequency Bands and Operation Of WCDMA

The proposed spectrum allocations for UTRA are shown in Fig. 6.1. 3^{rd} Generation (3G) radio access supports both Frequency Division Duplex (FDD) and Time Division Duplex

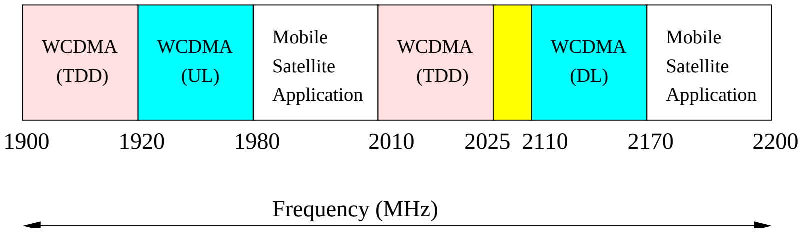

Figure 6.1: The proposal spectrum allocation in UTRA.

(TDD) operations. As seen from Fig. 6.1, the paired bands of 1920-1980 MHz and 2110-2170 MHz are allocated for FDD operation in the uplink and downlink, respectively, and the remaining unpaired bands are allocated to TDD mode [10]. The operating principles of these two schemes are shown in Fig. 6.2. The UL and DL signals are transmitted using different carrier frequencies f_1 and f_2, respectively, separated by a frequency guard band in FDD mode (Fig. 6.2(a)). On the other hand, the UL and DL transmission in the TDD mode take place at the same carrier frequency fc, but in different time slots, separated by a guard time (Fig. 6.2(b)).

6.1.2 Carrier Spacing in WCDMA

The carrier spacing of WCDMA spectrum has a raster of 200 kHz and can vary from 4.2 to 5.4 MHz. Fig. 6.3 shows the operator bandwidth of 15 MHz with three cell layers [4]. The result of [4] has shown that larger spacing can be applied between operators than within one operator's bands in order to avoid interoperator interference. Interfrequency measurements and handovers are supported by WCDMA to utilize several cell layers and carriers. UTRA defines several physical channels across the air interface.

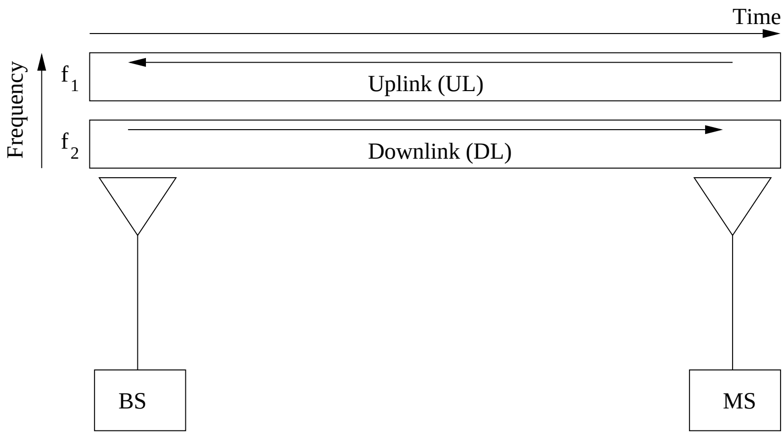

(a)

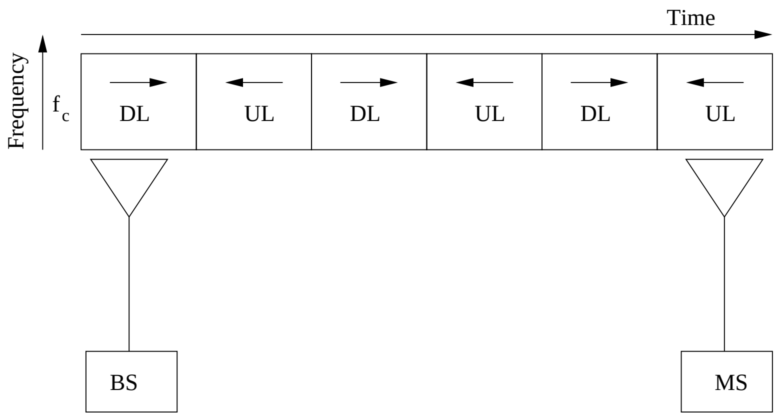

(b)

Figure 6.2: 6.2(a) Principle of FDD and 6.2(b) TDD operation.

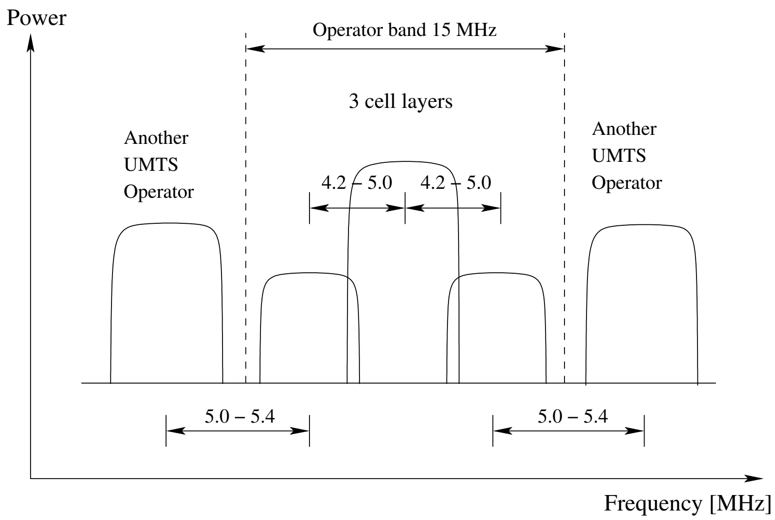

Figure 6.3: Frequency utilization in WCDMA (uplink or downlink) [6].

6.1.3 Uplink Dedicated Physical Channels

There are two types of uplink dedicated physical channels, the uplink Dedicated Physical Data Channel (UL-DPDCH) and the uplink Dedicated Physical Control Channel (UL-DPCCH). The DPDCH and the DPCCH are I/Q code multiplexed within each radio frame. Fig. 6.4 shows the frame structure of the uplink dedicated physical channels. Each radio frame of length 10 ms is split into 15 slots, each slot of length $T_{slot} = 0.666$ ms, corresponds to one power-control period. Each slot has four fields to be used for pilot bits, Transmit Power Control (TPC) commands, Feedback Information (FBI), and an optional Transport Format Combination Indicator (TFCI). The pilot bits are used for channel estimation in the receiver, the TPC bits carry the power control commands for the downlink power control, the FBI bits are used when closed loop transmission for the downlink diversity is used in the downlink (In FBI, the S field is (consisting of 0, 1, or 2 bits) used for Site Selection Diversity Transmission (SSDT) signalling, while the D field is (consists of 0 or 1 bit) used for closed loop mode transmit diversity signalling. The D field consists of 0 or 1 bit). The TFCI informs the receiver about the instantaneous transport format combination of the transport channels mapped to the uplink DPDCH transmitted simultaneously. A change of TFCI in uplink (UL) means that the power in the UL varies according to the change in data rate. A change of output power is required during UL compressed frames since the transmission of data is performed in a shorter time interval. The ratio of the amplitude between the DPDCH codes and the DPCCH code will also vary. The power step due to a change in TFCI shall be calculated in the User Equipment (UE) so that the power transmitted on the DPCCH shall follow the inner loop power control. The power change by TFCI is defined as the relative power difference between the averaged power of original (reference) timeslot and the averaged power of target timeslot without transient duration [39]. There is one and only one uplink DPCCH on each radio link; however, there may be zero, one or several uplink DPDCHs on each radio link. Each DPDCH frame on a single code carries 150×2^k bits, where k = 0..6, corresponding to a spreading factor of $256/2^k$ with the 3.84 Mcps chip rate. The spreading factor of the uplink DPCCH is always equal to 256, i.e. there are 10 bits per uplink DPCCH slot.

Multi-Code (MC) operation is possible in the uplink dedicated physical channels when higher data rates are needed. It allows up to six parallel codes to be used. Fig. 5.15 illustrates that we can transmit one DPCCH and up to six parallel DPDCHs simultaneously. It is beneficial to transmit with a single DPDCH for as long as possible, for reasons of

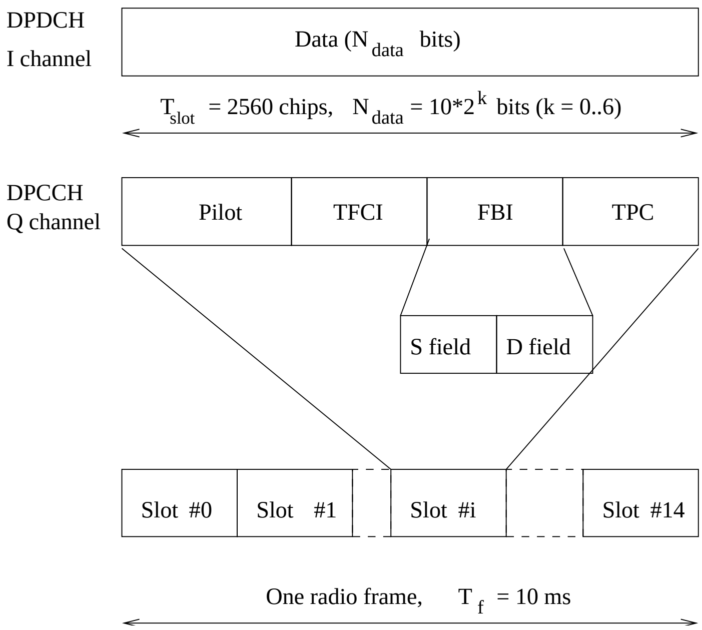

Figure 6.4: Frame structure for uplink DPDCH and DPCCH.

terminal amplifier efficiency, because MC transmission increases the peak-to-average ratio of the transmission, which reduces the efficiency of the terminal power amplifier [6].

6.1.4 Uplink Common Physical Channels

Physical Random Access Channel (PRACH)

The Physical Random Access Channel (PRACH) is used to carry the RACH. The random-access transmission is based on a Slotted ALOHA approach with fast acquisition indication. The User Equipment (UE) can start the random-access transmission at the beginning of a number of well-defined time intervals, denoted by access slots. There are 15 access slots per two frames and they are spaced 5120 chips apart. (See Fig. 6.5(a))

The structure of the Random Access Transmission (RAT) is shown in Fig. 6.5(b). The random-access transmission consists of one or several preambles of length 4096 chips and a message of length 10 ms or 20 ms. Each preamble consists of 256 repetitions of a signature of length 16 chips. There are a maximum of 16 available signatures.

Fig. 6.6(a) shows the structure of the message part of the RAT. The 10 ms message frame is split into 15 slots, each of length $T_{slot} = 2560$ chips. Each slot consists of two parts, a data part to which the transport channel is mapped and a control part that carries Layer 1 control information. The data and control parts are transmitted in parallel. A 10 ms message part consists of one message part radio frame, while a 20 ms message part consists of two consecutive 10 ms message part radio frames. The data part consists of $10 * 2^k$ bits, where k = 0, 1, 2, 3, with corresponding spreading factors of 256, 128, 64, and 32 respectively.

The control message part consists of 8 known pilot bits to support channel estimation for coherent detection and 2 TFCI bits. This corresponds to a spreading factor of 256 for the control message part. The total number of TFCI bits in the random-access message is $15 * 2 = 30$. The TFCI of a radio frame indicates the transport format of the transport channel mapped to the simultaneously transmitted data message part of radio frame. In case of a 20 ms PRACH message part, the TFCI is repeated in the second radio frame.

Physical Common Packet Channel(PCPCH)

The Physical Common Packet Channel (PCPCH) is used to carry the CPCH. The CPCH transmission is based on CSMA-CD approach with fast acquisition indication. The UE can start transmission at the beginning of a number of well-defined time-intervals, relative

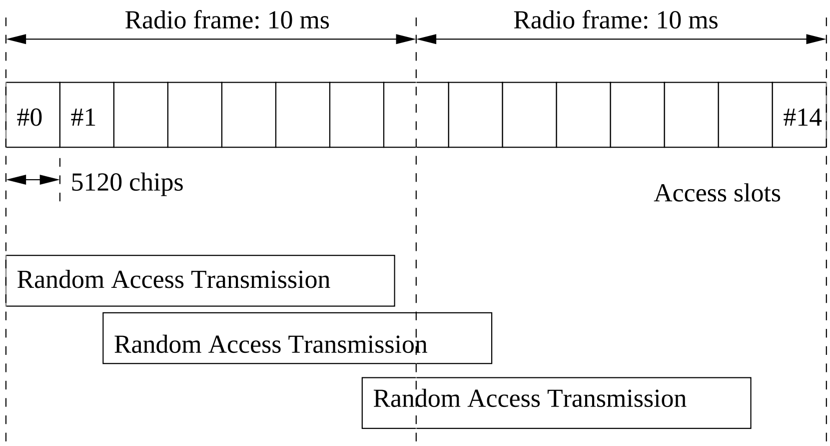

(a)

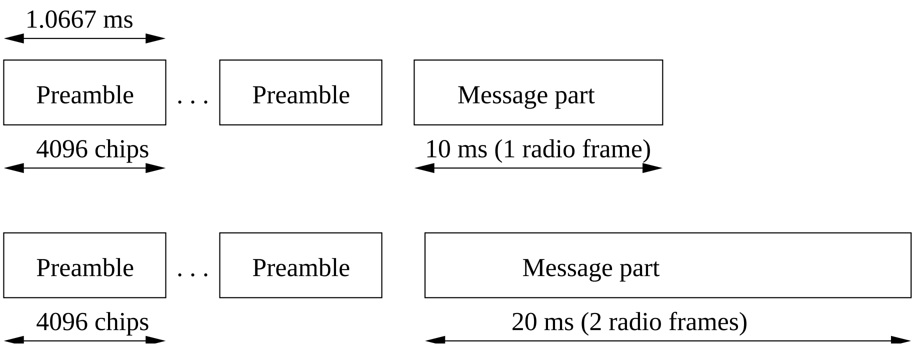

(b)

Figure 6.5: 6.5(a) RACH access slot numbers and their spacing, 6.5(b) Random access transmission sequence.

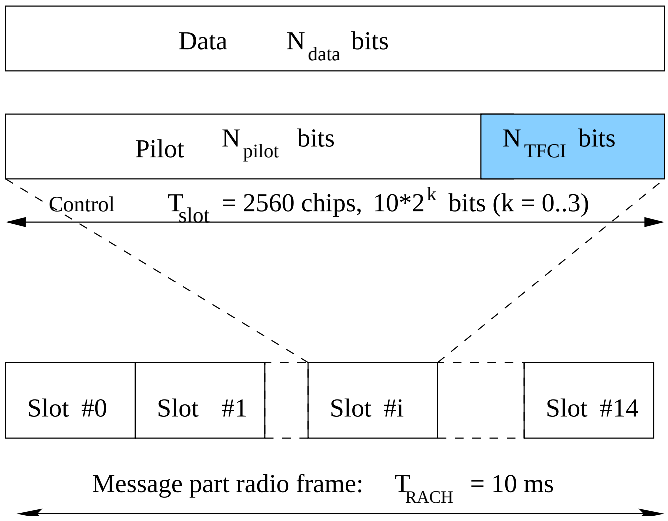

(a)

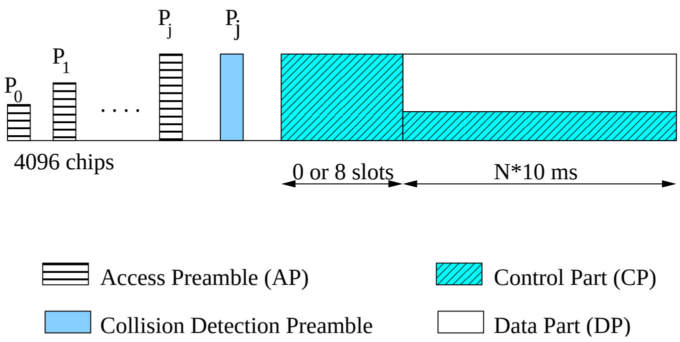

(b)

Figure 6.6: 6.6(a) Structure of the message part of RAT, 6.6(b) Structure of the CPCH random access transmission.

to the frame boundary of the received Broadcast Channel (BCH) of the current cell. The structure of the CPCH access transmission is shown in Fig. 6.6(b). The PCPCH access transmission consists of one or several Access Preambles (AP) of length 4096 chips, one Collision Detection Preamble (CDP) of length 4096 chips, a DPCCH Power Control Preamble (PCP) which is either 0 slots or 8 slots in length, and a message of variable length $N \times 10$ ms [6] [5].

Each CPCH message part consists of up to N_{Max} 10 ms frames [8], with each 10 ms frame split into 15 slots, each slot having $T_{slot} = 2560$ chips. Every slot consists of a data part that carries higher layer information and a control part that carries Layer 1 control information. The data and control parts are transmitted in parallel. The control part of the CPCH message part has a spreading factor of 256, and it uses the same slot format as the control part of the Common Packet Channel Power Control-Preamble (CPCH PC-P).

6.1.5 Deployment of WCDMA Air Interface

The channel structure of WCDMA air interface shows that it is to be deployed for the packet mode operation in general. The system capacity and the quality of service are governed by the way in which the available channels are utilized and how the interference arising in the system is handled. The channel utilization ultimately depends on the type of traffic the system has to handle and to this end it is necessary to examine the type of traffic expected in the third generation cellular systems.

6.2 3G Traffic Model

The third generation cellular mobile communication systems are expected to extend the wireline communication system capabilities including the transport of voice, data, and multimedia traffic, to wireless communication. Further, it recognizes that the bulk of this traffic will consist of asymmetrical flows such as Internet traffic where a user inputs modest amounts of traffic while attempting to receive traffic in bulk quantities. The traffic model developed by the 3^{rd} Generation Partnership Project (3GPP) reflects this nature and supposedly represent the traffic in futures cellular mobile communication systems. The 3GPP traffic model has three tiers, namely, session, packet call, and packet as illustrated in Fig. 6.7. A packet service session contains one or several packet calls depending on the application. During a packet call several packets may be generated, so that the packet call constitutes a bursty sequence of packet [6]. For instance, in a www browsing, a session may correspond to the downloading of a www document [7], [40]. After a portion of the document is downloaded to MS the user take some time to read it, before initiating the downloading of the next part of the document. Thus it is possible that a session contains several packet calls.

The traffic behaviour of Fig. 6.7 can be modeled by assuming that the respective events involved can be represented by the following stochastic processes.

- Session arrival is a Poisson process, (N_s, Number of sessions per unit time)
- Packet call arrival is a Geometrically distributed random process (N_{pc} = number of packet calls per session, D_{pc} = packet call inter-arrival time)

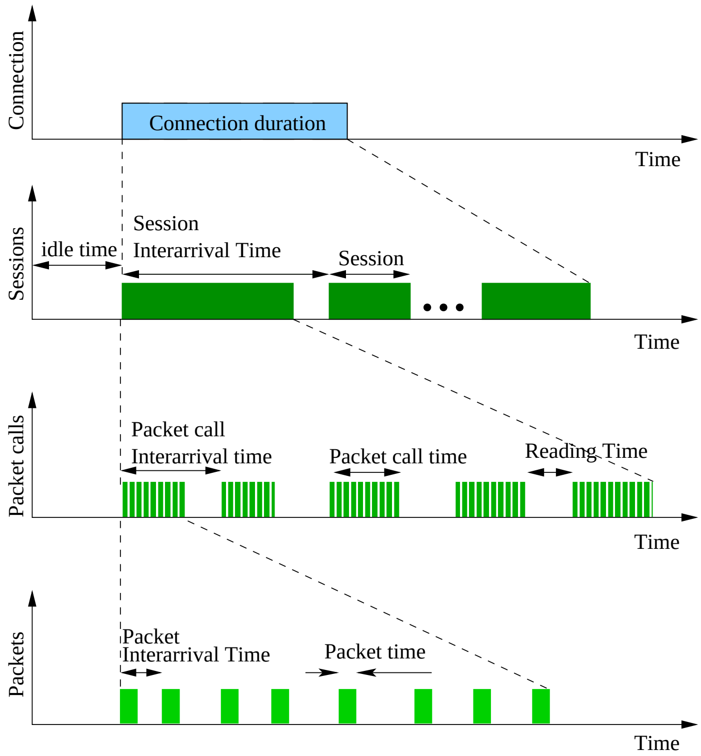

Figure 6.7: Three tier traffic model representing packet mode traffic.

- Packet arrival is a Geometrically distributed random process (N_d = number of packets per packet call, D_a = packet inter-arrival time)
- Packet length, S_d, is a Pareto distribution with cut-off (k, α)

6.2.1 Sessions, Packet calls, and Packets

Sessions arrive according to Poisson process and are classified into new sessions or handover sessions [40]. The duration of the inactivity periods of these sessions are classified as belonging to a Pareto distribution [41]. A new packet for a given session is generated in accordance with the data traffic type. After a packet is generated, the relevant buffer is updated. When all the packets corresponding to the given data session have been generated, and there is no data in the buffer, the data session ends.

The models presented here can be viewed as source models that describe how data packets are generated at the source and how they arrive at the buffers in the network. The traffic model can use a packet size distribution that suits best for the traffic case under consideration. Each layer of traffic can be modelled with an active (ON) period and an inactive (OFF) period. In case of a packet call, an ON period may include one or more requests by the user, and the user may make more requests before all the current requests are completed [41]. The OFF period represents the thinking time of a user, and typically indicates the existence of a significant pause in the communication activity. The results in [41] suggest that the durations of ON and OFF periods belong to Weibull and Pareto distributions, respectively.

6.2.2 Packet size

The packet size can be described by a Pareto distribution with cut off. Accordingly, the packet size is defined with the following formula [42]:

$$packet\ size = min(P,\ m) \tag{6.2.1}$$

where P is normal Pareto distributed random variable ($\alpha = 1.1, k = 81.5\ bytes$) and m is maximum allowed packet size [42]. The data rate and average inter-arrival times for this type of traffic is given in Table 6.1. The probability density function (PDF) of packet size is given by [42],

Table 6.1: Inter-arrival time between packets for Pareto traffic [42]

Date rates [$kbps$]	Average Inter-arrival time between packets [sec]
8	0.5
32	0.125
64	0.0625
144	0.0277
384	0.0104
2048	0.0019

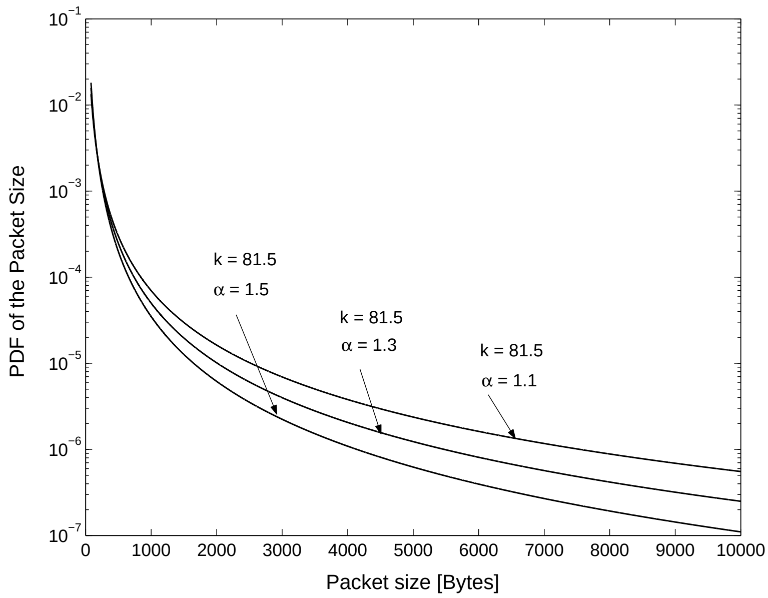

Figure 6.8: PDF of packet size (Pareto distribution) [41].

$$f_n(x) = \frac{(\alpha \cdot k^{\alpha})}{x^{\alpha+1}} \tag{6.2.2}$$

This is shown in Fig. 6.8. α determines the heaviness of the tail of the distribution. When α is close to 1, the distribution becomes heavier and the traffic becomes more bursty [43].

6.2.3 On Period Distribution

The traffic can be modelled with an active (ON) period and an inactive (OFF) period. An ON period may include more than one direct requests by the user, because the user may make another requests before all the current requests are completed. These are described in [41]. ON period can be described by a Weibull distribution. The PDF of Weibull distribution s given by,

$$\rho(t) = \left(\frac{k}{\theta}\right) \cdot \left(\frac{t}{\theta}\right)^{k-1} \cdot e^{-(t/\theta)^k} \tag{6.2.3}$$

where k determines the shape of the distribution. The distribution is light tailed when $k > 1$, heavy tailed when $k < 1$, and becomes negative exponential distribution when $k = 1$ [41]. The results in [41] illustrates the Weibull distribution for $k = 0.91$ to 0.77 and $\theta = e^{4.4}$ to $e^{4.6}$, respectively Fig. 6.9(a).

6.2.4 Off Period Distribution

The results in [41] suggest that the duration of an OFF period belong to a Pareto distribution with a probability density function

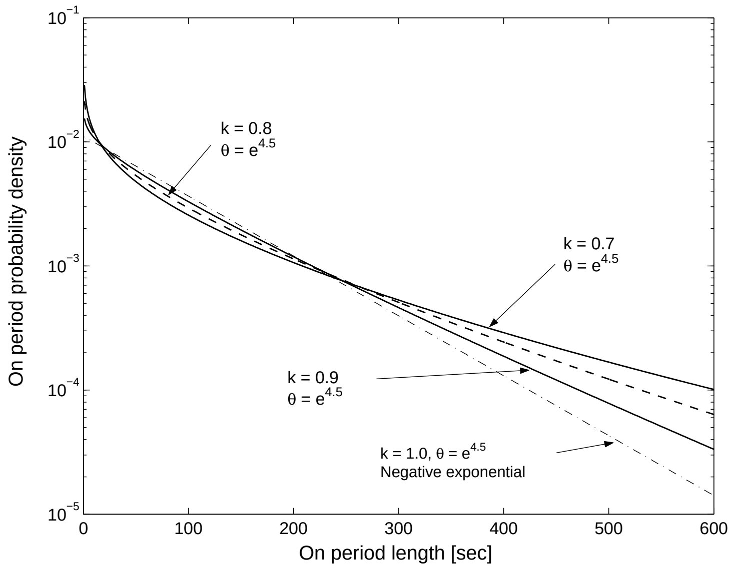

(a)

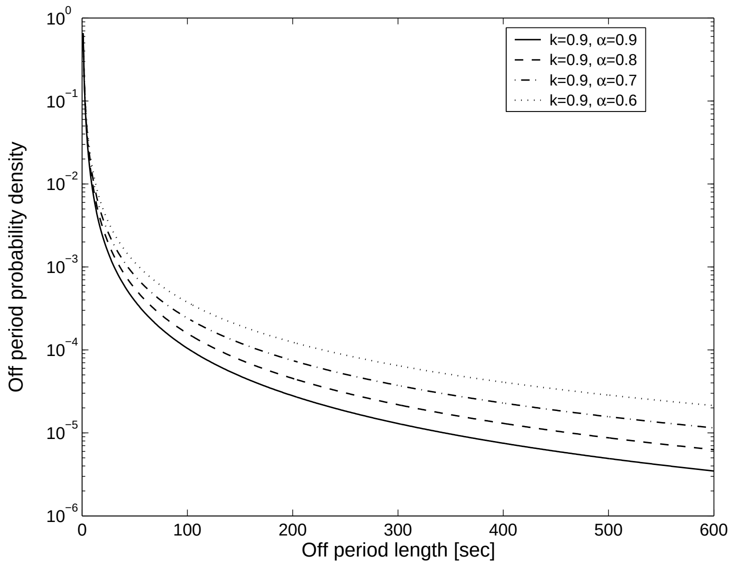

(b)

Figure 6.9: 6.9(a) PDF of ON period in Weibull distribution, 6.9(b) PDF of OFF period in Pareto distribution [41].

$$\rho(t) = \frac{(\alpha \cdot k^{\alpha})}{t^{\alpha} + 1} \tag{6.2.4}$$

where k represents the smallest value of OFF period. A Pareto distribution has infinite mean if $\alpha \leq 1$, and infinite variance if $\alpha \leq 2$. The WWW traffic data suggests that an α value of 0.91 to 0.58 [41], would be representative of Internet traffic. Fig. 6.9(b) shows an example of an OFF period probability density function for different values of α

6.3 Conclusions

This chapter is reviewed the WCDMA air interface. It also described a framework for the modelling and simulation of traffic in 3G cellular systems. It was shown that the basic 3G traffic model stipulated for the cellular mobile communication systems can be constructed for simulation using the next-event time advance approach. It was possible to examine the system behaviour in terms of the number of users in the system, the delay in queue per user, and the probability of a user being blocked by the system. The next stage of this investigation is to expand the system model to include non-uniform user distribution in cell space, as well as the multi-cell environment. The use of adaptive sectorisation to enhance the overall system capacity is also to be investigated

Chapter 7

Modelling of 3G Traffic for WCDMA Cellular Systems

In the last chapter, we described the 3G traffic model that has been proposed by the 3GPP. This chapter deals with the computer simulation of this model for typical parameters particularly related to Internet. We exploit this model to examine the cellular mobile system activity under packet mode operation. We define a System Activity Factor which could be used as a measure of interference in the system and then link it to the estimation of system capacity.

7.1 Computer Modelling of 3GPP Traffic

The 3GPP traffic model when taken to represent www traffic, a session is characterised by download of several web documents (i.e., packet calls) with long reading times between the documents (Fig. 7.1). The packet call size is typically of the order of 12 Kbytes (480 byte packet $\times$ 25 packets) and the reading time ranges from few seconds to few minutes. The packet size is taken as belonging to Pareto distribution with cut-off [42], with the

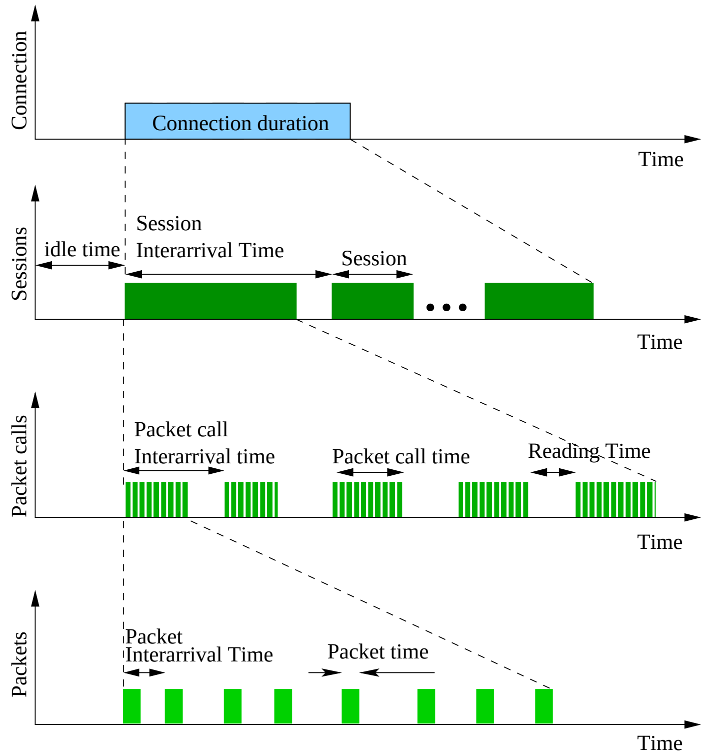

Figure 7.1: 3G traffic model representing www traffic.

parameters shown in Table 7.1.

7.2 The 3GPP Traffic Model Simulator Features: Activity Factors

The traffic simulator is a time driven program (written in MATLAB) which takes the events into account as the simulated time advances. The events are recognized as the start and ending of idle times, arrival of sessions, the departure of sessions, arrival of packet-calls, and packets. The simulated time is advanced to the next event time at the onset of next event. The active state of a user is indicated by the presence of a packet

Table 7.1: Packet size in web traffic.

Sessions per user	packet size
1	$1 \times 25 \times 480 = 12\ Kbytes$
5	$5 \times 25 \times 480 = 60\ Kbytes$
10	$10 \times 25 \times 480 = 120\ Kbytes$
20	$20 \times 25 \times 480 = 240\ Kbytes$

Table 7.2: Simulation parameters for 3GPP traffic simulator.

Data rate, R	64 kbps
Chip rate, W	3.84 Mcps
S_d (Pareto mean)	480 bytes
N_{pc}(Geometric mean)	5 packet-calls
D_{pc}(Geometric mean)	10, 30, 60 sec
N_d (Geometric mean)	25 packets
D_d	62.5 ms
k	81.5
α	1.1
Idle time, D_i (exp mean)	10, 60 sec

within a packet call during a session. The simulation is based on the traffic parameters shown in Table 7.2.

When the system completes serving a user, the number of users remaining in the system is used to determine whether the system will become idle or go on to serve a new user in the queue. An arrival event causes the system status to change from idle to busy or the number of users in the system to increase by 1. Similarly, a departure event causes the system status to change from busy to idle or the number of users remaining in the system to decreases by 1. Note that the number of users in the system gives a direct estimation of the system capacity.

7.2.1 Case of Single Session per Connection

The simulation begins with the system in empty state. A user enter the system starting with an idle time D_i. It is assumed that there is only one session per user and mean packet size is 12 Kbytes. Fig. 7.2(a) shows the traffic generated by individual users with a packet-call mean time of 10 sec. Fig. 7.2(b) shows how the number of active users in the system at any given time is varied with simulation time. (An active user is one that is engaged in the transmission of a packet) Fig. 7.3(a) shows the user activity during a session as indicated by the User Activity Factor (UAF), which we define as,

$$UAF = \frac{(Sum\ of\ ON\ periods\ of\ a\ user\ during\ a\ session)}{(Total\ session\ time)}. \tag{7.2.1}$$

Assume that there are 20 www users in the system. As mentioned before it is assumed that there is only one session per user, and according to the parameters of Table 7.2

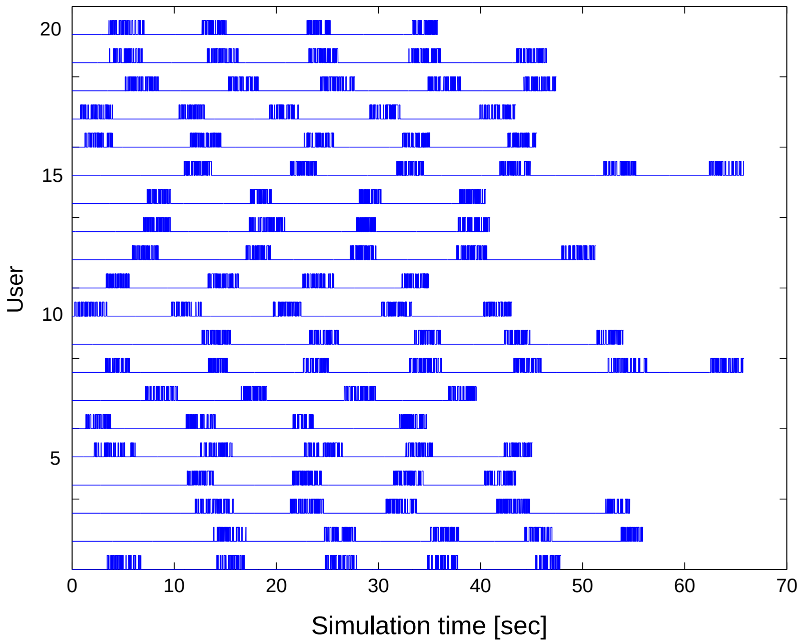

(a)

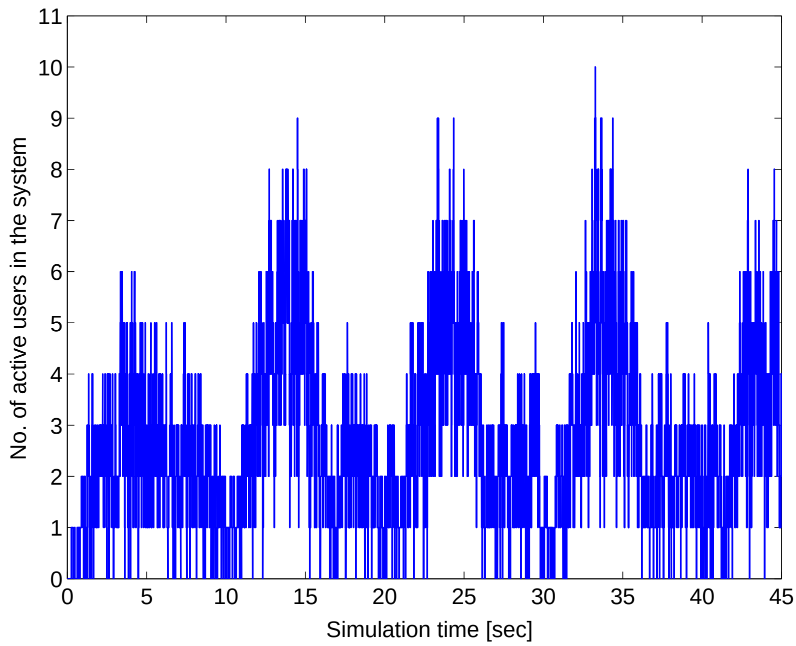

(b)

Figure 7.2: 7.2(a) Activity of individual users against simulated time. Average packet-call interarrival time is 10 sec, 7.2(b) The number of active users in the system vs the simulation time. Average packet-call interarrival time is 10 sec.

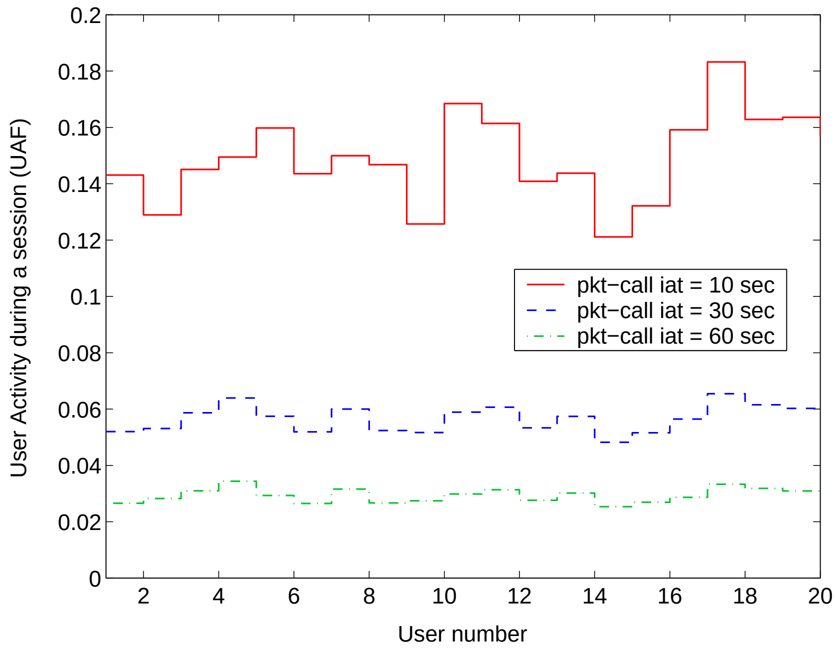

(a)

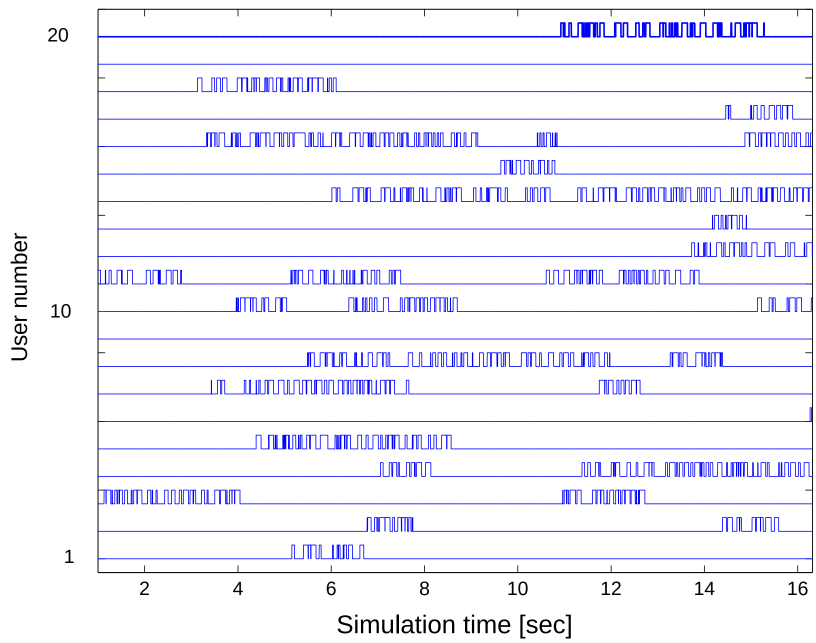

(b)

Figure 7.3: 7.3(a) The user activity factor against different users, for different packet call inter arrival times, 7.3(b) Activity (busy/idle) of individual users per session against simulated time. Average packet-call inter arrival time is 10 sec.

a varying number of packet calls are generated within the session. Similarly a varying number of packets are generated within the packet call. Fig. 7.3(b) shows the busy/idle state of the system with respect to each user against the simulated time, when the packet call mean is 10 sec. Fig. 7.4(a) shows the active number of users in the system as a function of simulated time. We define the System Activity Factor (SAF) at any given time as the ratio between the active number of users in the system at that time, and the total number of users in the system. Fig. 7.4(b) shows the behaviour of the system activity factor against the simulated time over the duration of the shortest session. (Shortest session is taken here to make sure that all 20 users contribute to the system activity with equal probability). Fig. 7.4(b) also shows the time average of the system activity factor (Average System Activity Factor) over the duration of the shortest session. Fig. 7.5(a) shows that the Average System Activity Factor (ASAF) is a function of packet call inter-arrival time. Note that it takes a negative exponential form.

7.2.2 Case of Multiple Session per Connection

Fig. 7.5(b), Fig. 7.6(a), and Fig. 7.6(b) show the dependence of ASAF on the number of session involved. In all cases, the ASAF rapidly decreases with the increasing session inter-arrival time, and reaches a steady value when the session inter-arrival time is of the order of 500 sec. Also it is clear that the ASAF is less dependent on packet inter-arrival time as the session inter-arrival time gets bigger. This convergence is most prominent when a call consists of a large number of sessions (Fig. 7.6(a) and Fig. 7.6(b)).

To estimate the system capacity, it is assumed that perfect power control is in place

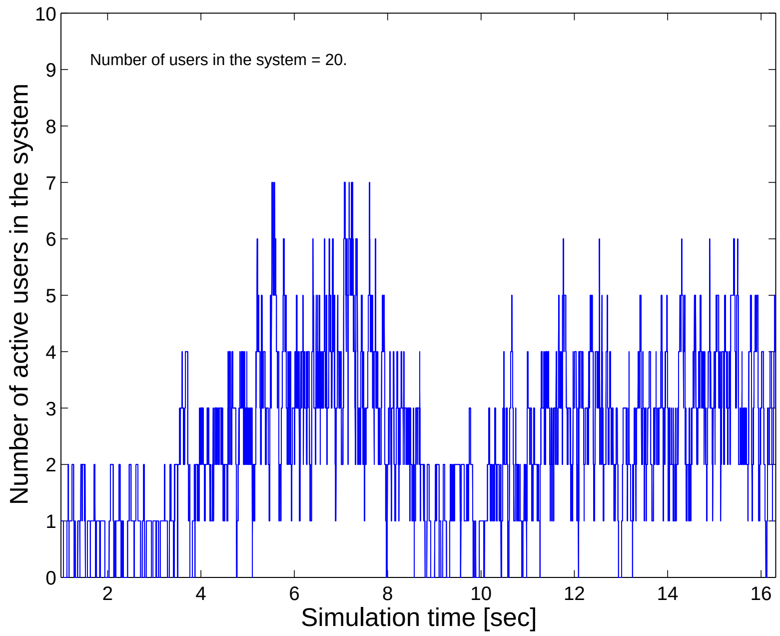

(a)

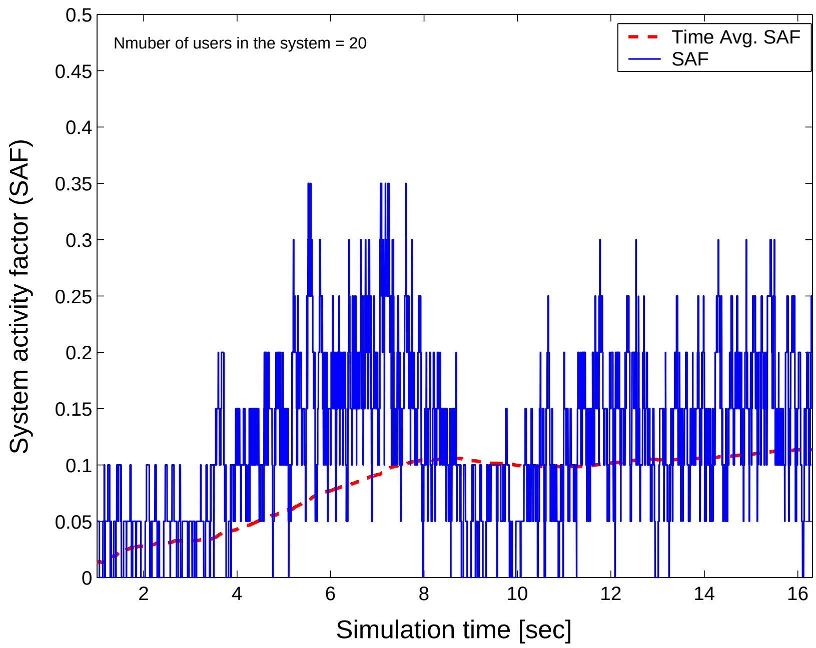

(b)

Figure 7.4: 7.4(a) The number of active users in the system against the simulated time. (Average packet-call interarrival time is 10 sec), 7.4(b) The system activity factor and its time average against the simulation time. (Average packet-call inter-arrival time is 10 sec).

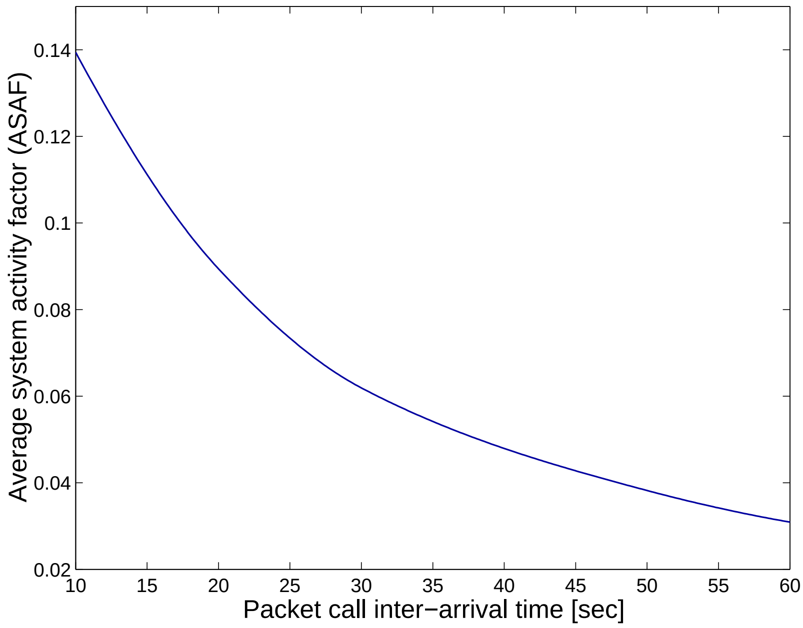

(a)

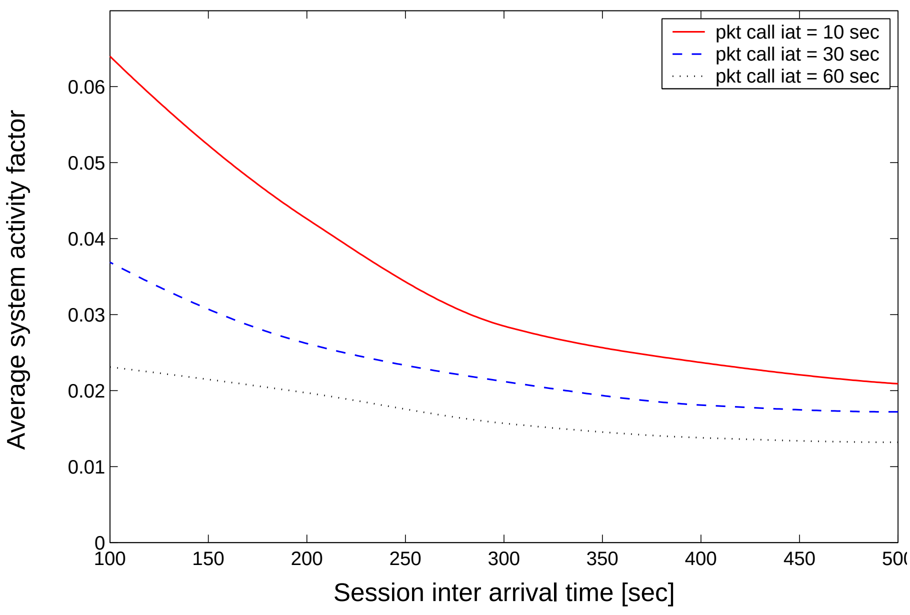

(b)

Figure 7.5: 7.5(a) Average system activity factors against packet call inter-arrival time. Number of sessions per user = 1, 7.5(b) Average system activity factors against session inter-arrival time. (Packet call inter-arrival (mean) times are ,10, 30, 60 sec). Number of sessions per user = 5.

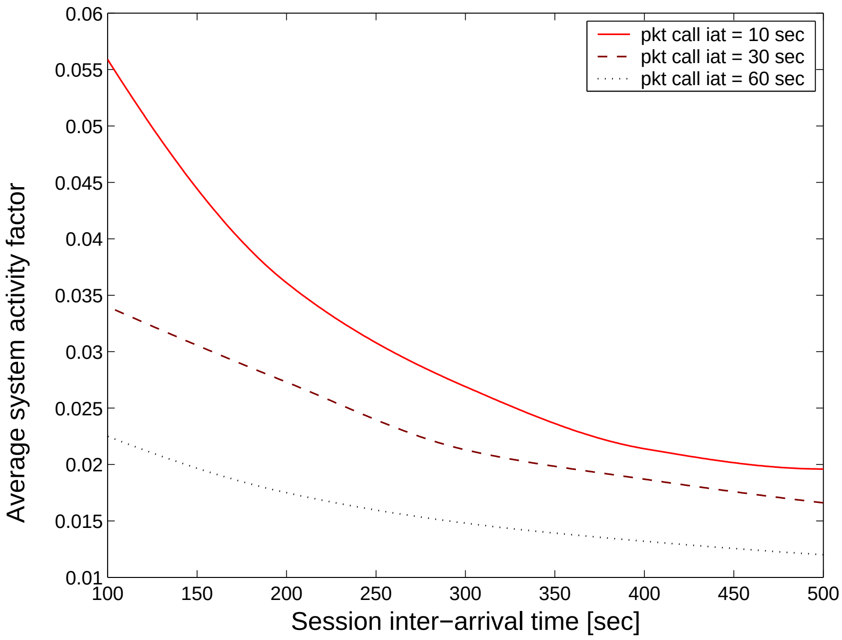

(a)

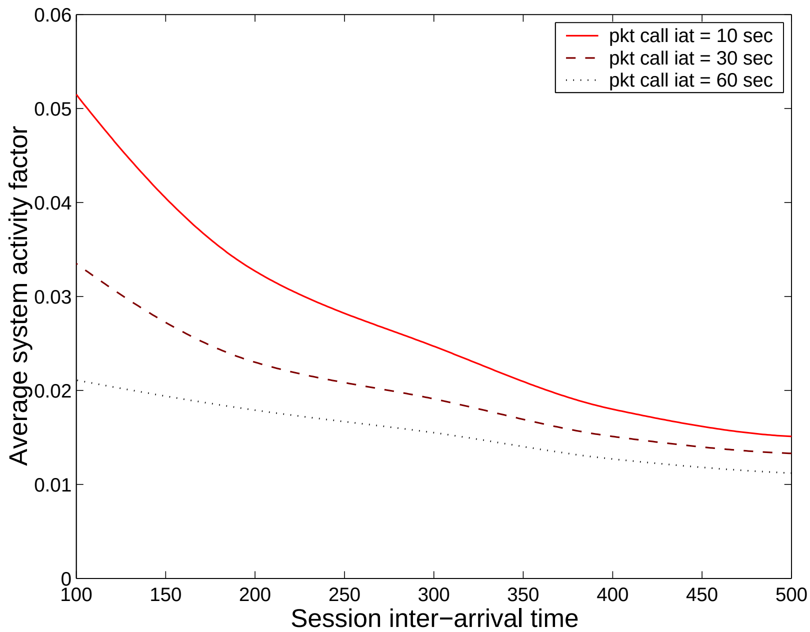

(b)

Figure 7.6: 7.6(a) Average system activity factors against session inter-arrival time. (Packet call inter-arrival (mean) times are 10, 30, 60 sec). Number of sessions per user = 10, 7.6(b) Average system activity factors against session inter-arrival time. (Packet call inter-arrival (mean) times are 10, 30, 60 sec). Number of sessions per user = 20

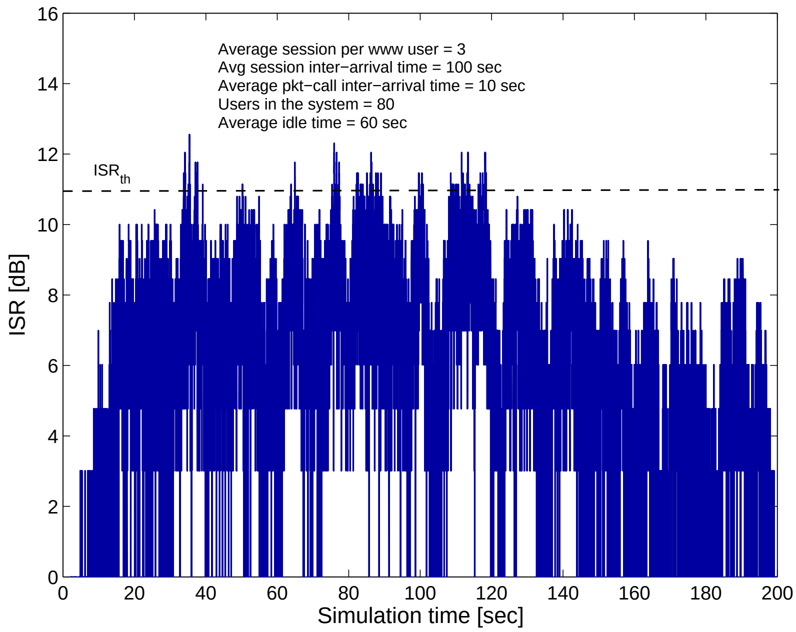

Figure 7.7: The system ISR Vs the simulation time. Number of users in the system = 80, average idle time = 60 sec, and session inter-arrival time = 100 sec.

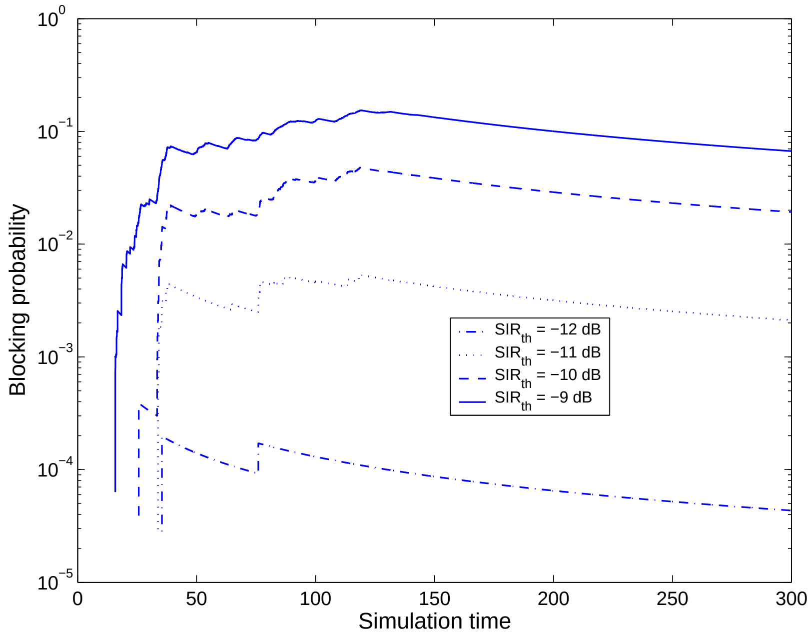

Figure 7.8: The system blocking probability Vs the simulation time. Number of users in the system = 80, average idle time = 60 sec, and session inter-arrival time = 100 sec.

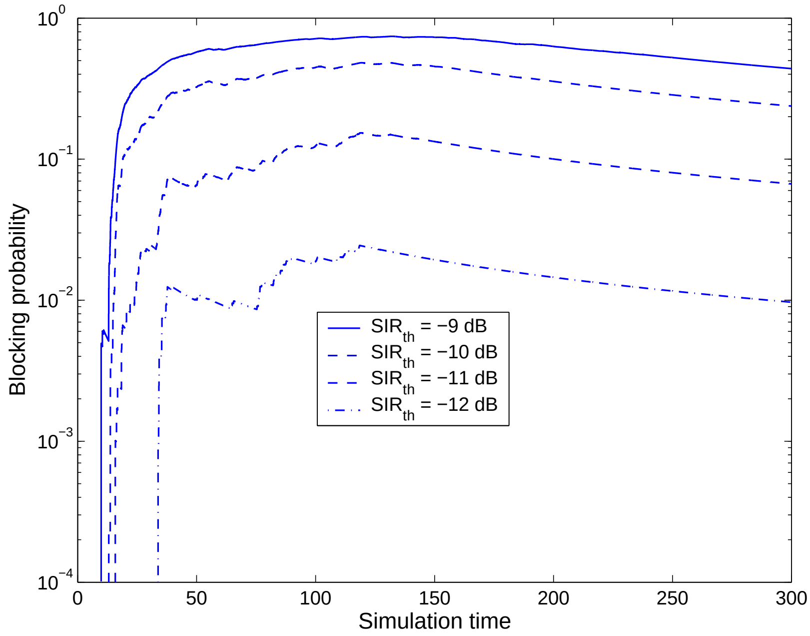

Figure 7.9: The system blocking probability Vs the simulation time. Number of users in the system = 80 with 5 reserved users, average idle time = 60 sec, and session inter-arrival time = 100 sec.

and the single cell scenario prevails. Interference is generated only when a user is in active state. Fig. 7.7 shows the system Interference-to-Signal-Ratio (ISR) when the total number of users is 80. The system blocking probability is shown in Fig. 7.8. Fig. 7.9 shows the system behaviour when a known amount of capacity is reserved for a given number of users. In this case the reserved users are guaranteed the connection and therefore their (user) activity factor is taken as 1. When a user chooses to transmit, the sector's BS will check whether the current ISR ($ISR_{current}$) is greater than the maximum (threshold) allowed ISR (ISR_{th}). If $ISR_{current}$ is greater than the threshold, ISR_{th}, the user is blocked. Therefore, the call blocking probability can be defined as

$$P_b = P_r(ISR_{current} > ISR_{th}) \tag{7.2.2}$$

In WWW services, where there are long inactivity periods within a connection and similar inactivity periods between packet-calls within a session, it allows many users to share the scarce radio resources. Monitoring this situation can lead to efficient resource allocation and management providing high capacity and large throughput. Different services pose different packet characteristics and the system performance can be quite different for these services. A good radio resource management algorithm can exploit long inactivity periods and bursty nature of data traffic to achieve large capacity and high throughput at a reasonable quality of service [40].

7.2.3 Case of Reserved Capacity

Since the capacity of a CDMA system is determined by the tolerable interference, the system activity factor has a direct bearing on the system capacity. To investigate this relationship we can define a threshold value for the signal-to-interference ratio that is acceptable for the quality of service intended, and then determine the number of active users the system can support. In doing so, it is necessary to identify the services that require guaranteed bandwidth and reserve capacity for those connections. The remaining capacity could be shared by the rest of the users, subjected to the fact that at instants of increased system activity, access to system would be denied for some. The system performance under this condition can be measured in terms of the probability of blocking of users seeking access to the system.

Fig. 7.10 shows the system activity in terms of interference-to-signal ratio (ISR) over a period of time. As shown in Fig. 7.10, the system blocking probability (P_b) can be found

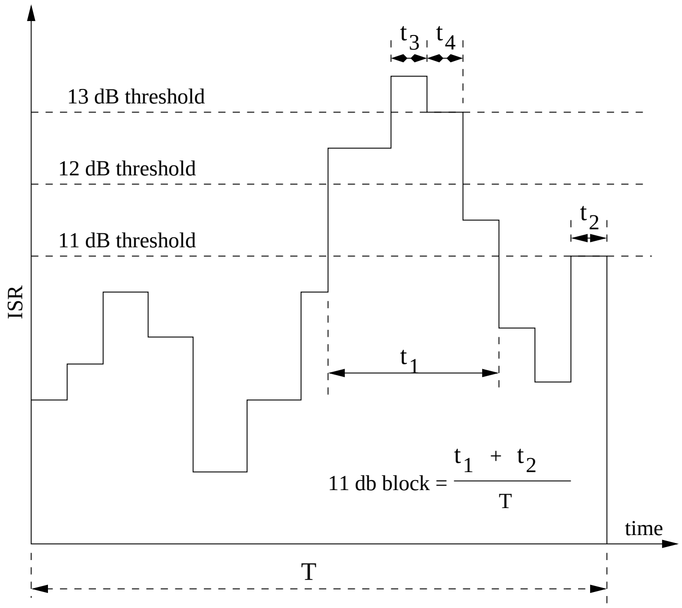

Figure 7.10: System activity (in term of ISR) against time.

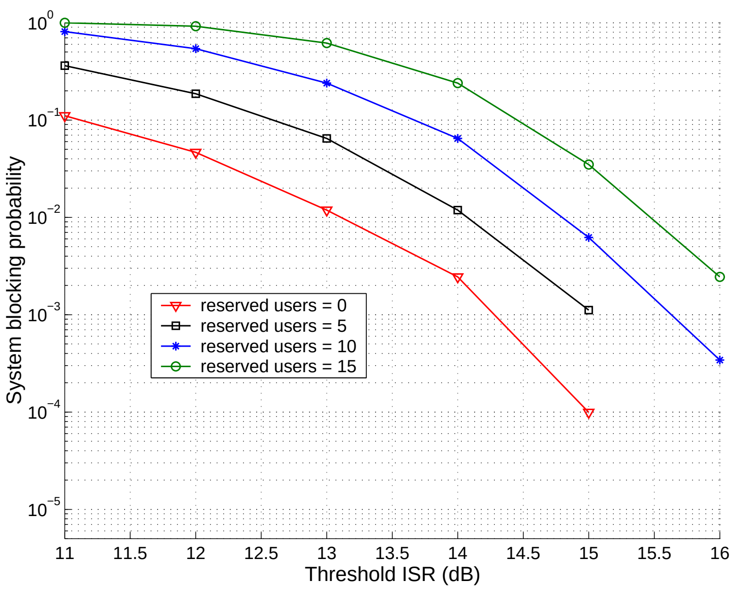

Figure 7.11: System blocking probability vs threshold ISR with capacity reservation. No. of users = 80.

with respect to a given interference-to-signal ratio threshold (which reflects the quality of service), as the fraction of the time the system activity causes the ISR to exceed the acceptable threshold (7.2.3).

$$i.e., \qquad P_b = \frac{sum\ of\ times\ ISR\ exceeds\ threshold}{total\ time\ duration} \tag{7.2.3}$$

Fig. 7.11 shows the system blocking probability as a function of quality of service (measured in terms of the acceptable interference-to-signal threshold). The results shown in Fig. 7.11 corresponds to 80 users in the system, each, on average, having three sessions per connection, session arrivals being Poisson. Each session, on the average, has 5 packet calls and the packet-call arrival time is geometrically distributed. Each packet call contains an average of 20 packets, and the packet arrival time is also geometrically distributed. Fig. 7.11 also shows the situation arrising from reserving bandwidth for a set number of users for guaranteed service.

7.3 Case of Adaptive Sectorisation and Hot Spots

In this investigation of WCDMA system capacity with packet mode operation, the number of users the system can support is evaluated using a computer simulation. The simulation environment follows that described in Chapter 4, and as shown there a multi-cell structure with sectorised cells is considered. The cell radius is taken as unity and the conventional hexagonal cell pattern is assumed. A uniformly distributed mobile population is generated with random locations within home and the 18 neighbour sectors, along with a Hot Spot

Table 7.3: Simulation parameters for WCDMA and Adaptive sectorisation.

Data rate, R	64 kbps
Chip rate, W	3.84 Mcps
ISR_{th}	8 dB dB
Blocking probability	1% dB
Packet length	480 bytes
Number of packets per packet-call	25 packets
Number of packet-call per session	5 packet-calls
Number of session per connection	5 sessions
ASAF	6.5%

(HS) located in the home sector. The simulation is based on the system parameters shown in Table 7.3. Simulations for three adaptive sector configurations were carried out to estimate the uplink capacity taking both intra-sector and inter-sector interference into account. For each loading (in terms of users), the simulation was run for more than 20,000 repetitions to obtain an average value for the blocking probability.

Fig. 7.12(a) shows the system blocking probability as a function of the number of users all of whom operate in packet mode with a constant bit rate of 64 kbps. The average system activity factor (found by previous results) is taken to be 6.5%. It can be seen from the graph that the system capacity, at 1% blocking, is 65 users per sector for an ISR_{th} of 8 dB, and 150 users per sector for an ISR_{th} of 12 dB. Fig. 7.12(b) shows the case of reserved capacity for a set number of users in the system. It is clear that with reserved capacity for five users the loss in system capacity is equivalent to about 40 packet mode users.

Fig. 7.13 shows the case of adaptive sectorisation with hot spots involvement. Fig. 7.13(a) shows the home sector and neighbour sector capacity against the hot spot to non-hot spot

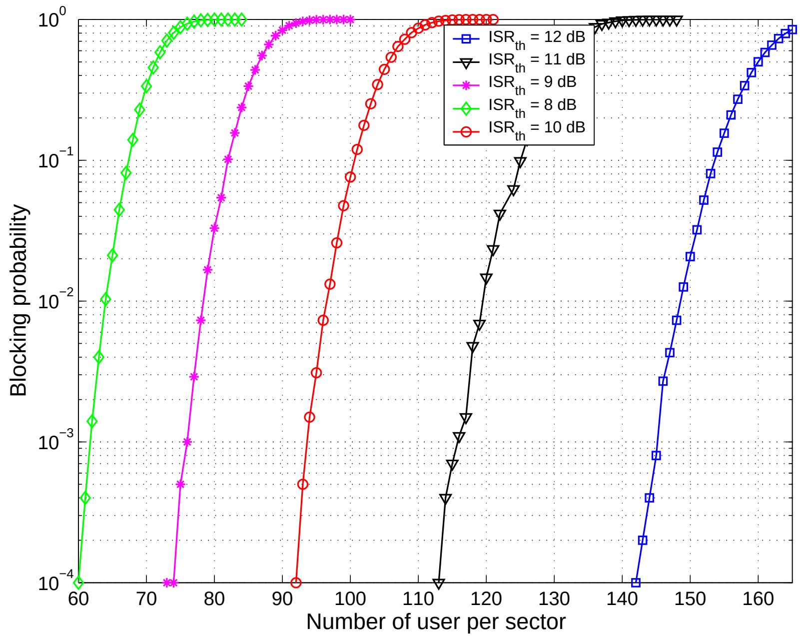

(a)

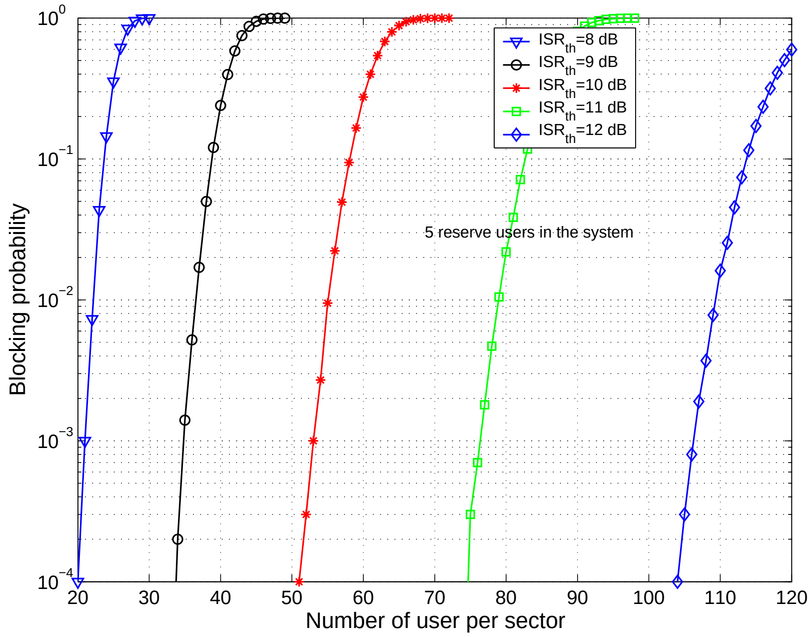

(b)

Figure 7.12: System blocking probability versus number of users per sector for different ISR_{th}. (Average idle time = 10 sec, packet inter-arrival time = 10 sec, and session inter-arrival time = 100 sec. 7.12(a) Reserved capacity = 0 users. 7.12(b) Reserved capacity = 5 users)

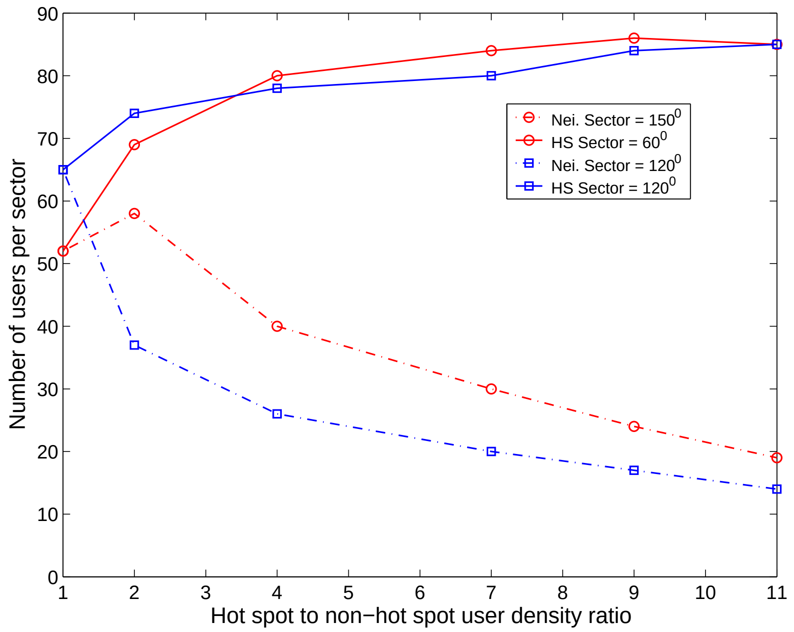

(a)

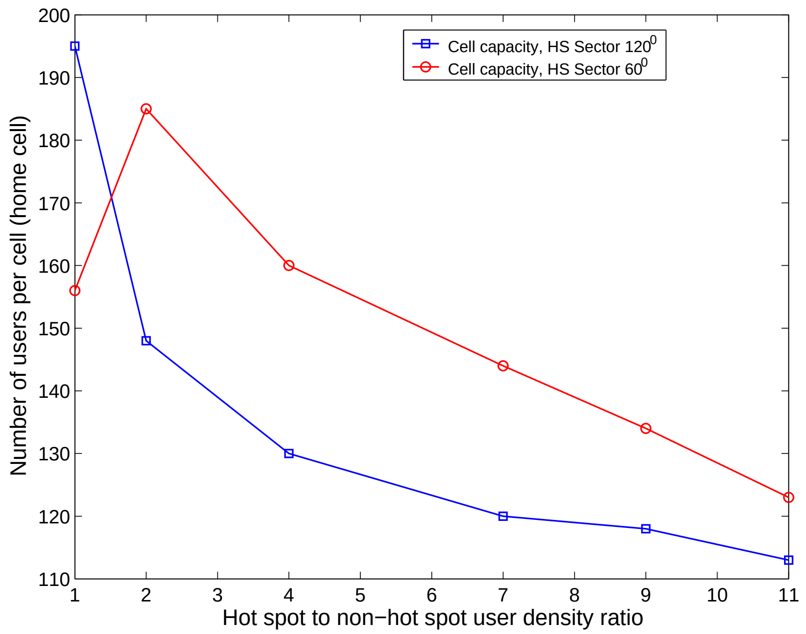

(b)

Figure 7.13: 7.13(a) Home and neighbour sector capacities versus hot spot to non-hot spot user density ratio at different HSS sizes (ISR_{th} = 8 dB), 7.13(b) Cell capacity versus hot spot to non-hot spot user density ratio at different HSS sizes. (ISR_{th} = 8 dB).

user density ratio with and without adaptive sectorisation. (Adaptive sectorisation corresponds to the case of HSS = 60^0 and the neighbour sector = 150^0). Fig. 7.13(b) shows the cell capacity against the user density ratio with and without adaptive sectorisation. It can be observed that, at an overall blocking probability of 1%, there is a capacity gain of about 37 users at a user density ratio of 2, when adaptive sectorisatoin is in place.

7.4 Conclusions

This chapter presented the simulation results of capacity assessment based on the 3G traffic model that incorporates packet mode operation. the performance parameters User Activity Factor and a System Activity Factor were defined to take into account of the two scenarios, namely, single and multiple sessions per user. The system blocking probability with capacity reservation for users requiring guaranteed bandwidth was examined. The application of adaptive sectorisation in these situations was also studied. The results indicate that a significant capacity improvement can be achieved by using adaptive sectorisation.

Chapter 8

Conclusions

In this investigation we reviewed the basic concepts underlying cellular wireless communication systems in order to bring the issue of capacity in CDMA cellular systems to the forefront. In particular, we considered the case of capacity improvement in cellular CDMA systems when non-uniform user distributions (hot spots) are involved in the coverage area. The system capacity was estimated in terms of the number of users the cell (or sector) could accommodate while providing an acceptable quality of service.

The quality of service is measured in terms of the system blocking probability which in turn reflects the acceptable signal-to-interference ratio. In order to calculate the interference arising in the system we considered a sectorised multi-cell model, with a hot spot located in the home sector, and the rest of the mobile population evenly distributed in the neighbour sectors. In calculating interference at sector BSs, both intra and inter sector interference were taken into account. The random locations of the mobile users in home and neighbour sectors and the normal radio signal propagation environment, including path-loss and slow fading (shadowing) were considered.

We studied the possibility of using adaptive sectorisation as a means of reducing interference in sectors where it appears crucial in a bid to increase the overall capacity of the system and found that this is achievable. We also found that the adaptive sectorisation could be easily implemented using finite antenna beam switching, and for that purpose practical array antennas could be employed.

The capacity improvement obtainable with adaptive sectorisation (in the presence of hot spots) is a function of user density in the hot spot in comparison to the user density in the rest of the cell, and we have shown that this improvement is significant particularly when the user density in hot spot is an order of magnitude higher than that of the rest of the coverage area.

We extended our investigation to cover the case of WCDMA systems by incorporating a 3G traffic model and estimating the system capacity with defined performance measures by given user activity and system activity factors. We have shown that with packet mode operation, the system capacity is enhanced to a great deal and that this enhancement is heavily dependent upon the type of traffic involved (as characterised by the 3G traffic parameters). It is possible to trade-off the system capacity with quality of service by allowing a limited number of users a guranteed bandwidth and still make capacity gains for those that operate in packet mode, although this trade-off appears rather expensive.

The concept of adaptive sectorisation to combat the capacity diminishing effect associated with hot spot formation, can be utilized in the case of WCDMA systems as well. Our studies show that at particular user density ratios, adaptive sectorisation can provide a higher capacity in comparison to normal case. However, when packet mode operation is in place the user density ratio depends not only on the user location but also on the user activity factor. Therefore, further investigations are necessary to identify and quantify the nature and amount of capacity improvement possible with adaptive sectorisation.

Bibliography

[1] J. S. Lee and L. E. Miller, *CDMA Systems Engineering Handbook.* Boston - London: Artech House, September 1998.

[2] F. H. Blecher, “Advanced mobile phone service,” *IEEE Transactions on Vehicular Technology*, vol. 29, no. 2, pp. 238–244, May 1980.

[3] W. C. Jakes, *Microwave Moible Communications.* John Wiley and Sons, 1974.

[4] R. Prasad, W. Mohr, and W. Konhauser, *Third Generation Mobile Communications Systems.* Boston - London: Artech House, 2000.

[5] T. Ojanpera and R. Prasad, *Wideband CDMA for Third Generation Mobile Communications.* Artech House, 1998.

[6] H. Holma and A. Toskala, *WCDMA for UMTS: Radio Access for Third Generation Mobile Communications.* John Wiley & Sons, West Sussex, England, 2000.

[7] T. Ojanpera and R. Prasad, *Wideband CDMA for Third Generation Mobile Communications.* Artech House, Boston, MA, 1998.

[8] J. P. Castro, *The UMTS Network and Radio Access technology.* John Wiley and Sons Ltd, 2001.

[9] R. Steele and L. Hanzo, *Mobile Radio Communications Secondary and Third Generation Cellular and WATM Systems*, 2nd ed. John Wiley & Sons, LTD.

[10] K. Takeo and S. Sato, "The proposal of CDMA cell design scheme considering change in traffic distributions," in *IEEE*, 1998, pp. 229–233.

[11] S. Faruque, *Cellualr Mobile Systems Engineering.* Boston-London: Artech House, 1996.

[12] W. C. Y. Lee, *Mobile Cellular Telecommunications Systems.* McGraw-Hill Book Company, 1989, ch. 6.

[13] R. C. V. Macario, *Personal and Mobile Radio Systems.* Peter Peregrinus Ltd, 1991.

[14] K. S. Gilhousen, I. M. Jaccobs, R. Padovani, L. A. W. A. J. Viterbi, and C. E. Wheatley, "On capacity of a cellular CDMA system," *IEEE Trans. Veh. Tech.*, vol. 40, pp. 303–312, May 1991.

[15] J. S. Wu, J. K. Chung, and C. C. Wen, "Hot-spot traffic relief with a tilted antenna in CDMA cellular networks," *IEEE Trans. Vch. Tech.*, vol. 47, pp. 1–9, Feb 1998.

[16] T. W. Wong and V. K. Prabhu, "Optimum sectorizational for CDMA 1900 base stations," in *IEEE VTC'97*, vol. 2, 1997, pp. 1177–1181.

[17] M. Mahmoudi, E. S. Sousa, and H. Alavi, “Adaptive sectorsize control in a CDMA system using butler matrix,” in *IEEE 49th VTC’99*, vol. 2, 1999, pp. 1355–1359.

[18] A. Wacker, J. L. Steffens, K. Sipila, and K. Heiska, “The impact of the base station sectorisation on WCDMA radio network performance,” in *IEEE 50th VTC’99 - Fall*, vol. 5, 1999, pp. 2611–2615.

[19] J. L. Steffens, A. Wacker, and P. Aikio, “The impact of the radio network planning and configuration on the WCDMA network capacity and quality of service,” in *IEEE 51st VTC2000-Spring Proceeding*, Tokyo, Japan, May 2000, pp. 1006–1010.

[20] S. C. Yang, *CDMA RF System Engineering*. Boston - London: Artech House, 1998.

[21] R. Prasad, *CDMA for Wireless Pesonal Communications*. Boston - London: Artech House, 1996.

[22] C. Joseph, J. Liberti, and T. S. Rappaport, *Smart Antennas for Wireless Communications*. Prentice Hall PTR, 1999.

[23] S. Glisic and B. Vucetic, *Spread Spectrum CDMA Systems for Wireless Communications*, 1996, ch. 5, pp. 247–258.

[24] C. U. Saraydar and A. Yener, “Capacity enhancement for CDMA systems through adaptive cell sectorization,” in *Wireless Conf. and Networking Conf.*, vol. 3, 1999, pp. 1139–1143.

[25] A. Chatovich and B. Jabbari, “Effect of non-uniform traffic load on erlang capacity of CDMA,” in *IEEE 49th VTC’99*, vol. 2, 1999, pp. 1658–1663.

[26] R. Ganesh and K. Joseph, "Effect of non-uniform traffic distributions on performance of a cellular CDMA system," in *IEEE*, 1997, pp. 598– 602.

[27] O. Adrian, S. G. Haggman, and A. Pietila, "Study of the impact of non-uniform spatial traffic distribution on the system parameters of CDMA cellular system," in *IEEE ICPWE'99*, 1999, pp. 394–398.

[28] M. Hata, "Emprirical formula for propagation loss in land mobile radio services," *IEEE Transactions on Vehicular Technology*, vol. 29, no. 3, pp. 317–325, Aug. 1980.

[29] J. Viterbi, A. M. Viterbi, K. S. Glihousen, and E. Zehavi, "Soft handoff extends CDMA cell coverage and increased reverse link capacity," *IEEE Journal on Sel. Area in Com.*, vol. 12, pp. 1281–1288, Oct 1994.

[30] *www.celwave.com/index.php?sid=c0e46ad491f02233c2bdcae4bb70f10e&p=340&l=1 (*please download PCS patterns*, **ALE1903H.199**).*

[31] J. M. Holtzman and D. J. Goodman. Kluwer Academic publishers, 1994, ch. Simulation Results on CDMA Forward Link System Capacity, pp. 145–159.

[32] T. Ottosson and A. Svensson, "Multi-rate schemes in DS/CDMA systems," in *Proc. VTC 1995*, vol. 2, Chicago, IL, Jul. 1995, pp. 1006–1010.

[33] A. L. Johansson and A. Svensson, "On multirate DS/CDMA schemes with interference cancellation," in *Wireless Personal Commun.*, vol. 9, Jan. 1999, pp. 1–29.

[34] C. L. I and R. D. Gitlin, "Multi-code CDMA wireless personal communications networks," in *Proc. ICC 1995*, vol. 2, Seattle, WA, Jun. 1995, pp. 1060–1064.

[35] M. Saquib, R. Yates, and N. Mandayam, "Decorrelation detectors for a dual-rate synchronous DS/CDMA system," in *Wireless Personal Commun.*, vol. 9, Nov. 1998, pp. 1966–1983.

[36] F. H. P. Fitzck, R. Morich, and A. Wolisz, "Comparison of multi-code link layer transmission strategies in 3Gwireless CDMA," in *IEEE Communi. Magazine*, Oct. 2000, pp. 58–64.

[37] T. Wong and V. K. Prabhu, "Capacity growth for CDMA system: Multiple sectors and multiple carriers deployment," in *IEEE 48th VTC'98*, vol. 2, 1998, pp. 1608–1611.

[38] E. Dahlman and K. Jamal, "Wide-band services in a DS-CDMA based FPLMTS system," in *Proc. of VTC'96, Atlanta, Georgia*, May 1996, pp. 1656–1660.

[39] 3GPP, "Technical specification group radio access networks; UE radio transmission and reception (FDD)," 3G TS 25.101.v3.2.0 (2000-03), Tech. Rep., 2000.

[40] N. D. Tripathi, "Simulation based analysis of the radio interface performance of an IS-2000 system for various data services," in *IEEE Proc. VTC-Fall'01*, vol. 3, Atlantic City, NJ, USA, October 7-11 2001, pp. 1797–1882.

[41] S. Deng, "Empirical model of WWW document arrivals at access link," in *IEEE Proc. ICC'96*, vol. 3, 1996, pp. 1797–1882.

[42] UMTS, "Selection procedures for the choice of radio transmission technologies of the UMTS," TR 101 112 V3.2.0 (1998-04), Tech. Rep., April 1998.

[43] M. Cheng and L. F. Cheng, “Uplink system performance of high-speed IS-95 CDMA with mixed voice and bursty data traffic,” in *Proc. of IEEE PIMRC'98*, Boston, MA, USA, Sep 1998, pp. 1018–1022.

[44] T. S. Rappaport, *Wireless Communications: Principles and Practise.* Prentice Hall, Upper Saddle River, NJ.

[45] R. Giuliano, F. Mazzenga, and F. Vatalaro, “Adaptive cell sectorisation for UMTS third generation CDMA systems,” in *IEEE VTC'01 Spring*, May 2001, pp. 6–9.

[46] F. R. Connor, *Antennas*, 2nd ed. London: Edward Aronld, 1989, ch. 4.

[47] M. R. Garcia, J. E. B. Lati, J. M. R. Terez, and A. D. Estrella, “Capacity analysis of an integrated wideband CDMA systems,” in *EUROCOMM 2000. Information System for Enhanced Public Safety and Security, IEEE/AFCEA*, 2000, pp. 204–211.

[48] K. Dimou, C. Rosa, T. B. Sorensen, J. Wigard, and P. E. Mogensen, “Performance of uplink packet services in wcdma,” in *Proc. of IEEE VTC'03 Spring*, 2003.

[49] C. Y. Huang, H. Y. Su, S. Vitebsky, and P. C. Chen, “Schedulers for 1xev-do: Third generation wireless high-speed data systems,” in *Proc. of IEEE VTC'03 Spring*, 2003.

[50] N. Enderle and X. Lagrange, “User satisfaction models and scheduling algorithms for packet-switched services in umts,” in *Proc. of IEEE VTC'03 Spring*, 2003.

[51] A. S. Anpalagan and E. S. Sousa, “Reverse link performance analysis of a cellular CDMA network with fixed overlapping sectors in non-uniform angular traffic,” in *IEEE ICC'01*, 2001.

[52] T. Nguyen, and P. Dassanayake, and M. Faulkner, “Capacity of CDMA Cellular Systems with Adaptive Sectorisation and Non-uniform Traffic,” in *Proc. IEEE 54th VTC Fall*, vol. 2, Atlantic City, NJ, USA, Oct. 2001, pp. 1163–1167.

[53] T. Nguyen, P. Dassanayake, M. Faulkner, and R. Berangi, “Influence of Hot Spot on Capacity of Cellular CDMA Systems with Adaptive Sectorisation,” in *International Symposium on Telecommunications (IST) 2001*, vol. 1, Tehran, Iran, September 1-3 2001, pp. 574–577.

[54] T. Nguyen, P. Dassanayake, and M. Faulkner, “Handling of non-uniform traffic in CDMA cellular using adaptive sectorisation,” in *1st ATcrc Telecommunications and Networking Conference*, Esplanade Hotel and Curtin University, Western Australia, April 4-5 2001, pp. 59–60.

[55] T. Nguyen, P. Dassanayake, and M. Faulkner, “Traffic model for third generation cellular mobile communication system,” in *4th International Conference On Modelling and Simulation*, Victoria University, Melbourne Australia, Nov. 11-13 2002, pp. 180–184.

[56] T. Nguyen, P. Dassanayake, and M. Faulkner, “Capacity CDMA systems with high bit rate user and adaptive sectorisation,” in *3rd Australian Communications Theory Workshop*, vol. 1, Canberra Australia, February 4-5 2002, pp. 67–70.

[57] T. Nguyen, P. Dassanayake, and M. Faulkner, “Computer modelling of 3G cellular traffic,” in *2nd ATcrc Telecommunications and Networking Conference*, Esplanade

Hotel, Western Australia, October 16-18 2002, pp. 146–149.

[58] T. Nguyen, P. Dassanayake, and M. Faulkner, "Use of adaptive sectorisation for capacity enhancement in CDMA cellular systems with non-uniform traffic," *Accepted to publish in Wireless Personal Communications, Kluwer.*

[59] T. Nguyen and P. Dassanayake, "Estimation of intercell interference in CDMA macro cells," in *Australian Telecommunications Networks and Applications Conference*, Melbourne Australia, Dec. 8-10 2003.

[60] T. Nguyen, P. Dassanayake, and M. Faulkner, "System activity in WCDMA system with packet mode traffic," in *3rd ATcrc Telecommunications and Networking Conference*, Melbourne Australia, Dec. 11-12 2003.

[61] H. Holma and K. Heiska, "Performance of high bit rates with WCDMA over multipath channels," in *IEEE VTC'99*, Houston, TX, May 1999, pp. 25–29.

[62] J. Muckenhein and U. Bernhard, "A frame for load control in 3rd generation CDMA networks," in *IEEE Proc Globecom'01*, 2001.

[63] 3GPP, "Technical specification group radio access networks UTRA FDD, radio transmission and reception," 3G TS 25.104 (v3.2.0), Tech. Rep., March 2000.

[64] M. Elsey, E. Farrell, and C. Johnson, "Matching WCDMA site configuration with coverage and capacity requirements," in *3G Mobile Communication Technologies*, March 26-28 2001, pp. 73–77.

[65] D. Bertsekas and R. Gallager, *Data Network*, 2nd ed. Prentice Hall, 1992, ch. 3.

[66] C. Lee and R. Steele, "Effect of soft and softer handoffs on CDMA system capacity," *IEEE Trans. Veh. Tech.*, vol. 47, no. 3, August 1998.

[67] C. A. Balanis, *Antenna theory analysis and design*, 2nd ed. Widley, 1997, ch. 6, pp. 257–267.

[68] S. Ogawa, A. Higashi, A. Ito, H. Horitani, K. Hatta, and T. Ueda, "WCDMA system experiments," in *IEEE VTC'00-Spring Proceeding*, Tokyo, Japan, 2000, pp. 143–147.

[69] B. C. Sowden and K. W. Sowerby, "Variable bit rate traffic modelling for dimensioning 3g cdma systes," in *Proc. of IEEE VTC'03 Spring*, 2003.

[70] S. Kumar and S. Nanda, "High data rate packet communications for cellular networks using CDMA: Algorithms and performance," *IEEE Journal on Selected area in Comm.*, vol. 17, no. 3, pp. 472–492, March 1999.

[71] W. C. Y. Lee, *Mobile Communications Design Fundamentals*, 2nd ed. John Wiley and Sons, INC, 1993.

[72] T. H. Wu and E. Geraniotis, "CDMA with multiple chip rates for multi-media communicaions," in *Proc. 28th Annual Conf. Information Sciences and Systems*, Princeton Univ., Mar. 1994, pp. 992–997.

[73] J. Lai-Steffens, A. Wacker, and K. Sipila, "Verification of 3g radio network dimensiong rules with static network simulation," in *Proc. of VTC'00*, 2000, pp. 478–482.

[74] A. Sabharwal, D. Avidor, and L. Potter, "Sector beam synthesis for cellular systems using phased antenna arrays," *IEEE Transactions on Vehicular Technology*, vol. 49, no. 5, pp. 1784–1792, Sep. 2000.

[75] G. K. Chan, "Effects of sectorization on the spectrum efficiency of cellular radio systems," *IEEE Transactions on Vehicular Technology*, vol. 41, no. 3, pp. 217–225, Aug. 1992.

[76] X. Yang, S. G. Niri, and R. Tafazolli, "Sectorization gain cdma cellular systems," in *Proc. of 3G Mobile Comm. Tech., 2000.* 1^{st} *Int. Conf.*, 2000, pp. 70–75.

[77] T. Lee and R. Arnott, "System performance of multi-sector smart antenna base station for wcdma," in *Proc. of IEE 3G Mobile Comm. Tech., 2001.* 2^{nd} *Int. Conf.*, Mar. 2001, pp. 1–6.

[78] H. D. Schotter, H. Elders-Boll, and A. Busboom, "Adaptive multi-code cdma systems for variable data-rates," in *Proc. of IEEE ICPWC'97*, 1997, pp. 334–337.

[79] S. W. Wang and I. Wang, "Effects of soft handoff, frequency reuse and non-ideal antenna sectorization on cdma system capacity," in *Proc. of IEEE VTC'93, Secaucus, NJ.*, May 1993, pp. 850–854.

[80] H. D. Schotter, H. Elders-Boll, and A. Busboom, "Multi-code cdma with variable sequence-sets," in *Proc. of IEEE ICPWC'97*, 1997, pp. 628–631.

[81] Z. Guo and K. B. Letaief, "Performance of vsf-cdma and mc-cdma in multirate systems," in *Proc. of IEEE VTC'01 Spring*, 2001.

[82] L. Zhang and T. T. Lee, “Dynamic packet scheduling for wireless channel with varying capacity,” in *Proc. of IEEE VTC’03 Spring*, 2003.

[83] W. Matragi and S. Nanda, “Capacity analysis of an integrated voice and data cdma system,” in *Proc. of IEEE VTC’99 Spring*, 1999, pp. 1658–1663.

[84] M. Alam and A. U. H. Sheikh, “Performance of multirate cdma transmission in cellular environment,” in *Proc. of IEEE VTC’99*, 1999, pp. 1688–1692.

[85] T. Ottosson and T. Palenius, “The impact of using multicode transmission in the wcdma system,” in *Proc. of IEEE VTC’99 Spring*, 1999, pp. 1550–1554.

[86] S. Ramakrishna and J. M. Holtzman, “A comparison between single code and multiple code transmission schemes in a cdma system,” in *Proc. of IEEE VTC’98 Spring*, May 1998, pp. 791–795.

[87] L. E. Aguado, T. O’Farrell, and J. W. Harris, “Performance evaluation of multiple bit-rate traffic mixing utra,” in *Proc. of IEE 3G Mobile Comm. Tech., 2000.* 1^{st} *Int. Conf.*, 2000, pp. 411–415.

[88] M. Sagfors, R. Ludwig, M. Meyer, and J. Peisa, “Buffer management for rate varying 3g wireless links supporting tcp traffic,” in *Proc. of IEEE VTC’03 Spring*, 2003.

[89] D. I. Kim, E. Hossain, and V. K. Bhargava, “Integrated rate and error control in variable spreading gain wcdma systems,” in *Proc. of IEEE ICC’01*, 2001.

[90] I. Koo, S. Bang, Jeehwan, and K. Kim, “Erlang capacity of smart antenna cdma system considering the sector operation,” in *Proc. of IEEE VTC’03 Spring*, 2003.

[91] R. P. Narrainen and F. Takawira, "A traffic model for a power controlled cdma system," in *Proc. of IEEE Comm. and Signal Processing, COMSIG'98*, 1998, pp. 51–56.

[92] M. Mahmoudi and E. S. Sousa, "Sectorized antenna system for cdma cellular networks," in *Proc. of IEEE VTC'97*, vol. 1, 1997, pp. 6–10.

[93] K. Goto, T. Suzuki, and T. Hattori, "Cell size adaptive in w-cdma cellular system," in *Proc. of IEEE VTC'02 Spring*, 2002.

[94] C. U. Saraydar and A. Yener, "Adaptive cell sectorization for cdma systems," *IEEE Journal on Selected Areas in Comm.*, vol. 19, no. 6, pp. 1041–1051, Jun. 2001.

[95] B.-S. Bae, K.-T. Jin, and D.-H. Cho, "Performance analysis of an integrated voice/data cdma system with dynamic admission/access control," in *Proc. of IEEE VTC'01 Spring*, 2001.

[96] S. Kumar and S. Nanda, "An access scheme for high speed packet data service on is-95 based cdma," in *Proc. of IEEE Computer and Comm.*, 1997, pp. 472–477.

[97] A. H. Solana, A. V. Bardaji, and F. C. Palacio, "Performance analysis of packet scheduling strategies for multimedia traffic in wcdma," in *Proc. of IEEE VTC'02 Spring*, 2002.

[98] M. Cesana and A. Capone, "Impact of mixed voice and data traffic on the umts-fdd performance," in *Proc. of IEEE Globecom'02*, 2002.

Appendix A

Published Papers

1. T. Nguyen, P. Dassanayake and M. Faulkner, "Use of Adaptive Sectorisation for Capacity Enhancement in CDMA Cellular Systems with Non-uniform Traffic," *Wireless Personal Communications, vol. 28, pp. 107-120, February 2004. Kluwer Academic Publishers.*

2. T. Nguyen, P. Dassanayake and M. Faulkner, "Capacity of CDMA Cellular Systems with Adaptive Sectorisation and Non-uniform Traffic," *IEEE Proc. VTC Fall 2001*, Atlantic City, NJ USA, October 7 - 11, Vol. 2, pp.1163-1167.

3. T. Nguyen, P. Dassanayake, M. Faulkner and R. Berangi, "Influence of Hot Spot on Capacity of Cellular CDMA Systems with Adaptive Sectorisation," *International Symposium on Telecommunications (IST) 2001*, Tehran, Iran, 1-3 September 2001 pp. 574-577.

4. T. Nguyen, P. Dassanayake and M. Faulkner, "Handling of Non-uniform traffic in

CDMA Cellular Using Adaptive Sectorisation," *1st ATcrc Telecommunications and Networking Conference*, Esplanade Hotel and Curtin University, 4-5 April 2001, pp. 59-60.

5. T. Nguyen, P. Dassanayake and M. Faulkner, "Capacity CDMA Systems with High Bit Rate User and Adaptive Sectorisation," *3rd Australian Communications Theory Workshop*, 4-5 February 2002, Canberra Australia, pp.67-70.

6. T. Nguyen, P. Dassanayake and M. Faulkner, "Computer Modelling of 3G Cellular Traffic", *2nd ATcrc Telecommunications and Networking Conference*, Esplanade Hotel, 16-18 October 2002, pp.146-149.

7. T. Nguyen, P. Dassanayake and M. Faulkner, "Traffic Modelling For Third Generation Cellular Mobile Communication Systems," *4th International Conference on Modelling and Simulation*, Victoria University, Melbourne Australia, 11-13 November 2002, pp180-184.

8. T. Nguyen and P. Dassanayake, "Estimation of Intercell Interference in CDMA Macro Cells," *Australian Telecommunications Networks and Applications Conference*, 8 - 10 December 2003, Melbourne Australia.

9. T. Nguyen, P. Dassanayake and M. Faulkner, "System Activity in WCDMA System with Packet Mode Traffic," *3rd ATcrc Telecommunications and Networking Conference*, 11-12 December 2003, Melbourne Australia.

Appendix B

Density of Mobile Population

Let ρ be the density of mobile population in a cell. If the hexagonal cell radius is R, and there are N users in the interfering cell, assuming that the users are uniformly distributed in the cell, the user density (users per unit area) is given by,

$$\begin{aligned}
\rho &= \frac{Number\ of users\ per\ cell}{Area\ of\ one\ hexagon} \\
&= \frac{N}{6\left(\dfrac{1}{2}R^2\sin(60^0)\right)} \\
&= \frac{N}{6 \times \dfrac{R^2\sqrt(3)}{4}} \\
&= \frac{2N}{3\sqrt{3}R^2}
\end{aligned} \tag{B.0.1}$$

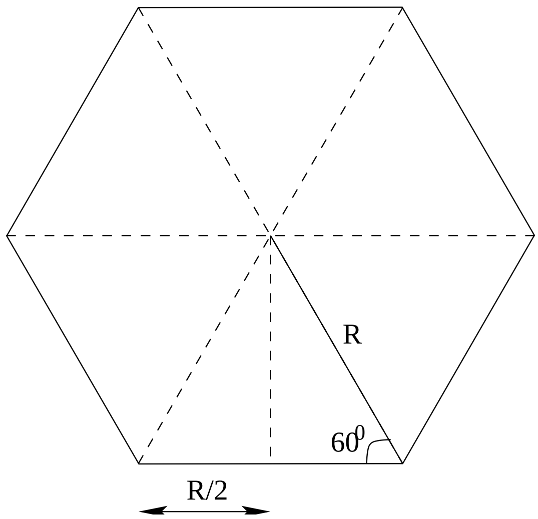

Figure B.1: Hexagon cell.

Appendix C

Linear Antenna Array

C.1 A linear array consisting of N elements

Assume that all elements of the array are identical and fed with currents of same magnitude but progressively increasing phase shift. The Array Factor (AF) of such an array can be obtained by considering its elements as point (isotropic) sources and taking the vector sum of radiations from individual elements [67]. Accordingly (Fig. C.1(a)) the Array Factor is found as,

$$AF(\theta) = \sum_{n=0}^{N-1} exp(j \cdot n(k \cdot d \cdot sin(\theta) + \beta), \tag{C.1.1}$$

where N is the number of elements, k is a constant with value $2\pi/\lambda$, d is the spacing between elements, λ is the free space wavelength, and β is the phase difference between feed currents in successive elements.

Broadside Array

For a broadside array the direction of maximum radiation is when $\theta = 0^0$ and for maximum value $\theta = 0^0$,

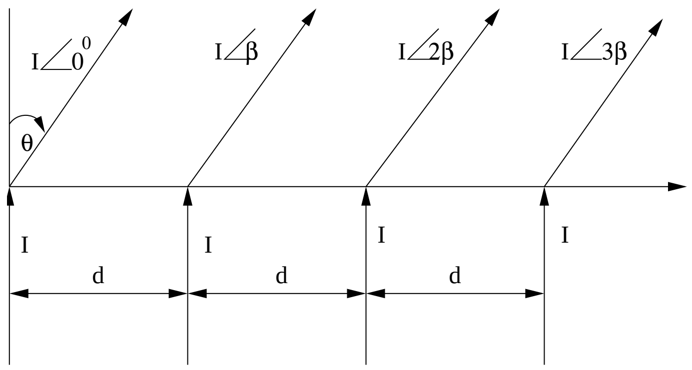

(a)

Figure C.1: 4-element array of isotopic sources.

Since,

$$\psi = k \cdot d \cdot \sin(\theta) + \beta = 0 \tag{C.1.2}$$

when $\theta = 0^0$,

$$\psi = \beta = 0 \tag{C.1.3}$$

Thus, for a broadside array, it is necessary that all the elements of the array have the same phase excitation. To avoid any grating lobes the largest spacing between the elements should be less than one wavelength ($d_{max} < \lambda$) [67].

End-Fire-Array

Some times it may be desirable to direct the main beam along the axis of the array (end-fire). In this case we have $\theta = \pm 90^0$. To direct the maximum toward $\theta = 90^0$,

$$\psi = k \cdot d \cdot \sin(\theta) + \beta \mid_{\theta=90^0} = 0 \Rightarrow \beta = -d \cdot k \tag{C.1.4}$$

If the maximum desired direction is $\theta = -90^0$, then $\beta = k \cdot d$. If the element separation is $d = \lambda/2$, end-fire radiation exists in both direction ($\theta = 90^0$ or ($\theta = -90^0$). If the element spacing is a multiple of a wavelength ($d = n \cdot \lambda$, where $n = 1, 2,$) then, in addition to having end-fire radiation in both directions, there will be grating lobes. Again, to avoid any grating lobes, the maximum spacing between the elements should be less than $\lambda/2$ [46].

C.2 Practical Antenna Array

A practical antenna array is obtained by replacing the isotropic radiators by practical radiation elements. Typically they are based on half-wave dipoles. In this study, we use the RFS (Radio Frequency System) Ltd dipole as the practical antenna element.

Adaptive Array

The arrays considered so far provide fixed beams which are directed towards the broadside or the end-fire direction. In applications such as cellular mobile systems where adaptive sectorisation is required, there is a need to scan the beam in various directions, and two of the most common methods used are mechanical scanning and electronic scanning. In case of mechanical scanning, the array can be rotated mechanically through 360^0 to give all-round coverage and is used when the rotating structure is not too large. In other cases electronic scanning is preferred.

In an array of several equally spaced elements, the main beam points in a direction at an angle θ_s to the normal when the phase difference between adjacent elements is given by [46],

$$\beta = k \cdot d \cdot \sin(\theta_s) \tag{C.2.1}$$

Thus, by varying the phase difference β, the beam can be steared through various directions θ_s as shown in Fig. C.2. However, it is to be noted that for element spacing of about half wavelength, beam steering is restricted to about 60^0 to avoid grating lobes [46].

Since the resultant AF of the linear array is a summation of exponentials, it can be represented by the vector sum of phasors each of unit amplitude and progressively increasing phase difference β relative to the adjacent. Fig. C.3 illustrates the case of an array of 4 elements. For an N element antenna array with element spacing equal to $\lambda/2$, the AF can be found by substituting (C.2.1) into (C.1.1). Then,

$$AF(\theta) = \sum_{n=0}^{N-1} exp(j \cdot n \cdot \pi(\sin(\theta) + \sin(\theta_s)), \tag{C.2.2}$$

where $0^0 \leq \theta \leq 360^0$ and $\theta_s = [-45^0 \;\; -15^0 \;\; 15^0 \;\; 45^0]$. The resultant antenna pattern ($AP(\theta)$) is found by pattern multiplication (i.e., it is the product of the $AF(\theta)$ and the pattern of a single element of the array, $A(\theta)$).

$$i.e. \qquad AP(\theta) = A(\theta) \times AF(\theta) \tag{C.2.3}$$

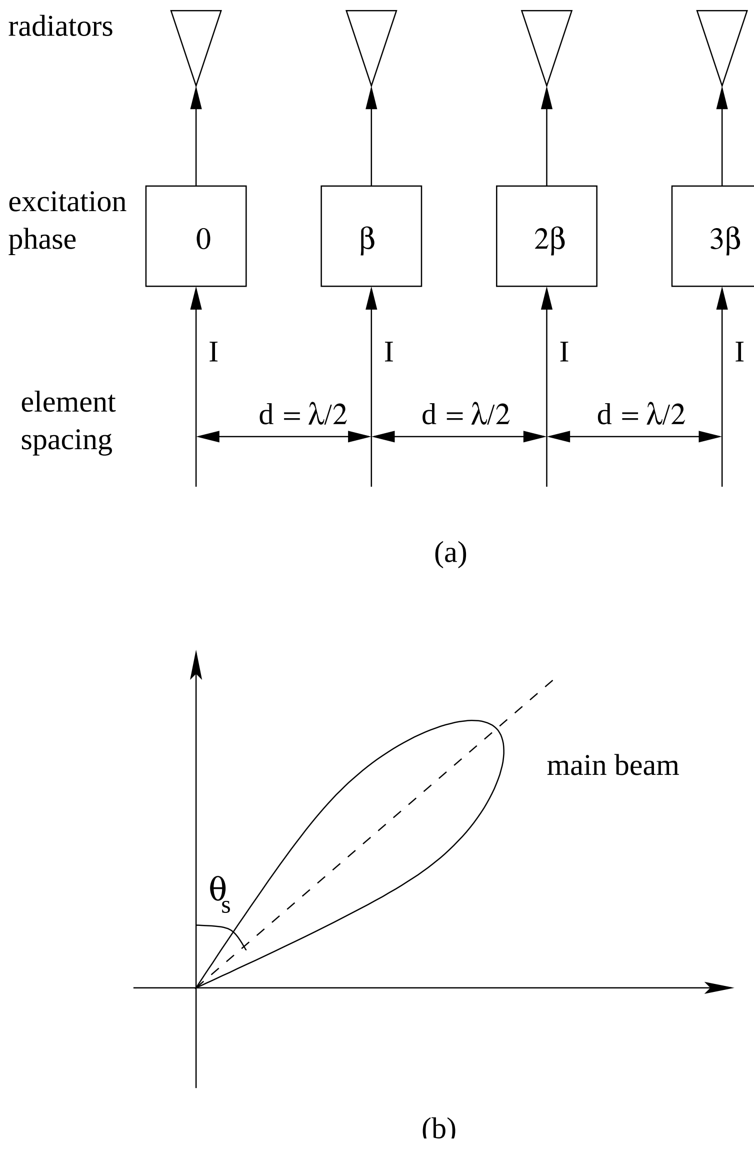

Figure C.2: (a) array of radiators fed with currents of progressive phase advance. (b) direction of the main beam.

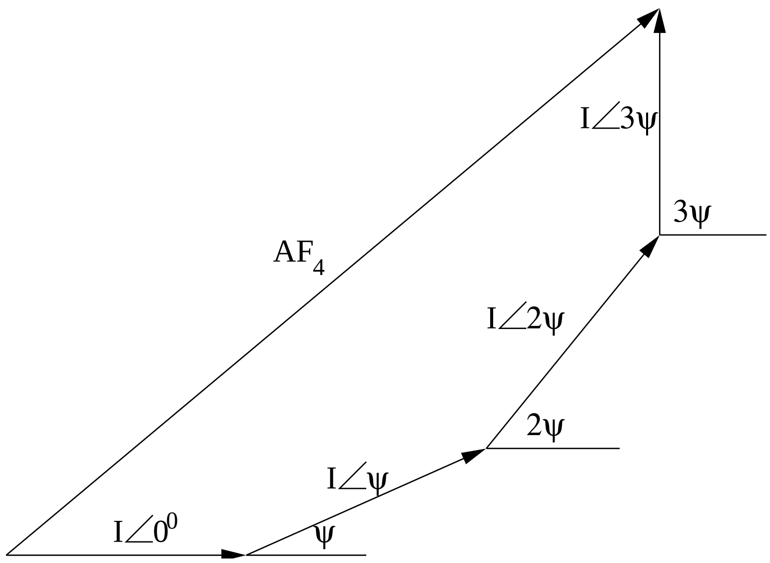

Figure C.3: Phasor diagram of $AF(\theta)$ for a four element array.

$AF(\theta)$ is a function of the element spacing and the array excitation phase. By varying the element spacing d and/or phase difference β between excitation of elements, the characteristics of $AF(\theta)$ and hence the resultant array pattern can be controlled.